CSIRO Intelligent Grid Research Cluster
Project #3

A report on life cycle costing, greenhouse gas abatement and optimal siting

Gerard Ledwich and Fushuan Wen (QUT)
D. Jayaweera and S. Islam (CUT)

June 2011

Contents

Chapter 1. Introduction and Summary 9
1. Sizing the distributed generation with life cycle costing and greenhouse gas abatement effects 10
2. Radial basis function neural network based short-term wind power forecasting with Grubbs test 11
3. Optimal siting and sizing of distributed generators based on a modified primal-dual interior point algorithm 11
4. Optimal siting and sizing of distributed generators in distribution systems with plug-in electric vehicles 12
5. A hybrid approach for planning distributed generation employing chance constrained programming 12
6. Risk control in transmission system planning with wind generators 13
7. Generation Scheduling with Fluctuating Wind Power 13
Chapter 2. Sizing the Distributed Generation with Life Cycle Costing and Greenhouse Gas Abatement Effects 15
1. Background 15
2. The test network 18
3. The developed methodology 20
4. The Software Development 22
5. Case studies 23
6. Conclusions 30
References 32
Chapter 3. Radial Basis Function Neural Network Based Short-term Wind Power Forecasting with Grubbs Test 34
1. Introduction 34
2. RBF neural network 35
3. Construction of the RBF model 37
4. Prediction results and analysis 39
5. Conclusion 41
References 41
Chapter 4. Optimal Siting and Sizing of Distributed Generators Based on a Modified Primal-Dual Interior Point Algorithm 43
1. Introduction 43
2. The optimal siting of DGs 44
3. The optimal sizing of DGs 46
4. The MPDIPA for optimizing the sizing of DGs 47
5. Case studies 52
6. Conclusions 56
References 56
Chapter 5. Optimal Siting and Sizing of Distributed Generators in Distribution Systems with Plug-in Electric Vehicles 58
1. Introduction 58
2. Chance Constrained Programming 61
3. Modeling of Uncertainties 61
4. The Mathematical Model 65
5. Solving Strategies 70
6. Case studies 73

7. Conclusion 80
References 80
Chapter 6. A Hybrid Approach for Planning Distributed Generation Employing Chance Constrained Programming 83
1. Introduction 84
2. Overview of the planning method 86
3. Problem formulation 88
4. Modeling of uncertain factors 89
5. Solution method 90
6. Application example 95
7. Conclusion 97
References 97
Chapter 7. Risk Control in Transmission System Planning with Wind Generators 100
1. Background 100
2. The developed method 101
3. Case study 101
4. Conclusion 105
References 106
Chapter 8. Generation Scheduling with Fluctuating Wind Power 107
Nomenclatures 107
1. Introduction 108
2. The MILP-UC Formulation 110
3. Scenario Generation and Reduction 113
4. Generation Scheduling with Wind Power 117
5. Case Studies 118
6. Conclusion 125
References 125
Concluding Remarks 129
Appendix A 131
Appendix B 133

List of Tables

Table 3.1 Critical Value $\lambda_{\alpha,n}$ of Grubbs Test 37

Table 3.2 Comparison of MAPE among different forecast hours between RBF and BP Neural Network Predictions 41

Table 4.1 The states of three phase switches 52

Table 4.2 The loss sensitivity on the bus voltage of the four buses in the IEEE 123-node test feeder 53

Table 4.3 The siting and sizing of DGs after the optimization 54

Table 5.1 The original loads 74

Table 5.2 Probability distribution parameters of the load growth 75

Table 5.3 The candidate schemes for the types, siting and sizing of DGs 75

Table 5.4 The retail prices and on-grid prices in the planning period 76

Table 5.5 The investment and maintenance costs of a plug-in EV as well as electricity price adjustment coefficients in the planning period 76

Table 5.6 The investment, maintenance and operating costs of renewable DGs in the planning period 76

Table 5.7 The investment and maintenance costs of fueled DGs in the planning period 77

Table 5.8 Optimal siting and sizing of DGs in the planning period 77

Table 5.9 The cost items in the planning period 77

Table 6.1 The parameters of candidate RE-DGs 95

Table 6.2 Details of RE-DG planning schemes 95

Table 6.3 Comparison of costs between scheme A and scheme B 95

Table 6.4 The over-limitation of nodal voltage 95

Table 7.1 Comparisons of the three planning schemes for the 18-bus system 102

Table 7.2 Comparisons of the optimal planning schemes using the developed model and the investment minimization model for the 18-bus system 103

Table 7.3 The probability of not violating branch power flow limits 104

Table 7.4 Comparisons of the optimal planning schemes using the developed model and the investment minimization model for the 46-bus system 104

Table 8.1 System Data 1 118

Table 8.2 System Data 2 119
Table 8.3 System Data 3 119
Table 8.4 Generation Scheduling with Forecasted Wind Power 120
Table 8.5 Scenarios Generated 121
Table 8.6 Generation Scheduling with Varying Wind Power 122
Table 8.7 The Impact of Prediction Errors 123
Table 8.8 The Impact of Ramping on Prediction Errors 123
Table 8.9 Total Operating Costs under Different Spinning Reserve Constraints 124
Table A1 Bus data of the 18-bus system 131
Table A2 Branch data of the 18-bus system 131
Table B1 Bus data of the 46-bus system 133
Table B2 Branch data of the 46-bus system 134

List of Figures

Fig 2.1 Life Cycle Cost phases of a generating unit (Modified from (Taylor, June 2003)) 17

Fig 2.2 Schematic diagram of the proposed test network 19

Fig 2.3 Overview of the generation size optimisation algorithm with LCC and GHG 20

Fig 2.4 Total installed capacities of generating technologies needed to meet weekly operating conditions with base case loading 23

Fig 2.5 Sum of the generating unit sizes vs. variation in system load 24

Fig 2.6 LCC for different DG unit combinations in 25 years 25

Fig 2.7 GHG emission for 25 year project life 26

Fig 2.8 Total LCC for 25 year project life 26

Fig 2.9 GHG based ranking 27

Fig 2.10 LCC based ranking 27

Fig 2.11 Equally weighted ranking based on both GHG and LCC 28

Fig 2.12 LCC Cost–benefit analysis with different DG technologies 29

Fig 2.13 LCC and GHG emission variation with generating unit combinations 29

Fig 3.1 RBF Neural Network Structure 35

Fig 3.2 Sample data after preprocessing 38

Fig 3.3 Result of wind power forecast after 1h 40

Fig 3.4 RPE diagram of wind power forecast after 1h using RBF Neural Network 40

Fig 4.1 The computational procedure of the MPDIPA 52

Fig 4.2 The diagram of the IEEE 123-node test feeder 52

Fig 4.3 The loss sensitivity on the bus voltage in the IEEE 123-node test feeder 53

Fig 4.4 The variations of the network loss in the iteration process 54

Fig 4.5 The voltage at every bus in the IEEE 123-node test feeder without DGs 55

Fig 4.6 The voltage at every bus in the IEEE 123-node test feeder with DGs 55

Fig 4.7 The dual gap in each iteration 55

Fig 5.1 The flowchart of the developed CCP based method for optimal siting and sizing of DGs in Distribution Systems 60

Fig 5.2 The relationship between a wind unit's output power and the wind speed 63

Fig 5.3 The relationship between the output power of a solar generating source and the illumination intensity 64

Fig 5.5 The flowchart of the GA-embedded Monte Carlo simulation procedure 72

Fig 5.6 The IEEE 37-node test feeder 73

Fig 5.7 The optimal sizing of each kind of DGs in each year during the planning period 78

Fig 5.8 The proportion of the annually added capacity of each kind of DGs during the planning period 78

Fig 5.9 The voltage variations at each node of the test feeder with added DGs in the planning period 79

Fig 6.1 Flowchart of the hybrid planning scheme for DG 87

Fig 6.2 The flowchart of system state analysis 92

Fig 6.3 Flow chart of RE-DGs planning based on Harmony Search 94

Fig 6.4 Single-line diagram of the IEEE 37-node test feeder 96

Fig 6.5 The cost comparison between scheme A and scheme B 97

Fig 8.1 The piecewise linear energy cost function 111

Fig 8.2 The normal distribution fit by simple MCS and LHS 115

Fig 8.3 The schematic depiction of the generation of a scenario fan 116

Fig 8.4 The Framework of the Stochastic Unit Commitment 118

Fig A1 18-bus system 132

Fig B1 46-bus system 136

LIST OF ACRONYMS

ACO	ant colony optimisation
AENS	average energy not supplied
ANN	Artificial neural network
ARMA	autoregressive moving average
BP	back propagation
CAIDI	customer interruption duration index
CBD	central business district
CCP	chance-constrained programming
CPLEX	optimization software
DE	differential evolution
DG	distributed generation
DPSO	discrete particle swarm optimisation
DSTATCOM	distribution static Var compensator
EENS	expected energy not supplied
GA	genetic algorithm
GHG	greenhouse gas
HS	harmony search
IEEE	leading professional body
IPLAN	software
LCC	life-cycle costing
LP	linear programming
LQR	linear quadratic regulator
MAPE	mean absolute percentage error
MATLAB/SIMULINK	analysis software
MILP	mixed-integer linear programming
MPDIPA	modified equations of the primal-dual interior point algorithm
PABL	the probability of not violating all the branch power flow limits
PBL	the probability of not violating each branch power flow limit
PEV	plug-in electric vehicles
PSL	probability of not violating system power flow limit
PSM	margin of system power flow
PSM	probability for the security margin of system power flow
PSO	particle swarm optimisation
PV	photovoltaic
RBF	radial basis function

CHAPTER 1. INTRODUCTION AND SUMMARY

Distributed Generators (DGs) are usually small and modular generation units located near the customers. Their generation power ranges from a few kilowatts to several megawatts (generally below 10 megawatts). It includes mainly combustion engines with liquid or gaseous fuel, micro turbine, solar power (photovoltaic power and solarthermal power), wind power, biomass power, fuel cell and so on.

With enhanced awareness of energy conservation, emission reduction and environmental protection, DGs have been increasingly employed in modern power systems, especially in distribution systems. DGs can not only reduce energy losses, delay the expansion of transmission systems and hence investment, but can also enhance the security and stability of the power system concerned, improve voltage quality, increase energy utilization and reduce pollution emission.

However, if the siting and sizing of DGs are not properly determined, these advantages cannot be fully exploited. With this in mind, it is the objective of this report to systematically address the siting and sizing issues of DG, and to evaluate the greenhouse gas abatement effect.

In addition to the current chapter, the following seven chapters will be presented, followed by concluding remarks.

Chapter 2: Sizing the distributed generation with life cycle costing and greenhouse gas abatement effects

Chapter 3: Radial basis function neural network based short-term wind power forecasting with Grubbs test

Chapter 4: Optimal siting and sizing of distributed generators based on a modified primal-dual interior point algorithm

Chapter 5: Optimal siting and sizing of distributed generators in distribution systems with plug-in electric vehicles

Chapter 6: A hybrid approach for planning distributed generation employing chance constrained programming

Chapter 7: Risk control in transmission system planning with wind generators

Chapter 8: Generation scheduling with fluctuating wind power

A brief introduction of the next seven chapters (Chapters 2-8) is given below.

1. Sizing the distributed generation with life cycle costing and greenhouse gas abatement effects

Modern distribution networks operate with distributed generation, of which wind and PV can be primary technologies. With the recent developments, they share a considerable amount of loads compared to other DG technologies that may exist in a typical distribution network. Optimal planning algorithms are required to determine the type of generating technology to use, the machine ratings that will satisfy the demand and enable the system to be operated at minimal cost under constrained operating conditions.

A software program was developed and scripted using IPLAN programming language to work in conjunction with PSS/E software. The algorithms corresponding to the software development is presented in chapter 2.

A set of scenarios were developed and the most economical combinations of hybrid generating units, their performance, and individual merits with regard to objectives of this part of the project were investigated. The results suggest that the best possible combinations of various DGs such as wind and PV systems can be operated with critical supports of diesel units as supplement to the grid power supply.

Case studies presented are referring to constant cost factors of generating technologies and assets. However, the software program is developed to incorporate varying costs of generating technologies and assets that may have arisen through the inflation and life cycle effects. Such facilities in the software enables incorporation of the varying cost components of PV, wind etc, as well as the futuristic cost elements that may have arisen through subsidiaries given by governments for the use of particular generation technologies.

The investigations further suggest that the wind and diesel generating unit combination gives the most economical power generation for the particular network considered for the assessment, followed by wind, PV, diesel, and PV and diesel combinations.

The proposed algorithm gives not only the size of DG system and geographical location but also the operating condition of the week that determines the optimal condition. Such information is useful in reducing computation time of extended applications that include the security of energy supply to consumers by DG and the reliability improvement with DG unit combinations.

The priority ranking of LCC and GHG emission can be used by network regulators and policy makers for setting incentives or penalising those who adversely affect the environment. It also facilitates benchmarking distribution networks for the incentives as appropriate. The results coming out of the program can also be used as a potential platform for the carbon trade and extended applications. On the other hand, distribution network operators can use the proposed methodology to balance the benefits between different types of DG combinations and overall benefits of reducing LCC and GHG emission. Such an approach is necessary in meeting renewable energy targets and balancing the economy verses carbon trade.

2. Radial basis function neural network based short-term wind power forecasting with Grubbs test

Great efforts have been engaged in the implementation of renewable energy programs around the globe because of global warming and the deficiency of fossil fuel energy. In particular, the utilization of wind power, one of the main renewable energy resources, has experienced rapid development in recent decades. Wind power, however, comes the obvious disadvantages of intermittence and uncertainty which could significantly increase the difficulty of power system dispatching. The ever-increasing size, number and capacity of wind farms has brought the power industry the challenge of ensuring the secure and stable operation of power systems. Accurate forecasting of wind power generation plays an important role in power system dispatching and wind farm operation.

ANN has the ability to discover and approximate the nonlinear relationship through learning. The ANN based forecasting of wind speed and wind power has become a popular research focus in recent years. At present, Back Propagation (BP) neural networks and local feedback neural networks are usually employed. Based on the gradient descent rule, the BP algorithm is a local optimization algorithm. Many studies have revealed that the Radial Basis Function (RBF) neural network can achieve higher approximating accuracy, avoid being trapped in local minima, and has a faster learning curve. Furthermore, the RBF neural network, while having a simple structure, has strong capabilities of extrapolation and non-linear mapping between input and output.

Wind power forecasting can be classified as long-term, mid-term, short-term, or ultra short-term based on duration. In chapter 3, a RBF neural network based forecasting model is developed based on the wind speed, temperature, and historical wind generator outputs. The Grubbs Test is employed to check exceptional data. Prediction is conducted using the 2009 actual yearly data from a wind farm in Guangdong, China. The prediction achieved high accuracy with the prediction error below 10% most of the time. The simulation shows that the exceptional data must be eliminated in wind power forecasting in order to achieve higher precision of prediction.

3. Optimal siting and sizing of distributed generators based on a modified primal-dual interior point algorithm

As mentioned before, the advantages of DGs can be fully exploited if the siting and sizing of DGs are properly optimized. Inappropriate siting and sizing of DGs could even lead to an increase in network losses and a decrease of voltage quality at some buses.

Given this background, in chapter 4, a simple and practical approach for determining the suitable siting of DGs is first developed based on the loss sensitivity on every bus voltage. It can effectively reduce the solution space to a few buses. Secondly, after determining the optimal siting, the MPDIPA is employed to determine the sizing of DGs with the objective of optimizing the voltage profile at every bus. The modified equations of the Primal-Dual Interior Point Algorithm are then simplified to speed up the calculation procedure. IEEE 123-node test feeder is employed to verify the effectiveness of the proposed method. The results demonstrate that the proposed approach is

able to search for the optimal solutions quickly. At the same time, the voltage profiles are obviously improved and the network loss is decreased dramatically.

4. Optimal siting and sizing of distributed generators in distribution systems with plug-in electric vehicles

Due to the increasing penetration of DGs in distribution systems, the siting and sizing of DGs in distribution system planning is becoming increasingly important. Inappropriate siting and sizing of DGs could lead to many negative effects on the distribution systems concerned, such as the relay system configurations, voltage profiles and network losses. Another issue is that more and more attention is being paid to the applications of plug-in electric vehicles (PEV). However, some uncertainties such as the stochastic output power of a PEV due to its random charging and discharging schedule, that of a wind power unit due to the frequently variable wind speed, and that of a solar generating source due to the stochastic illumination intensity, volatile fuel prices and future uncertain load growth could lead to some risks in determining the optimal siting and sizing of DGs in distribution system planning. Hence, the optimal siting and sizing of DGs need to be carefully considered in distribution system planning.

In Chapter 5, for the simplicity of presentation, the load power of a PEV in the charging condition is regarded as the negative output power of the PEV and negative input power to the system concerned. Therefore, the load power of a PEV in both charging and discharging conditions is called the "output power" of the PEV. Moreover, the PEV is regarded as a kind of DG with stochastic output power.

Under the chance constrained programming framework, a new mathematical model is developed to handle some uncertainties such as the stochastic output power of a PEV, that of a renewable DG, that of a solar generating source, volatile fuel prices used by a fueled DG and future uncertain load growth in the optimal siting and sizing of DGs. Then, a Monte Carlo simulation embedded genetic algorithm approach is presented to solve the developed CCP model. Finally, the test results of the IEEE 37-node test feeder demonstrate the feasibility and effectiveness of the developed model and method.

5. A hybrid approach for planning distributed generation employing chance constrained programming

Siting and sizing of renewable energy distributed generation into existing distribution systems is essential to ensure the best benefits achievable from such resources while maintaining the secure and reliable operation of the distribution systems.

In this chapter, a novel planning methodology, based on chance constrained programming (CCP), has been proposed for optimally planning RE-DG into the distribution systems so as to maximize the benefits. In this chapter, the RE-DG planning problem is formulated as a stochastic optimization problem subject to security limitations as chance constraints. The model to be developed could not

only to yield the maximum benefits, but also maintain the performance of system under an uncertain environment. A new methodology is developed to evaluate the reliability of distribution systems with embedded RE-DGs, in which the intentional islanding operation of distribution grids in some cases is taken as an important way to improve system reliability and reduce outages. Based on the developed model and approach, the IEEE 37-node test system is employed to verify the effectiveness, and test results have demonstrated that the voltage profile and power flow can be significantly improved and the cost from loss of supply substantially reduced.

6. Risk control in transmission system planning with wind generators

Although wind power is clean and renewable, wind farms can bring about significant unfavorable impacts on power systems due to their stochastic, intermittent and uncontrollable characteristics. With the expansion of wind power generation and thus the increasing quota of wind energy in power systems, these adverse influences could become technical barriers to wind power integration, resulting in new challenges to transmission system planning (TSP) and operation. To address these challenges, new approaches should be applied in TSP to facilitate the integration of wind energy through increasing the power system's ability to defend against the influence.

To overcome the shortcomings discussed above, chapter 7 presents a probabilistic model for the power output of wind generators. The DC probabilistic power flow is calculated with the combined use of cumulants and Gram-Charlier series. Three risk-controlling strategies are then introduced to enhance the system's defense against security risks in allusion to the uncertain factors in TSP: probability of not violating each branch power flow limit (PBL), probability of not violating system power flow limit (PSL), probability for the security margin of system power flow (PSM).

Based on the above work, a TSP model with risk-controlling strategies is developed for a power system containing wind generators. A cost-benefit method is utilized to evaluate the planning schemes in order to maximize the overall benefit.

Two case studies demonstrate that it is possible to achieve a good trade-off among the security, reliability and economics of TSP schemes by employing risk-controlling strategies. Consequently, the security risks of a system associated with the uncertainties due to wind generators can be controlled using the developed TSP model.

7. Generation Scheduling with Fluctuating Wind Power

Current generation scheduling cannot fully integrate the most essential features of non-dispatchable generation technologies like wind power. This limitation is becoming an issue for grid operators as there is more and more public and political pressure to increase the penetration of renewable generation technologies, which depend on randomly varying weather conditions. Existing generation scheduling is however generally based on deterministic models and usually ignores the likelihood and the potential consequences of the random contingencies. Because of this limitation,

this chapter proposes a generation scheduling suitable for fluctuating wind power, which is also applicable to other renewable power generation.

There are two methods of incorporating the wind power into unit commitment. One is to take into account the wind power as a constant. In other words, the wind power can be forecast without errors. The other one is the stochastic approach. The two strategies are presented as follows. Uncertainties are observed in wind power generation, and a stochastic approach is most suitable for the modelling of generation. It is natural to apply a stochastic approach to a deterministic problem in the solution process.

In chapter 8, a stochastic optimization approach is proposed for the unit commitment problem considering the uncertainty of wind power generation, based on the mixed-integer linear programming (MILP). The problem is formulated as minimizing the total cost of thermal units. To consider wind power generation, scenarios are generated using scenario generation techniques. The stochastic problem is hence transformed to a deterministic one.

A 10-unit system and 100-unit system are employed to demonstrate the proposed model and method. It is shown by the simulation results that the expected scheduling cost by using stochastic programming is generally more than that using the deterministic model. This is because the stochastic model took into account the situation that the thermal units cannot meet the prediction error caused by the variation of wind power in time. Hence, the ramping capabilities of units and prediction accuracy of wind power are crucial when wind power varies.

CHAPTER 2. SIZING THE DISTRIBUTED GENERATION WITH LIFE CYCLE COSTING AND GREENHOUSE GAS ABATEMENT EFFECTS

1. Background

The assessment techniques and distributed generation (DG) technologies are significantly advancing with the increase in large scale and dispersed integration of DG. This evokes the need of a generic network that can be used as a common platform to assess the performance of techniques and DG technologies. It also provides researchers the platform for comparing alternative methods and further advances the solutions.

There are distribution networks which are well designed to absorb additional capacity of distributed generation. One must see research problems within a problem in order to understand and investigate solutions. In that context, use of robust distribution network models may not be always the right platform to assess the merits of DG. On the other hand, there are networks that inherit serious operating issues. They are either not suitable for the assessment of DG technologies or assessment techniques. This is because they may give pessimistic conclusions due to the unusual weakness of the network. Therefore, it is obvious that the right balance is necessary in order to test any technique or technologies. The reason being that if the assessment platform is significantly different from majority of distribution networks, the research conclusion comes through the investigation may not be a fair conclusion for DG techniques and their benefits to distribution networks.

The above facts demonstrate the need for a network that can fairly assess the characteristics of DG technologies and performance of techniques that are aimed at assessing the benefits of DG. Therefore, this report proposes a test network that is designed based on the concepts of realistic distribution networks. The network is stable under normal operating conditions and without the presence of distributed generation.

Modern distribution networks operate with distributed generation of which the wind and PV (Alderfer et al., 2000) can be primary technologies. With the recent developments, they share a considerable amount of loads compared to other DG technologies that may exist in a typical distribution network. The output of some of the renewable power generation technologies including Wind and PV varies throughout the year; however their output can be dispatched with the support of energy storage technologies. The optimum, efficient, and economical operation of renewable and new generation technologies requires the use of smart devices which would enables the smart coordination of DGs. Such an arrangement would reduce the use of fossil fuelled DGs such as

diesel units or in other words they may able to operate only when they are economical in the operating cycle.

There are algorithms in the published literature for investigating optimal generating unit combinations however they are mostly confined to single bus systems where the hybrid generation technologies are connected. The optimal planning algorithm requires determining the type of generating technology to use, the machine ratings that will satisfy the demand and to operate the system at minimum cost under constrained operating conditions (Inglis et al., 2010, Pan et al., 2009). The literature suggests that there are three main types of algorithms that can be used to solve a planning problem: constructive heuristic algorithms, conventional optimization algorithms and combinatorial algorithms (Romero et al., 1996, Gallego et al., 1998, Lavorato et al., 2009). They further highlights that the utilization of robust and efficient linear programming algorithms is vital parts in realising the tasks within the problem. Heuristic and conventional optimization algorithms as presented in (Garver, 1970), and are used to solve the linear programming (LP) problems associated with the optimisation. The LP algorithm provides a less complex method to formulate the problem and ensures that fast and efficient solutions to the problem with large systems. The LP algorithms consider all the specific characteristics of the problem and they incorporate various constraints associated with the optimal planning of the electrical system and its auxiliaries.

The determination of costs is an integral part of the feasibility study and design of any power system. In the past, comparisons of different generation technology alternatives, whether at the conceptual or detailed design stage, was based mainly on initial capital costs. In order to achieve better outcomes from assets, ongoing operation and maintenance costs must be considered as they consume more resources over the asset's service life cycle. Life Cycle Costing (LCC) is a process to determine the sum of all the costs associated with an asset or part thereof, including acquisition, installation, operation and maintenance, refurbishment, and disposal costs.

Life cycle costing adds together all the costs of alternatives over their life period and enables an evaluation on a common basis for the period of interest usually using discounted costs considering inflation. This enables decisions on acquisition, maintenance, refurbishment or disposal to be made in light of full cost implications. Life cycle cost can be calculated during any or all phases of an asset's life cycle. It can be used to provide input to decisions regarding asset design, manufacture states, installation, operation, support and disposal. Early identification of acquisition and ownership costs enables the decision-maker to balance performance, reliability, maintainability, maintenance support, and other goals against life cycle cost. Fig 2.1 shows an example of life cycle costing of a generating unit.

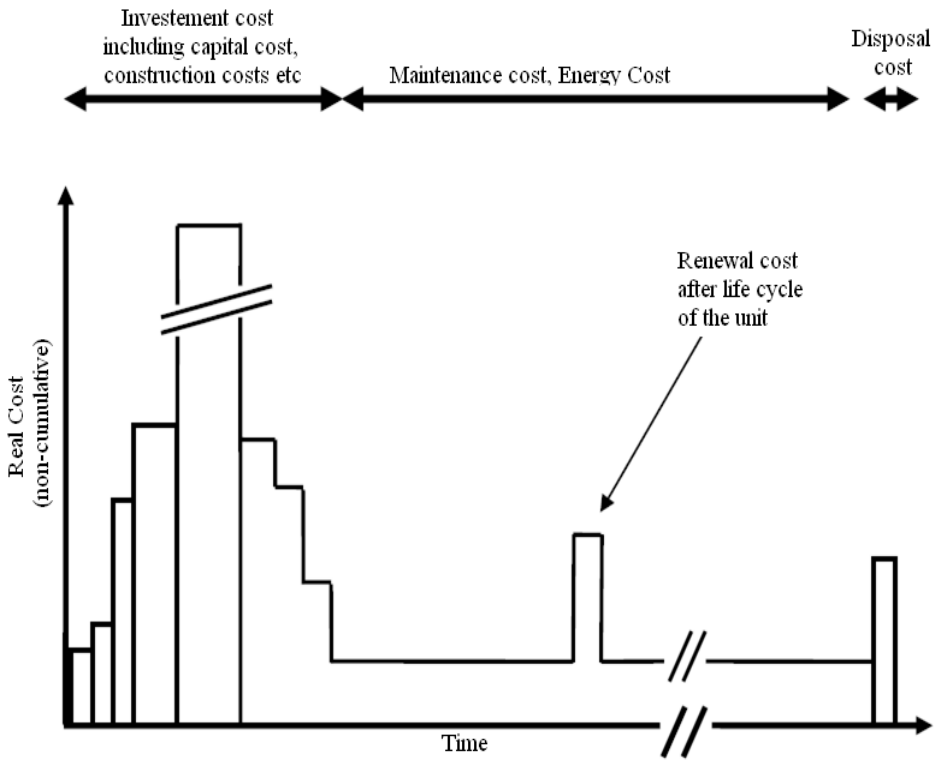

Fig 2.1 Life Cycle Cost phases of a generating unit (Modified from (Taylor, June 2003))

One of the environmentally hazardous outputs of conventional power generating units is the greenhouse gasses. Greenhouse gases are those gaseous constituents of the atmosphere, both natural and anthropogenic, that absorb and emit radiation at specific wavelengths within the spectrum of thermal infrared radiation emitted by the Earth's surface, the atmosphere itself, and by clouds. This property causes the greenhouse effect. Water vapour (H_2O), carbon dioxide (CO_2), nitrous oxide (N_2O), methane (CH_4) and ozone (O_3) are the primary greenhouse gases in the Earth's atmosphere (Wikipedia, 2000b).

According to the data provided on green house gas emissions by sector (Wikipedia, 2000a), the largest contributor towards the green house gas emission is the power industry and is responsible for highest percentage of carbon dioxide gas emissions. Such effects can be minimised with the integration of large-scale renewable distributed generation into power systems. Renewable power integration requires an adequate evaluation in order to assess the environmental impacts and economics of the overall production and utilization life cycle, including the construction and operation stages of renewable plants (Mikhail Granovskii et al., May 2006). For every kilowatt-hour of electricity produced, a proportion of CO_2 is emitted to the atmosphere, which is known as Greenhouse coefficient. For example, one kilowatt-hour of electricity produced by burning brown coal will emit approximately one kilogram of CO_2 into the atmosphere. The Australian Greenhouse Office annually determines each State's Greenhouse coefficient, based on their respective sources of electricity generation. The highest greenhouse coefficient in Australia was found in Victoria with a

value of 1.39 and this value is used as the basis to predict the worst case scenario (Emission Statement, 2010).

2. The test network

The proposed test network consists of 49 busses, 52 feeders, 25 transformers, 13 load points, 3 diesel units, 2 wind farms, and 1 PV farm with a total active and reactive peak load of 42MW, 6MVAr respectively. The network is developed in such way that it would operate healthy under normal operating conditions.

Fig. 2.2 shows the schematic diagram of the network. It is divided into three zones – Zone A, Zone B, and Zone C. One of the aims of zoning is to facilitate islanding and grid connected modes of studies. User need to provide the control mechanism that will prevent unintentional islanding. The added benefit of zoning is that the user can test the feasibility of mini/micro-grid associated research as well as issues of inter-connection of mini/micro-grids. User can also test the feasibility of the operation of a distribution network with the operation of distribution network autonomous controllers.

The detailed technical data associated with each of the zones A, B and C are given in detail in (Jayaweera et al., November 2010). It also provides various test case scenarios and details of the voltage and thermal loading distribution for the network. Under the normal operating conditions the network is steady state stable and there is no voltage limit (± 6 %) or thermal limit violations exist.

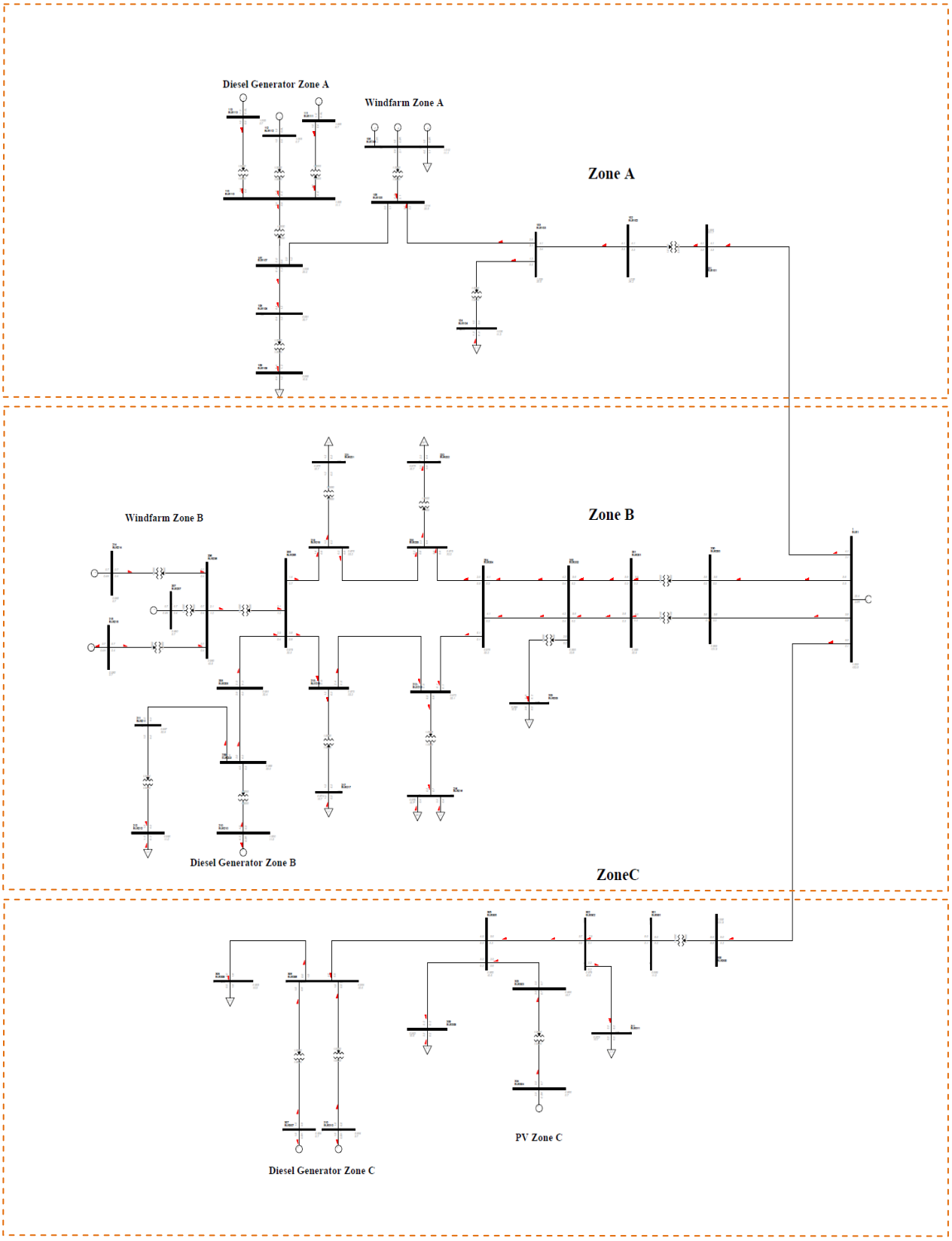

Fig 2.2 Schematic diagram of the proposed test network

3. The developed methodology

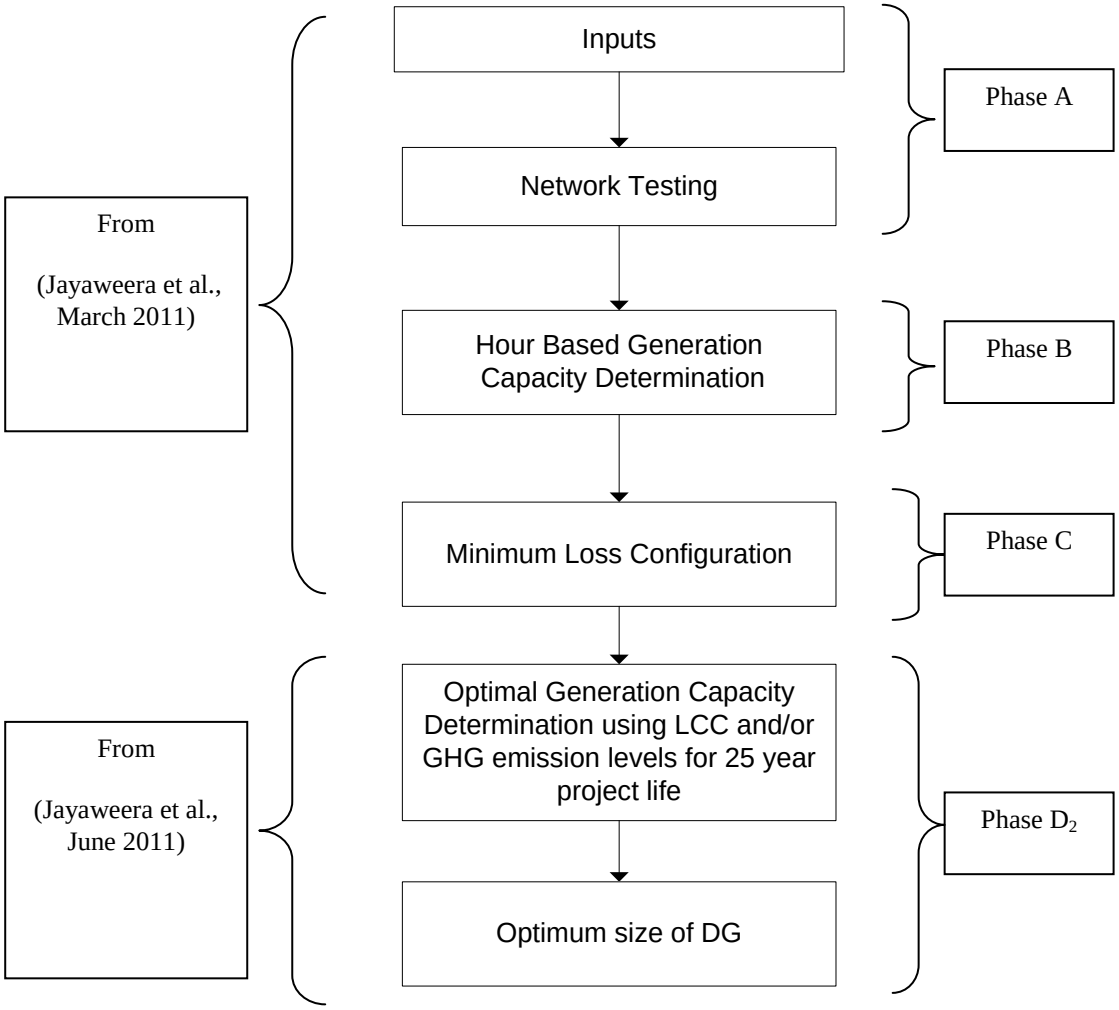

Fig 2.3 Overview of the generation size optimisation algorithm with LCC and GHG

Fig 2.3 shows the methodology used to determine the optimal DG sizes including diesels with life cycle costs (LCC) and green house gas (GHG) emissions over 25 years. The algorithm is divided into four sections namely Phase A, Phase B, Phase C, and Phase D_2. Phases A, B, and C are as explained in (Jayaweera et al., March 2011). The details for Phase D_2 are given in (Jayaweera et al., June 2011).

Phase A of the algorithm involves data inputs and the verification of the network base case (Jayaweera et al., November 2010) for network constraint violations. Upon entering the data, the network feasibility is checked by applying the Newton-Raphson algorithm. If the network converges for the operating condition without violating any constraints the operating state is deemed feasible. On successful convergence of the network, the program proceeds to Phase B of the algorithm.

In phase B, the most economical combination of DG units in the system including diesel units that best match the load and DG generation profile, for each hour of the year is determined. If it satisfies all the constraints, then the combination is saved and the operating costs associated with it is calculated and stored against the combination. On completion of the Phase B, the DG unit combination with the least operating costs is inputted to the next phase.

Phase C of the algorithm is used to determine how best the generation is allocated in such a way that the DG unit combination produces least amount of power losses. This is obtained by calculating the sensitivity of alteration of each DG unit capacity combination to reduce power losses of the network.

In phase D_2, the total LCC and GHG emission are calculated and the final results for the investigation is given as output. The diesel generators are operated only if they operate within the economical (efficient) region. The algorithm treats 40% to 100% of the rated output power of a diesel unit as the economic region of the efficiency curve.

The number of years of the project is flexible and in this investigation is set to 25 years. The investment cost includes the capital cost per MW for each unit, procurement and design costs, and installation costs respectively. The maximum ratings of the units are used for investment cost calculation. Depending on the life of the individual units in the system, replacement or renewal costs for the units are to be considered for the LCC calculation. The replacement can occur more than once within the 25 year period of the assessment. The disposal cost is included within the replacement cost.

Using the total generated power associated with each unit, the yearly costs associated with the operation and maintenance, energy/fuel costs, and cost of power losses can be calculated. This calculation assumes that the load profiles and magnitudes remain the same for the entire 25 year period. This facilitates simplified calculations neglecting the costs for network restructuring and reduces the computation time that is necessary for each year. Even though these elements are not incorporated, they can be embedded as an extension to the algorithm.

The cost of energy losses for the system is calculated assuming that all the energy lost in the network is supplied by the diesel generators. That is, diesel generators are assumed to generate the extra power required to meet the power loses of the network.

In this study, three options are offered to determine the optimal DG unit combination.

- Option 1 selects the optimal combination of DGs that includes diesels according to the total LCC for the whole period considered for the assessment (25 years).

- Option 2 considers the DG unit combination with the least GHG emission and therefore provides the best environmentally friendly generation of power.
- Option 3 is used to arrive at an output that is both economical and environmentally friendly. This is done by ranking the full array of combinations. First ranking set is determined based on the total LCC of combinations. Second ranking set is determined based on GHG emitting level of the combinations. Then, the priority ranking sets are combined together with weighting factors and the DG unit combination with the lowest value out of the combined rank considered as the most beneficial and economical combination for the power network. In this investigation, equal weighting factors are assumed with the objective of giving equal importance to reduce LCC and GHG emissions.

4. The Software Development

The algorithm proposed before is scripted using the PSS/E version 32 based IPLAN programming. IPLAN modules can be created through any text editing software and has the ability to interact with PSS/E software to produce the desired outcome. IPLAN programs interrogate the PSS/E via various routines and control the execution of inbuilt commands in the PSS/E via a series of PUSH commands. The values entered for the PUSH commands appear to the host application if they were entered from the terminal. It can access the whole information and data from the PSS/E software and can use the same to perform complex analytical and logical calculations to produce output values that can be fed back to the software.

PSS/E has a large collection of application program interface commands that can be used to input various types of data to execute different types of power flow calculation, create output reports etc. These commands can be either given at the program input terminal or can be given as inline commands using the IPLAN software enabling the seamless integration of the user defined subroutines with the actual inbuilt functions present in the PSS/E software package.

More details on IPLAN programming is given in (Jayaweera et al., March 2011), (Jayaweera et al., June 2011) and (Siemens Energy, March 2009).

5. Case studies

5.1 Impacts of load variation effects

The network loading is varied in percentage steps to determine the optimal size of generators taking into account network constraints, total life cycle costs, power losses. Fig. 2.4 shows the total installed capacities of operating conditions corresponding to weekly based scenarios in a sample year. The vertical axis gives the total installed capacities (MW) the wind, PV and diesel generators that will provide the minimum total life cycle costs, while the horizontal axis provides the combinations corresponding to each week calculated during the Phase B.

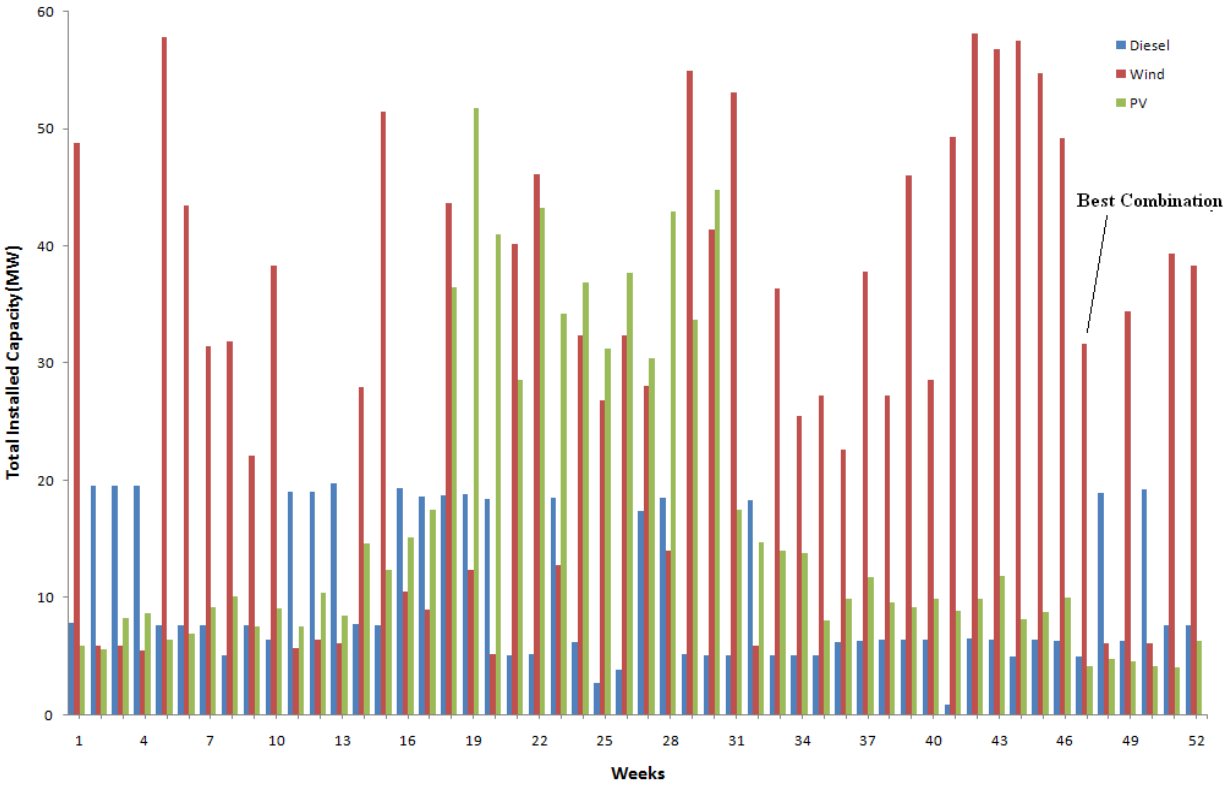

Fig 2.4 Total installed capacities of generating technologies needed to meet weekly operating conditions with base case loading

Each of the generating unit size corresponding to each week is fed into Phase C and thereafter Phase D of the algorithm in achieving the goals.

Installed capacity of the generating unit given at the week 47 gives the most economical combination that can fulfil all the operating condition of the year. This is highlighted in Fig 2.4. Thus, the week 47 is representative for selecting the least cost of operation scenario and provides the added benefit of optimal combination of distributed generating units. Identification of such an operating condition is infeasible without the application of exhaustive algorithms because of simultaneous variation of several factors through the simulation period.

Fig 2.5 shows the total installed capacity of most economic generating unit combination of all studies. Load at 90% of the base case load gives the largest required installed capacity to meet the operating conditions of the selected year. This is because the wind units of this scenario provide more power than other generating units. Network constraints and loading level together with physics of power flow limit injecting power from the generating stations that results higher demand from wind units resulting an increase in installed capacity. At 90% of full load, the penetration of Wind and PV is more than that was for the full load condition. This can be attributed to greater relaxation available in the network voltage limit and thermal limit constraints and indicates that the network mostly absorbs wind energy.

However, loading from 30% to 80% of the base load follows a linear variation of total installed capacity which contributes to most economical configuration.

Once the base case loading is increased above 100%, the most economic combination demands more power from diesel units, resulting in a reduced penetration level of wind power. This situation arises because the extra capital cost of wind units is not economical with larger installed capacities demanded by increased loading levels to meet a safe operating condition of the network. The network operation is infeasible beyond 130% of base load due to network constraints.

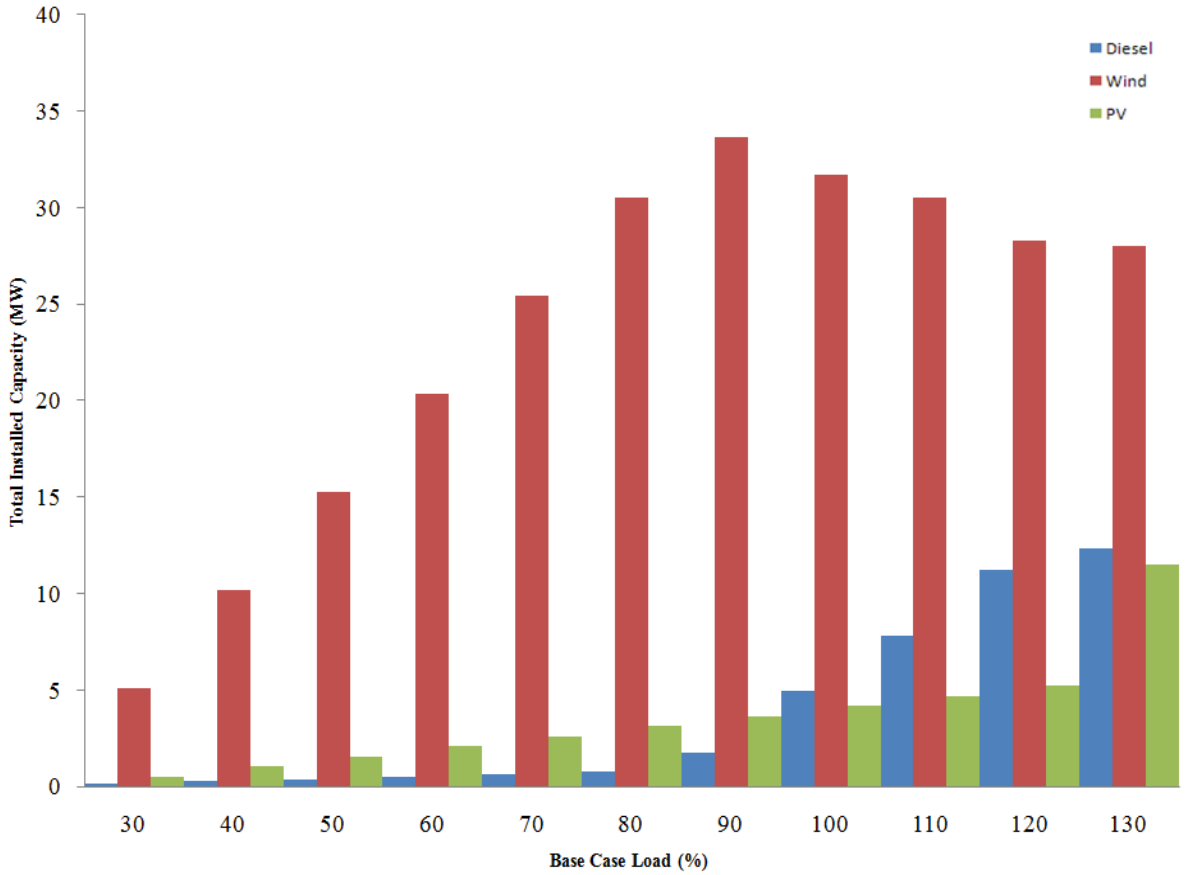

Fig 2.5 Sum of the generating unit sizes vs. variation in system load

5.2 Life cycle costs

Fig 2.6 shows the LCC incurred for the wind, PV and diesel generators for different DG unit combinations of the project for 25years. The total load demand for the 25 years is assumed as constant throughout. A depreciation rate of 7 % is used to calculate the net present value of the costs for each year in dollars. Results suggest that the week corresponding to the critical operating condition that determines the optimal DG size is not affected throughout and it remains at the 47th week.

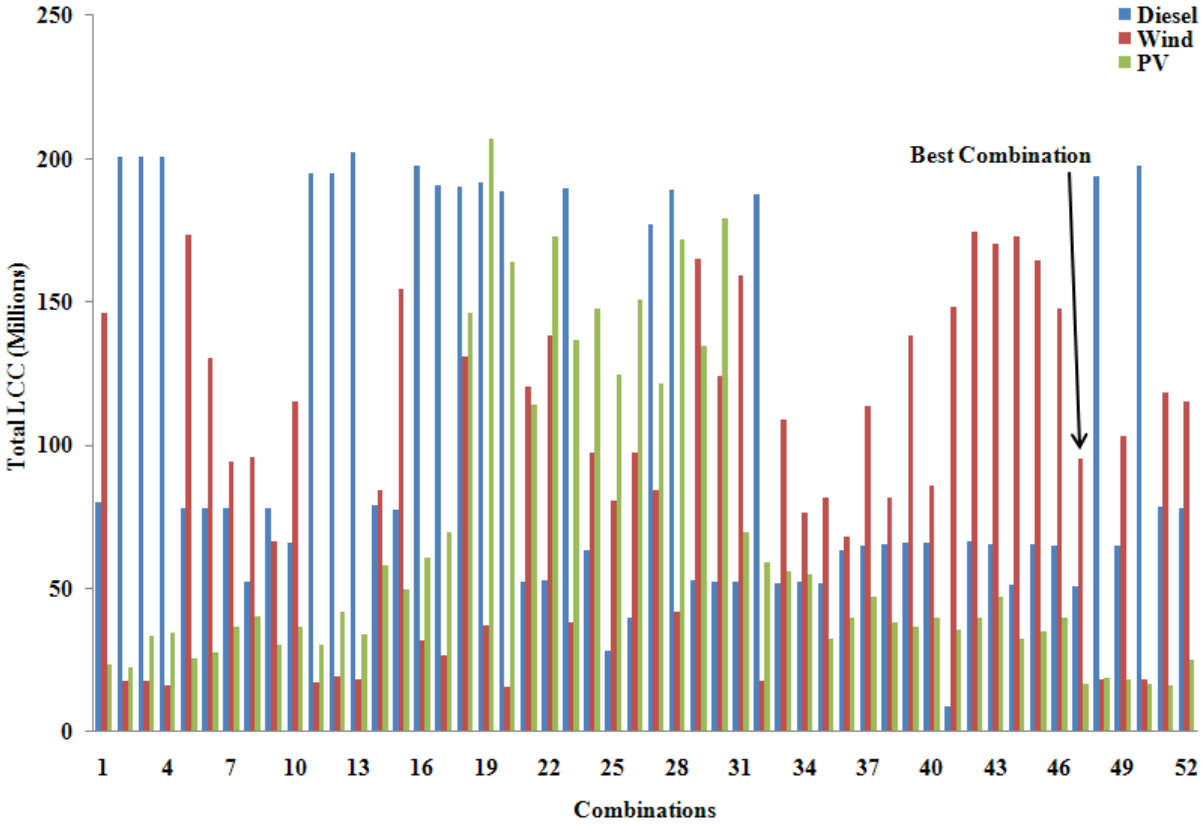

Fig 2.6 LCC for different DG unit combinations in 25 years

5.3 The GHG abatement

The green house gas abatement algorithm proposed in section 3 and (Jayaweera et al., June 2011) was incorporated into the LCC subroutine as an addition to investigate the environmental impacts for different DG unit combinations. Upon successful testing of the software, a series of studies were performed to verify the effectiveness of the three options given in the algorithm under Phase D_2 in section 3.

Fig 2.7 gives the green house gas emission in equivalent of CO_2 weight in tonnes for the 25 year study period. Results show that the DG unit combination corresponding to week 29 has the least GHG emission. Therefore, the operating condition at week 29 is the one that determines the most beneficial DG unit combination and size based on GHG.

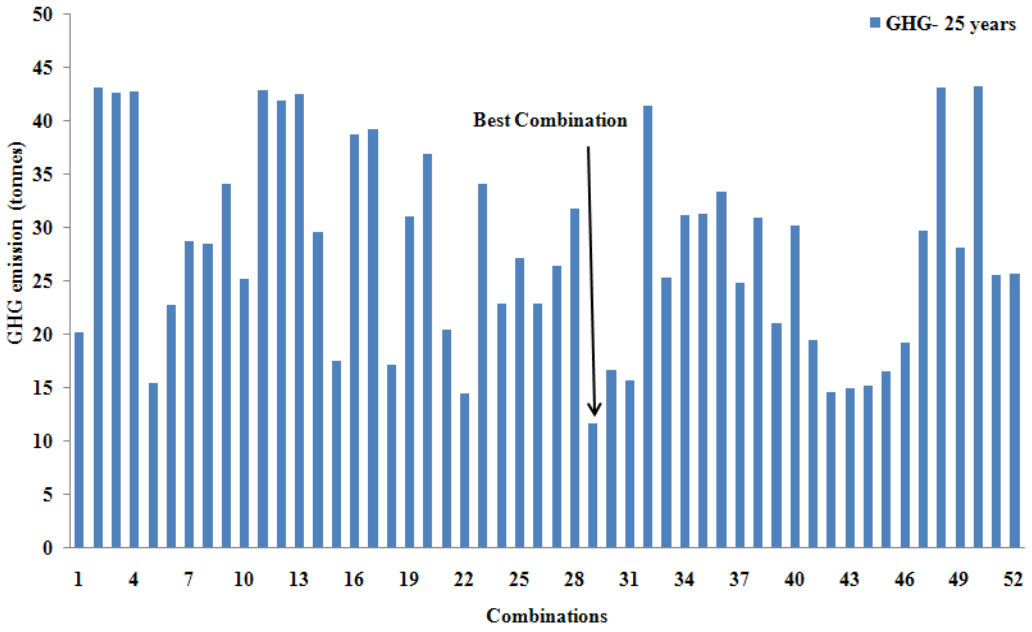

Fig 2.7 GHG emission for 25 year project life

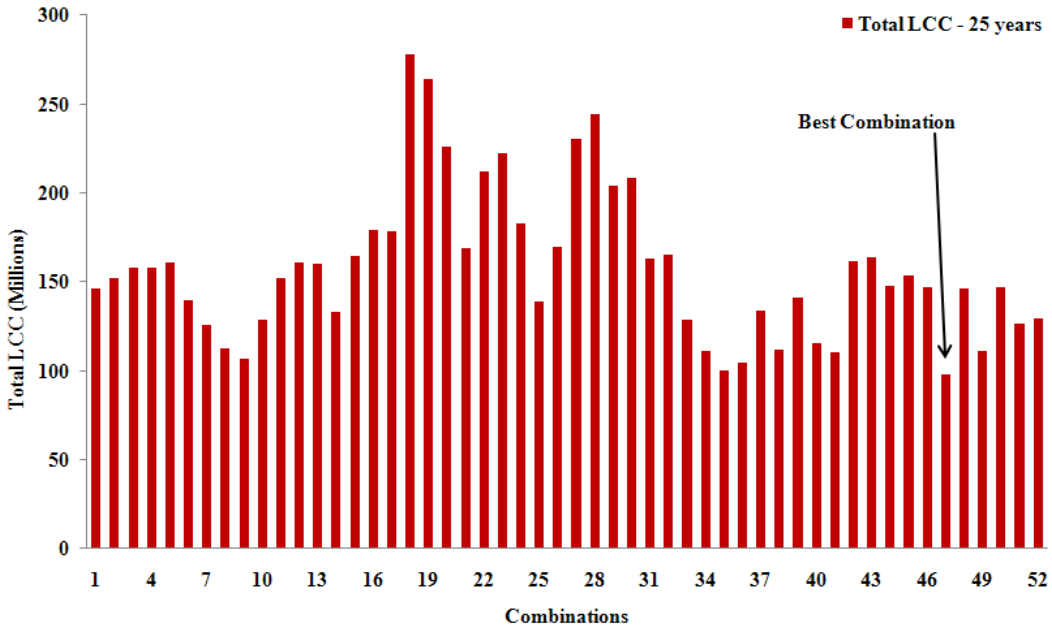

Fig 2.8 Total LCC for 25 year project life

Fig 2.8 shows the ascending order of ranking of various DG unit combinations taking into account GHG emission. The best rank (or the lowest position in the ascending order of ranks) results due to the operating condition at the 29th week. Fig 2.9 shows the ranking based on the LCC values. The results given in Fig 2.7and 2.8 are used to derive the combined priority list to determine the most favourable DG unit combination taking into account both GHG emission and LCC costs.

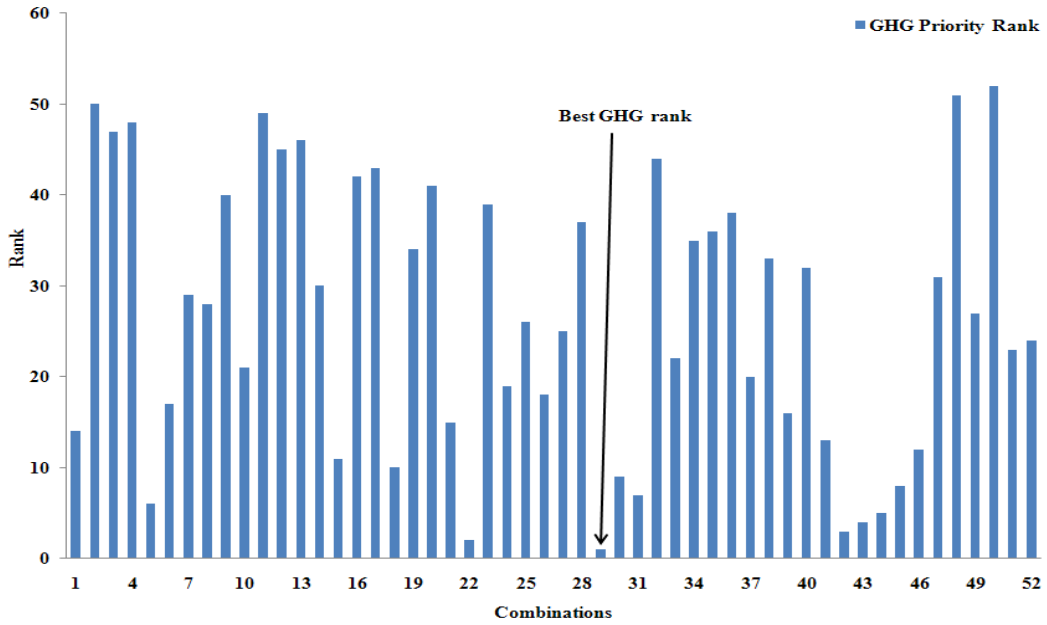

Fig 2.9 GHG based ranking

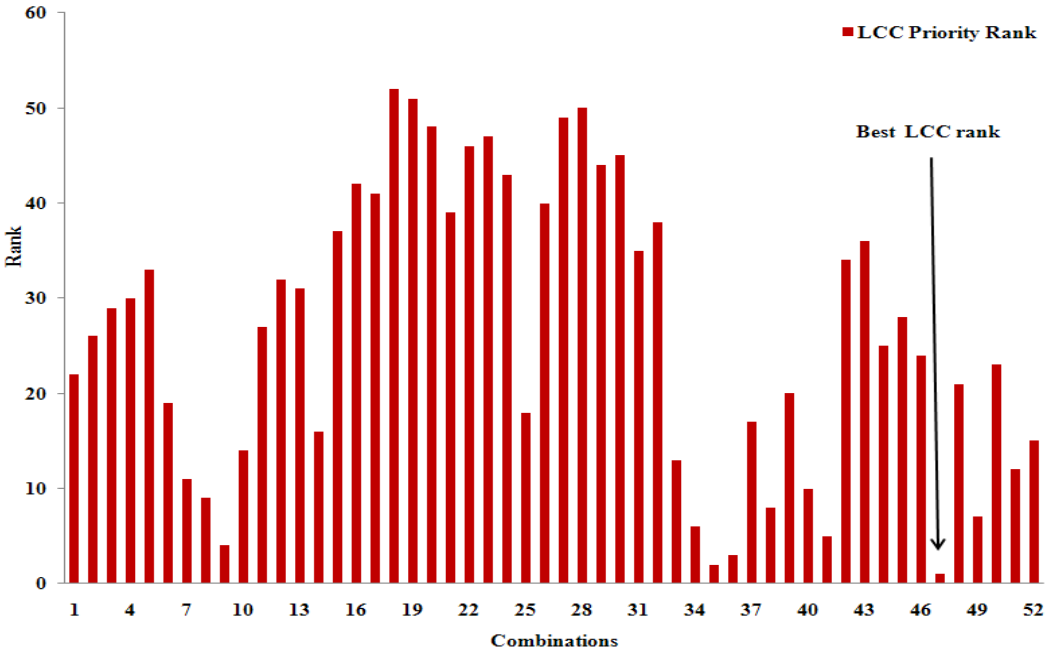

Fig 2.10 LCC based ranking

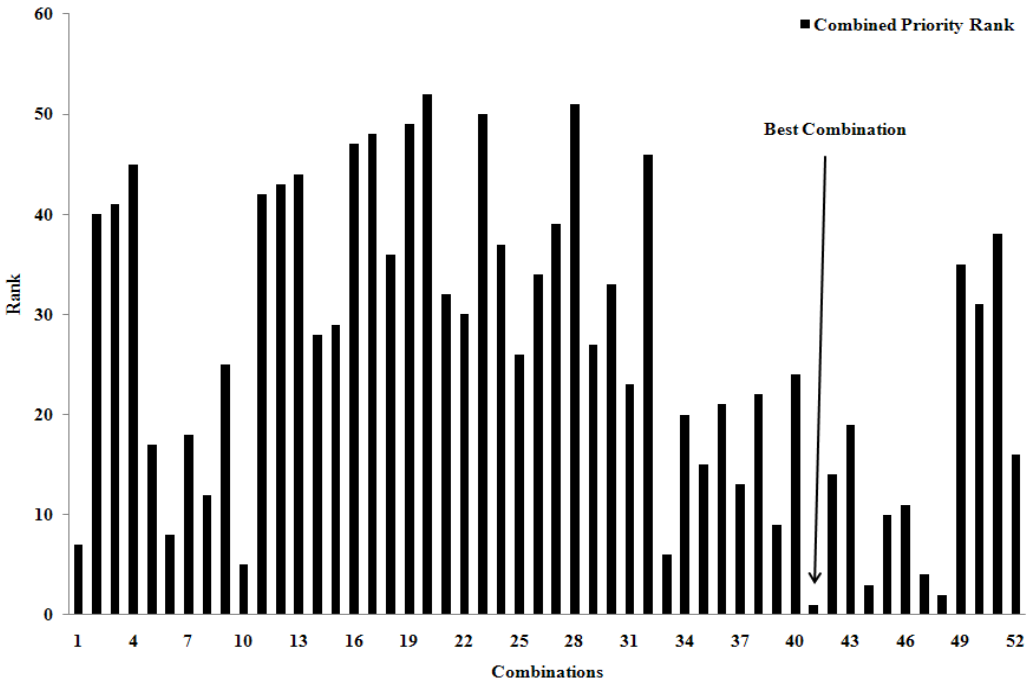

Fig 2.11 Equally weighted ranking based on both GHG and LCC

The ranks based on both GHG and LCC shown in Fig 2.11 is used to determine the best combination. Fig. 2.11 also shows that the optimal DG unit combination corresponds to 41st week; however it is not the best combination if either of the LCC and GHG was decoupled and treated individually. Of the two best combinations, week 47 has a better ranking with LCC consideration than week 29 with GHG priority. Detailed observations also suggest that the DG unit combination results through week 41 operating condition has a lower load share by diesel units and much higher load share by wind penetration. This results a better GHG ranking (lowest in the order) even though the LCC ranking is lower than week 47 resulting DG unit combination.

5.4 The GHG variation with combinations

The pie-chart presented in Fig 2.12 shows the summary of the variation in total LCC associated with the system when combinations of generation technologies were varied to supply the same load demand. The most economical combination was found to be that of a hybrid system with diesel and wind units. This combination offers 12% less cost than diesel, wind, and PV unit combination. The results further suggest that the wind-diesel operation is 22% more economical than that of PV-diesel operation for the test network considered for the assessment.

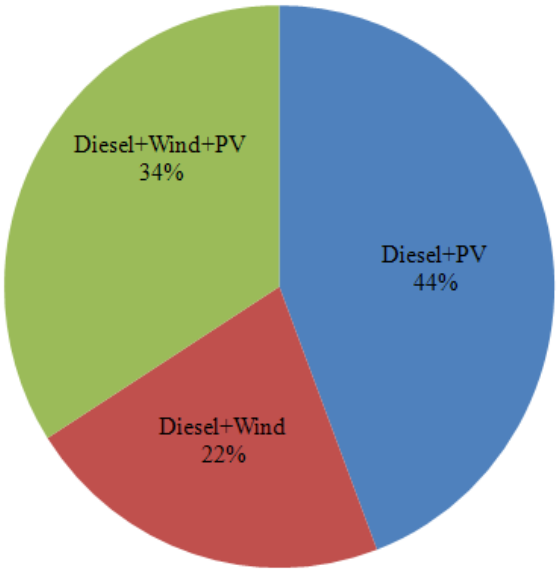

Fig 2.12 LCC Cost–benefit analysis with different DG technologies

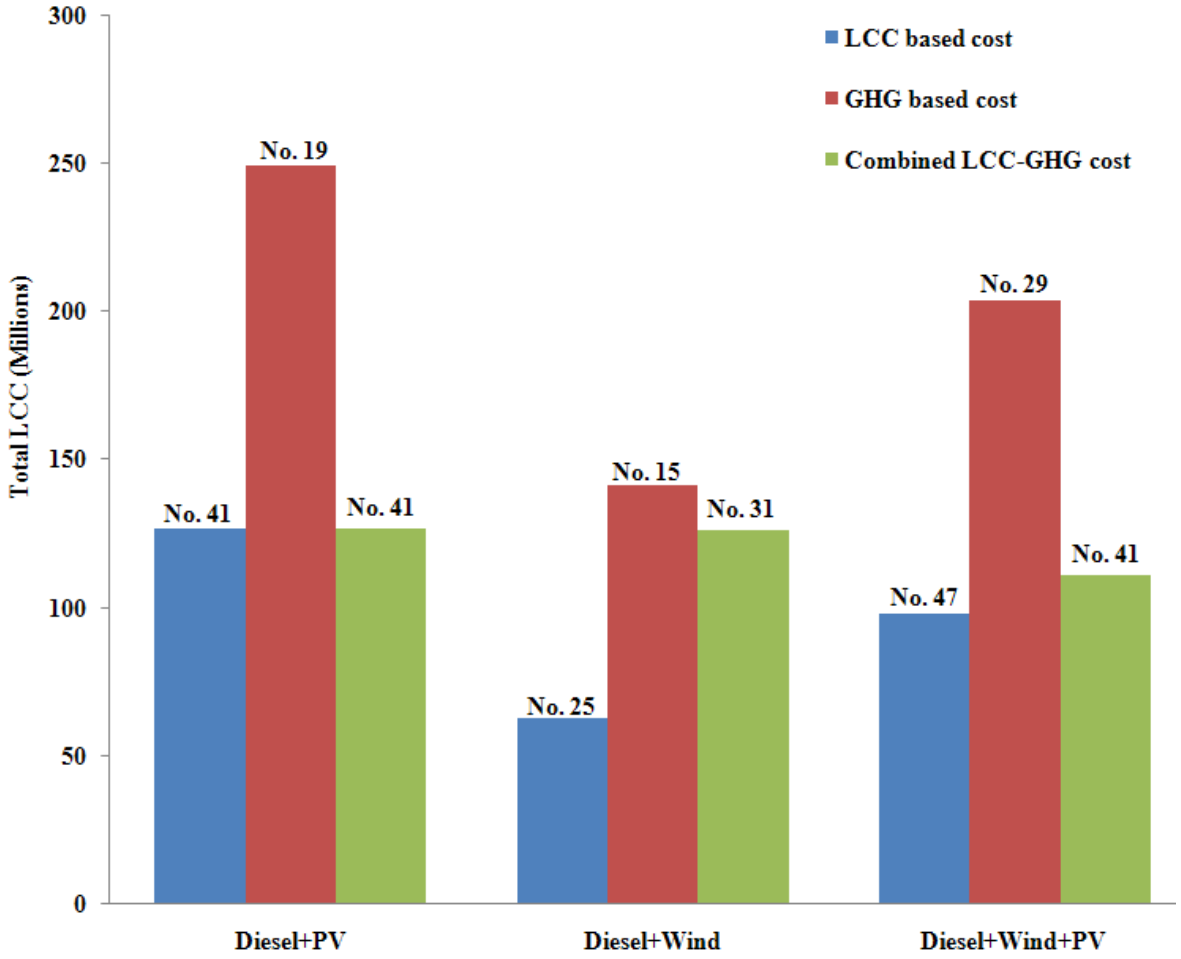

Fig 2.13 LCC and GHG emission variation with generating unit combinations

Fig 2.13 shows the summarised LCC and GHG emission cost variations in the context of diesel/PV, diesel/Wind, and diesel/Wind/PV operations. The bar charts in blue, red and green gives the total LCC corresponding to the optimal DG combination based only on LCC, based only on GHG, and

considering LCC and GHG with equal weighting factors respectively. The results in Fig. 2.13 suggest that the operating condition at the week 41 is the most critical operating condition in terms of determining the distributed generating unit combination that provides most benefits in terms of reducing LCC and GHG emissions for the test network considered for the assessment.

The case studies presented in this report refer to constant cost factors of generating technologies and assets. However, the software program facilitates incorporation of cost of different makes and ages of DG technologies in the formulation. Such facilities in the software enable to incorporate varying cost components of PV, wind and other DG technologies in addition to the futuristic cost elements that may arise through governmental subsidiaries and taxes set by governments for the sustainable energy future.

6. Conclusions

A test network is presented for the assessment of DG technologies and assessment techniques (Jayaweera et al., November 2010). Report presents technical data of the entire network component that are required for steady state analysis, time series characteristics of load, and the time series characteristics of wind and PV generation. The test network is designed in such a way that it is healthy under normal operating conditions. The proposed network is that it can be used to compare different techniques and to generalise techniques. Time series characteristics of wind and PV can be used to quantify average effects of intermittent technology performance and to identify hidden effects that can trigger significant impacts to the network operation. The technical data given in the report is for the steady state analysis. However, the users have the option to include transient and dynamic data of the equipment as necessary for their studies.

An algorithm is proposed for the calculation of the life cycle cost and green house gas abatement through the optimisation subroutines proposed in (Jayaweera et al., March 2011) and (Jayaweera et al., June 2011). The algorithm determines the most economical and environmentally friendly hybrid DG unit combination that can be accommodated to an active distribution network. The algorithm offers the most beneficial distributed generation unit mix and their capacities respective to the geographical location of the system. The software program was developed and scripting the algorithm using IPLAN subroutines to work in conjunction with PSS®E software (Siemens, June 2009). The program facilitates to differentiate the LCC benefits, GHG emission levels, and combined effects. Such options are vital in trading off the business objectives of distributed energy business.

A set of case studies are performed to investigate the specific features of the test system (Jayaweera et al., November 2010). The results conclude that the optimal DG size can be affected by not only

the constraints of the power system but also the greenhouse gas effects if a designer concerns overall benefits. For the particular network considered for the study shows that the best DG system and sizes are achieved through the operating condition of the 47th week if the network constraints and LCC is considered whereas combine effects of greenhouse gas emission effects, aging life of equipment, and network constraints moves the critical operating condition of the week to 29th week. In other words, week 29th operating condition determines the most beneficial DG system and the size for the network if those constraints are considered.

The application of the proposed weighting approach suggest that with equal weightings, the best DG system and the unit sizes results by the operating condition of 41st week. The case studies also show the vulnerability for sizes of DG and the type in balancing the LCC and greenhouse gas emission in an active distribution network. Thus, network planner needs putting extra effort in applying the balanced approach for global system benefits. Such approaches not only improve the network performance, but also reduce adverse impacts on the environment.

The most economical DG system of the network used for the assessment is the Wind and diesel system. This system offers 12% less cost than the system with diesel, wind, and PV units. The results further suggest that the wind-diesel operation is 22% economical than that of PV-diesel operation for the network.

The results conclude that the operating condition at the week 41 is the most critical operating condition in terms of determining generating unit combination that provides most benefits in terms of LCC and GHG emission for the test network.

The proposed algorithm gives not only the size of DG system and geographical location but also the operating condition of the week that determines the optimal condition. Such information is useful in reducing computation time of extended applications that include the security of energy supply to consumers by DG and the reliability improvement with DG unit combinations.

The importance priority ranking of LCC and GHG emission can be used by network regulators and policy makers for setting incentives or penalise those who adversely affects the environment. It also facilitates benchmarking distribution networks for the incentives as appropriate. The results comes out of the program can also be used as a potential platform for the carbon trade and extended applications. On the other hand, distribution network operators can use the proposed methodology to balance the benefits between different types of DG combinations and overall benefits of reducing LCC and GHG emission. Such an approach is necessary in meeting renewable energy targets and balancing the economy verses carbon trade.

References

ALDERFER, B. R., STARRS, T. J. & ELDRIDGE, M. M. (2000) Making Connections: Case Studies of Interconnection Barriers and their Impact on Distributed Power Projects. Golden CO, National Renewable Energy Laboratory.

EMISSION STATEMENT, P. L. (2010) http://www.emissionstatement.com.au/Climate_Change_Glossary_of_Terms.html

GALLEGO, R. A., MONTICELLI, A. & ROMERO, R. (1998) Comparative studies of non-convex optimization methods for transmission network expansion planning. IEEE Trans. Power Syst., 13, (3), 822–828.

GARVER, L. L. (1970) Transmission network estimation using linear programming. IEEE Trans. Power Appar. Syst., 89, (7), 1688– 1697.

INGLIS, S., AULT, G. W., ALARCON-RODRIGUEZ, A. & GALLOWAY, S. J. (2010) Multi-objective network planning tool for networks containing high penetrations of DER. Universities Power Engineering Conference (UPEC), 2010 45th International.

JAYAWEERA, D., SYED, I. & SANDEEP, S. (June 2011) Sizing the Distributed Generation with Life Cycle Costing and Greenhouse Gas Abatement.

JAYAWEERA, D., SYED, I. & SANDEEP, S. (March 2011) A software development and simulation of generation and cost optimised controller.

JAYAWEERA, D., SYED, I. & SANDEEP, S. (November 2010) Test Network for the optimal siting and dispatch assessment of distributed generation.

LAVORATO, M., RIDER, M. J., GARCIA, A. V. & ROMERO, R. (2009) Distribution network planning using a constructive heuristic algorithm. Power & Energy Society General Meeting, 2009. PES '09. IEEE.

MIKHAIL GRANOVSKII, IBRAHIM DINCER & ROSEN, M. A. (May 2006) Economic Aspects Of Greenhouse Gas Emissions Reduction By Utilisation Of Wind And Solar Energies To Produce Electricity And Hydrogen

PAN, F., ZONG, M. & ZHOU, M. (2009) Planning of distributed generation considering marginal capacity cost. Transmission & Distribution Conference & Exposition: Asia and Pacific, 2009.

ROMERO, R., GALLEGO, R. A. & MONTICELLI, A. (1996) Transmission system expansion planning by simulated annealing. IEEE Trans. Power Syst., 11, (1), 364-369.

SIEMENS ENERGY, I. (March 2009) Release 18.2 IPLAN Program Manual PSS®E 32.0.

SIEMENS, P. S. S. (June 2009) PSSE 32.0 Online Documentation.

TAYLOR, A. (June 2003) An Introduction to Life Cycle Costing Involving Structural Stormwater Quality Management Measures

WIKIPEDIA (2000a) http://en.wikipedia.org/wiki/Carbon_emissions_reporting.

WIKIPEDIA (2000b) http://en.wikipedia.org/wiki/Greenhouse_gas

CHAPTER 3. RADIAL BASIS FUNCTION NEURAL NETWORK BASED SHORT-TERM WIND POWER FORECASTING WITH GRUBBS TEST

Accurate prediction in wind power generation plays an important role in power system dispatching and wind farm operation. The Radial Basis Function (RBF) neural network, owing to its superior performance of linear/nonlinear algorithm with respect to fast convergence and accurate prediction, is very suitable for wind power forecasting. Based on the historical data from a wind farm composing of wind speed, environmental temperature, and power generation, the authors develop a short-term wind power prediction model for one-hour-ahead forecasting using a RBF neural network. Due to the existence of incorrect values in the original data, the Grubbs test is conducted to pre-process the samples. In the case study, the forecasting results are compared with the actual wind power outputs. The simulation shows that the presented method can provide accurate and stable forecasting.

1. Introduction

Great global efforts have been engaged in the implementation of renewable energy programs because of global warming and the deficiency of fossil fuel energy. Particularly, the utilization of wind power, one of the main renewable energy resources, has experienced rapid development in recent decades [Lei Ya-zhou, 2003]. Wind power, however, has obvious disadvantages of intermittence and uncertainty which could largely increase the difficulty of system dispatching. The ever-increasing size, number and capacity of wind farms has brought utility industry a challenge to ensure secure and stable operation of power systems. Accurate forecast of wind power generation plays an important role in power system dispatching and wind farm operation.

Although research activities have been widely carried out in the field of power generation in China and abroad, the prediction of wind power output is far from satisfactory and the prediction accuracy should be considerably improved to reach an acceptable level. The proposed prediction methods so far include statistic analysis [Y. Cancino-Solorzano and J. Xiberta-Bernat, 2009; J.A. Roney, 2007; M.C. Alexiadis et al, 1998], Kalman filter [P. Louka et al, 2008], time series analysis [Kamal L and Jafri Y Z, 1997; Z. Huang et al, 1995], Artificial Neural Networks (ANN) [Li Shuhui, 2003; M.Bilgili et al, 2007; T. Senjyu et al, 2006; T.G. Barbounis and J.B. Theocharis, 2006; Bei Chen et al, 2009; AlexiadiS M et al, 1998; T.G. Barbounis and J.B. Theocharis, 2007], Fuzzy Logic [T.G. Barbounis and J.B. Theocharis, 2007; Ioannis G. Damousis, 2004], and spatial correlation [T.G. Barbounis and J.B. Theocharis, 2007; Ioannis G. Damousis, 2004; M. C. Alexiadis et al, 1999].

ANN has the ability to discover and approximate the nonlinear relationship through learning. ANN based prediction of wind speed and wind power has become a popular research focus in recent

years. At present, BP (Back Propagation) neural networks and local feedback neural networks are usually adopted. Based on the gradient descent rule, the BP algorithm is a local optimization algorithm. Many studies have revealed that the Radial Basis Function (RBF) neural network can achieve higher approximating accuracy, avoid being trapped in local minima, and has a faster learning curve. Furthermore, the RBF neural network, while with simple structure, has strong capability of extrapolation and non-linear mapping between input and output.

According to the duration, wind power prediction can be classified as long-term, mid-term, short-term, or ultra short-term forecast. This chapter focuses upon the Short-term forecasting. With the data from a wind farm in Guangdong, China, the wind power is predicted in short-term by the developed RBF neural network and the prediction results are compared against the real measurements.

2. RBF neural network

The RBF Neural Network, due to the advantages addressed in the introduction, is very suitable for non-linear time series prediction, such as in wind power forecasting.

2.1 RBF Neural Network

RBF neural network is a forward network. As shown in Fig 3.1, the structure of RBF neural network is composed of the input, the hidden and the output layer. The function of the input layer is to transmit signals. The parameters of the activation function, which is a Green or a Gauss Function, are regulated by the hidden layer, where the nonlinear optimization strategy is used. Linear weights are adjusted by the output layer, and in general the linear optimization strategy is adopted.

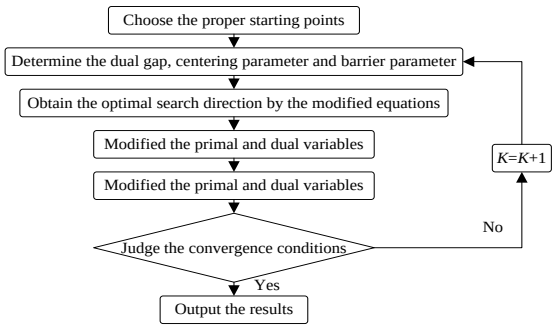

Fig 3.1 RBF Neural Network Structure

2.2 Learning Algorithm of RBF Network

There are three parameters to be solved in the RBF neural network learning algorithm. They are the center of the base function, the mean square deviation, and the weights from the hidden layer to the output layer. The common radial basis function is a Gauss function in the RBF neural network. Thus the activation function can be expressed as

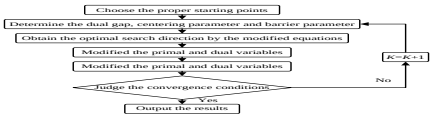

(1)

where  is the Euclidean norm, c and σ are respectively the center and the mean square deviation of the Gauss function.

From the structure of the RBF neural network, the output of the network is given as

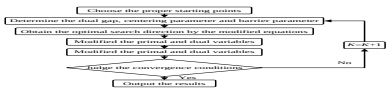 $j=1,2,\ldots,n$ (2)

where 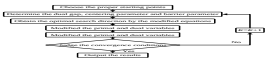 is the *p-th* input sample, p=1,2, …,*P*, with *P* as the total number of samples,  is the center of hidden layer nodes,  is the connection weights from the hidden layer to the output layer, i=1,2, …,*h* is the number of hidden layer nodes, and  is the real output of the *j-th* output node corresponding to the input sample.

Suppose d is the expected output. Then the mean square deviation of base function should be

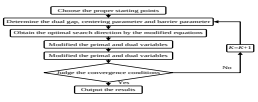

(3)

3. Construction of the RBF model

3.1 Selection of data sample

An asynchronous wind generator with a unit capacity of 600kW from a wind farm in Guangdong is selected in the case study for short term power output prediction. In the case study, only the daily period is considered. The wind speed in a wind farm is a nonlinear function influenced by many factors, with the wind speed being the primary one to determine the wind power generation. Another factor affecting the power output is the air density, which in turn is affected by the temperature. Because the wind engine has its own Yaw system and it can implement yawing automatically, the influence of the wind direction is not considered. Through analyzing the operation of the wind generator in the case study, the power output within the preceding time duration, the environmental temperature, and the wind speed of the succeeding time duration are selected as the input of training samples.

3.2 Sample Data Pre-processing

Some incorrect data are found by comparing and analyzing the original data, which include normal or abnormal outage data of wind turbine, fault data of wind instruments for wind turbine, and so on. These incorrect original data need to be pre-processed to reduce the prediction error.

In the work, the Grubbs Test is adopted to eliminate the exceptional data that are identified by

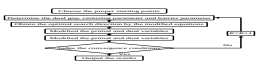

(4)

All satisfying (4) should be eliminated from that group of the test data, where is the critical value of Grubbs test determined by the test number *n* and the given sample significance level α, *s* is the sample variance, is the average value, and is the outlier. Some values are listed in Table I.

Table 3.1 Critical Value $\lambda_{\alpha,n}$ of Grubbs Test

n	**Significance level**	
	0.05	***0.01***
100	3.210	3.600
200	3.432	3.822
300	3.552	3.938
500	3.695	4.075
800	3.820	4.193
1000	3.877	4.247

Fig 3.2 shows the sample data after the pre-processing. After eliminating the exceptional values, the copied data is more stable than the original one.

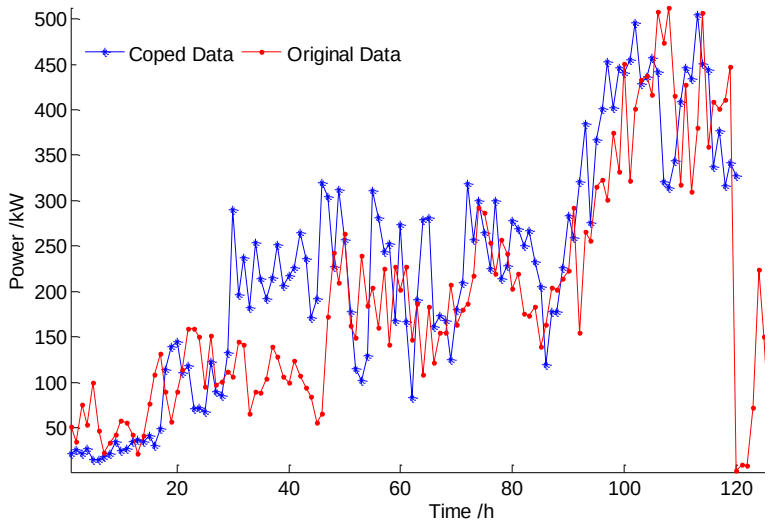

Fig 3.2 Sample data after pre-processing

3.3 Normalization of the samples

For most practical problems, there are many input parameters with the dimension and the order of magnitude of each input varying in a wide range. Furthermore, the systems involved are usually nonlinear. When the learning is conducted in a region far from zero, the learning speed could be very slow or even not converged. Therefore, normalization of the samples is necessary, such as that done in our project of wind power forecasting, where the input data are mapped to [-1,1]. After training, the outputs are inversely renormalized into the original data range.

3.4 RBF Network Model

Suppose that a time series is given as 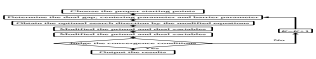 . If the succeeding M values are predicted with the preceding N values of the series, the former N values of every sample are the inputs of the RBF neural network, while the M values are the target outputs. Through learning, the input space  is mapped to output space  .

Training network works as follows.

Sample Input  Target Output 

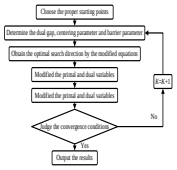

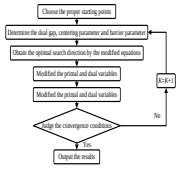

Predicting results are below.

Input Space 

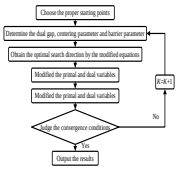

Output Space 

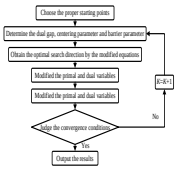

4. Prediction results and analysis

To demonstrate the performance of the developed predicted model, the sample data in 2009 is selected from the wind farm in Guangdong. The power output one-hour ahead is predicted using the developed model. The average data in each 12 minutes in an hour is recorded so that 5 data sets are obtained in each hour. During the modelling procedure, the data in the past 24 hours are selected as the training samples for carrying out the prediction with the predicted curve shown in Fig 3.3.

The effectiveness of the predicted model is verified quantitatively by the relative percentage error (RPE) and the mean absolute percentage error (MAPE) given by the following equations:

$$RPE= \quad (5)$$

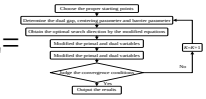

$$MAPE= \quad (6)$$

where  is the predicted power value,  is the observed power value, and N is the number of predicted data.

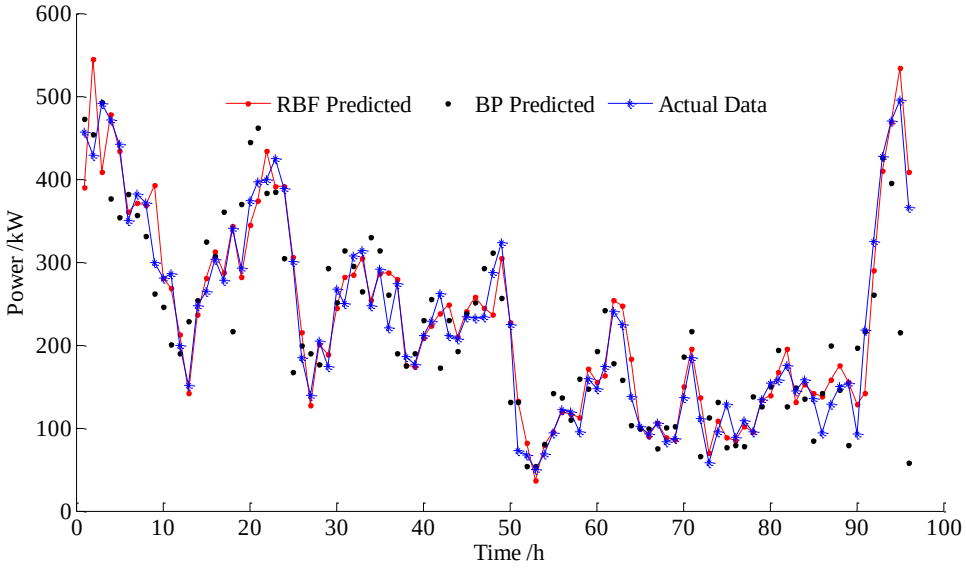

Fig 3.3 The result of wind power forecasting after 1h

The RPE diagram is shown in Fig 3.4, which is the contiguous one-hour wind power prediction in 96 hours. It is seen from the diagram that the number of one-hour prediction with error less than 20% is 82, i.e., 85% of the total prediction. The study on the prediction results shows that the other 15% prediction with large errors (>20%) is mainly caused by the fault data. The MAPEs of next hour wind power prediction in contiguous 24 hours, 48 hours, 72hours, and 96 hours are calculated separately (Table 3.2). In general, the prediction error is below 10%.

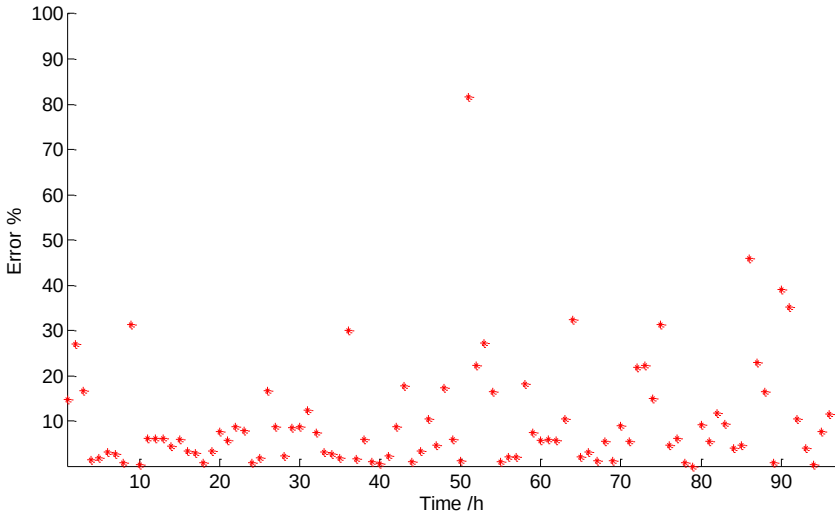

Fig 3.4 The RPE of wind power forecast after 1h using RBF Neural Network

The prediction results using the RBF neural network and the back-propagation (BP) neural network are compared in Table 2. The RBF neural network achieved significantly more accurate results, with the MAPE 7.12% for 24 hours, 7.30% for 48 hours, 8.97% for 72 hours, and 10.06% for 96 hours, all much lower than that of the BP network. Compared with some other existing methods, the

RBF neural network prediction also has better performance [YANG Xiu-yuan et al, 2005]. Another observation is that the prediction error increases along with the increase of the prediction hours.

Table 3.2 Comparison of MAPE among different forecast hours between RBF and BP Neural Network Predictions

Predicting hours	RBF	BP
24	7.12	12.97
48	7.30	16.73
72	8.97	20.83
96	10.06	23.84

5. Conclusions

A RBF neural network based prediction model is developed based on the wind speed, temperature, and historical wind generator outputs. Prediction is conducted using the real 2009 annual data from a wind farm in Guangdong, China. The prediction achieved high accuracy with the prediction error below 10% most of the time. The simulation shows that the exceptional data must be eliminated in wind power forecasting in order to achieve higher precision of prediction.

References

ALDERFER, B. R., STARRS, T. J. & ELDRIDGE, M. M. (2000) Making Connections: Case Studies of Interconnection Barriers and their Impact on Distributed Power Projects. Golden CO, National Renewable Energy Laboratory.

Lei Ya-zhou (2003). "Studies on wind farm integration into power systems." *Automation of Electric Power Systems*, 27, 84-89.

Y. Cancino-Solorzano and J. Xiberta-Bernat (2009). "Statistical analysis of wind power in the region of Veracruz (Mexico)." *Renewable Energy* , 34, 1628- 1634.

J.A. Roney (2007). "Statistical wind analysis for near-space applications." *Atmospheric and Solar-Terrestrial Physics*, 69, 1485-1501.

M.C. Alexiadis, P.S. Dokopoulos, H.S. Sahsamanoglou, I. M. Manousaridis (1998). "Short term forecasting of wind speed and related electrical power ." *Solar Energy*, 63, 61-68.

P. Louka, G. Galanis, N. Siebert, G. Kariniotakis, P. Katsafados, I. Pytharoulis, G. Kallos (2008). "Improvements in wind speed forecasts for wind power prediction purpose using Kalman filtering." *Journal of Wind Engineering and Industrial Aerodynamics*, 96, 2348-2362.

Kamal L and Jafri Y Z (1997). “Time series models to simulate and forecast hourly averaged wind speed in Quetta，Pakistan.” *Solar Energy*, 61, 23-32.

Z. Huang, Z.S. Chalabi, “Use of time-series analysis to model and forecast wind speed,” *Journal of Wind Engineering and Industrial Aerodynamics*, vol.56, pp. 311-322, May 1995.

Li Shuhui (2003). “Wind power prediction using recurrent multilayer perceptron neural networks.” *Proceedings of IEEE Power Engineering Society General Meeting*, 2325-2330.

M.Bilgili, B.Sahin, A.Yasar (2007). “Application of artificial neural networks for the wind speed prediction of target station using reference stations data.” *Renewable Energy*, 32, 2350-2360.

T. Senjyu, A. Yona, N. Urasaki, T. Funabashi (2006). “Application of Recurrent Neural Network to long-Term-Ahead Generating Power Forecasting for Wind Power Generator.” *IEEE Power Systems Conference and Exposition*, 1260-1265.

T.G. Barbounis and J.B. Theocharis (2006). “Locally recurrent neural networks for long-term wind speed and power prediction.” *Neuro computing*, 69, 466-496.

Bei Chen, Liang Zhao, Jian Hong Lu (2009). “Wind Power Forecast Using RBF Network and Culture Algorithm.” *International Conference on Sustainable Power Generation and Supply*, 1-6

AlexiadiS M, Dokopoulos P, Sahsamanoglou H (1998). “Short term forecasting of wind speed and related electrical power.” *Solar Energy*, 63, 61-68.

T.G. Barbounis and J.B. Theocharis (2007). “A locally recurrent fuzzy neural network with application to the wind speed prediction using spatial correlation.” *Neuro computing*, 70, 1525-1542.

Ioannis G. Damousis, Mihas C. Alexiadis, John B . Theocharis (2004).“A Fuzzy Model for Wind Speed Prediction and Power Generation in Wind Parks Using Spatial Correlation.” *IEEE Trans on Energy Conversion*, 19(2): 352-361.

M. C. Alexiadis, P. S. Dokopoulos, H. S. Sahsamanoglou (1999). “Wind-Speed and Power Forecasting based on Spatial Correlation Models.” *IEEE Trans on Energy Conversion*, 14, 836- 842.

Yang Xiu-yuan, Xiao Yang, Chen Shu-yong (2005). “Wind Speed and Generated Power Forecasting in Wind Farm.” *Proceedings of the CSEE*, 25(11): 1-5.

CHAPTER 4. OPTIMAL SITING AND SIZING OF DISTRIBUTED GENERATORS BASED ON A MODIFIED PRIMAL-DUAL INTERIOR POINT ALGORITHM

With the enhanced awareness of energy-saving, emission-reduction and environmental protection, distributed generators (DGs) have been increasingly employed in modern power systems, especially in distribution systems. DG can not only reduce energy losses, delay the expansion of transmission systems and hence the investment, but also enhance the security and stability of the power system concerned, improve voltage quality, increase energy utilization and reduce pollution emission.

However, these advantages can be fully explored if the siting and sizing of DGs are properly optimized. Inappropriate siting and sizing of DGs could even lead to the increase in network losses and the drop of voltage quality at some buses. Given this background, a sensitivity based approach is presented to identify the optimal siting of DGs. On the other hand, the optimal sizing of DGs is determined by the Modified Primal-Dual Interior Point Algorithm (MPDIPA) with an objective of maintaining the voltage profile at the optimal level. IEEE 123-node test feeder is employed to verify the effectiveness of the proposed method. The results demonstrate that the proposed approach is able to search for the optimal solutions quickly. At the same time, the voltage profiles are obviously improved and the network loss is decreased dramatically.

1. Introduction

At present, an increasing number of researchers in the power system area have realized that the traditional models of the power system—the centralized generation, long-distance power transmission and interconnection among large-area power networks could result in many increasingly prominent drawbacks. This is especially true when an accident occurs in some part of the power system; it will lead to a large area outage and a negative impact on the normal daily life of people, and even the safety and stability of social orders. If the power system which is interconnected with each other collapses, it will cause much more inestimable losses and consequences. The traditional model of power systems cannot meet the requirements in modern times. With the rise in promotion towards the utilization and exploitation of renewable energy sources, DG has been extensively applied in power systems due to its advantages, namely flexible operation, security and reliability, as well as environmental protection.

DG is usually a kind of small, modular, efficient and reliable generation units located near the customers [Wang Chengshan et al, 2006]. Its generation power ranges from a few kilowatts to several megawatts (generally below 10 megawatts). It mainly includes combustion engine with the

fuel of liquid or gas, micro turbine, solar power (photovoltaic power and photothermal power), wind power, biomass power and fuel cell etc. Combined with the traditional model, DG is playing an increasingly important and positive role in decreasing network losses, reducing electricity price, maintaining environmental and economical benefits, reducing the investment in generation capacity and delaying the upgrade of the transmission system. However, if the siting and sizing of DGs are not properly determined, these advantages cannot be fully explored.

Given this background, in recent years many researchers have done much work on this subject. In [N. Acharya et al, 2006], an efficient and analytical approach is developed for DG allocation in primary distribution networks with the objective of minimizing network losses. However, this approach may sometimes fail to find the global optimal solution. In [M. Gandomkar et al, 2005], an algorithm combining the Genetic and Tabu Search approaches is presented for DG allocation in radial distribution networks. The calculation results of a simple and small system indicate that this algorithm is better than genetic algorithm based approach. In [D. Singh, and K.S. Verma, 2005], a genetic algorithm based approach is employed for the siting and sizing of DG from the perspective of a generation company. With the objective of minimizing the energy cost or generation cost respectively, this approach optimizes time-varying voltages and loads.

In this chapter, a simple and practical approach for determining the suitable siting of DGs is developed based on the loss sensitivity on every bus voltage. It can effectively reduce the solution space to a few buses. Secondly, after determining the optimal siting, the MPDIPA is employed to determine the sizing of DGs with the objective of optimizing the voltage profile at every bus. The modified equations of the Primal-Dual Interior Point Algorithm are next simplified for speeding up the calculation procedure.

2. The optimal siting of DGs

The siting of DGs has an impact on the security and reliability, as well as the economic operation of the power system concerned. The solution space of the problem of optimizing the DG siting will dramatically expand as the bus number increases [Wang Zhiqun et al, 2005]. In order to maximize the benefits from DG, the optimal siting should be determined first. In this section, a practical method called the loss sensitivity on every bus voltage is developed.

2.1 The Loss Sensitivity on Every Bus Voltage

The polar form of real power flow equations in the Newton-Laphson method (N-R) can be formulated as

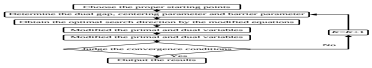

(1)

Where: and are the voltage amplitudes at bus and respectively; is the net injected power at bus ; and are respectively the conductance and susceptance between bus and bus ; is the voltage angle between bus and bus .

The total loss of the distribution network studied can be expressed as

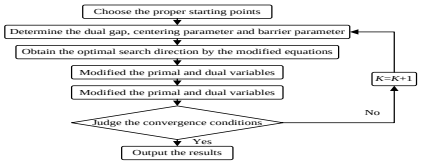

(2)

Where: is the real power output of the DG at bus; is the real power of the load at bus.

Therefore, the loss sensitivity on every bus voltage can be obtained as

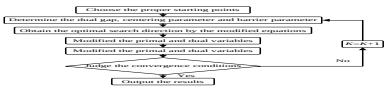

(3)

2.2 The Steps of Implementation

Using the results from the power flow calculation, the loss sensitivity on every bus voltage can first be evaluated. According to the values, the buses are ranked in ascending order. If the loss sensitivity on some bus voltage is the smallest one (less than zero) and the voltage at this bus is lower than the reference voltage, then increasing the voltage of this bus will lead to the decrease of the network loss to the greatest extent. Finally, this bus can be determined as the optimal siting of DGs.

3. The optimal sizing of DGs

After the optimal siting of DGs is carried out, the MPDIPA is employed to determine the optimal sizing of DGs concerned. Due to some simplifications are made to the modified equations, the calculation procedure of this approach is sped up.

3.1 The Objective Function

The objective function for the optimal sizing of DGs is to optimize the voltage profile at every bus in the distribution network. The mathematical model can be formulated as follows:

(4)

Where: is the number of nodes in the distribution network; is the reference voltage.

Some work has been done to employ the multi-objective optimization technique to solve the optimal sizing problem of DGs [G. Celli et al, 2005]. The advantages of this kind of methods are that several objectives can be optimized and realized at the same time. However, it is difficult to balance weightings among these objective functions. Here, a method combining the loss sensitivity on every bus voltage and the single objective function is employed in this chapter.

3.2 The Equality Constraints

The equality constraints corresponding to both active and reactive power balance equations are formulated as follows:

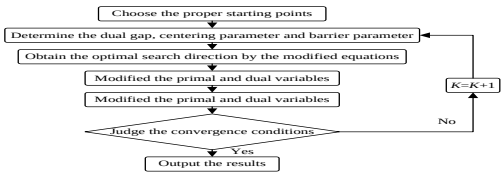

(5)

Where: and are the active and reactive power output of the DG at bus respectively; and are the active and reactive power of the load at bus respectively.

3.3 The Inequality Constraints

The inequality constraints considered here mainly include the upper limits of active and reactive power outputs of the DGs, the upper and lower limits of the voltage amplitude at every bus and the maximum permitted power flow in any feeder in the distribution network for respecting the thermal capacity limit:

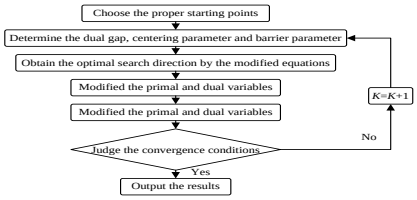

(6)

Where: is the number of DGs.

4. The MPDIPA for optimizing the sizing of DGs

The principles of the MPDIPA can be mathematically formulated as

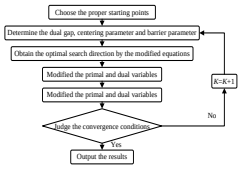

(7)

Where: is the objective function; is the set of the equality constraints; is the set of the inequality constraints; is the vector of the state variables.

4.1 The Lagrange Function

The MPDIPA employed here first transforms all inequality constraints in (7) into equalities by adding non-negative variables. Then, the non-negative conditions of slack variables are handled by incorporating them into logarithmic barrier terms; finally, a Lagrange function is built as follows by incorporating equalities into the objective function of (7):

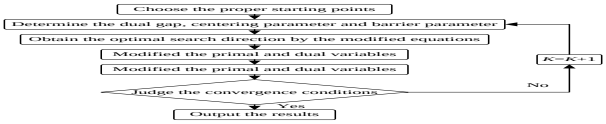

(8)

Where: ; and are the slack variables; are the Lagrange multipliers; is the barrier factor.

4.2 The Simplification of the Modified Equations

First, the Lagrange function (8) must satisfy the Karush-Kuhn-Tucker (KKT) optimality conditions [Yu-chi Wu et al, 1994]. Therefore, the optimal search direction is solved by the Newton's method and the following matrix can then be obtained:

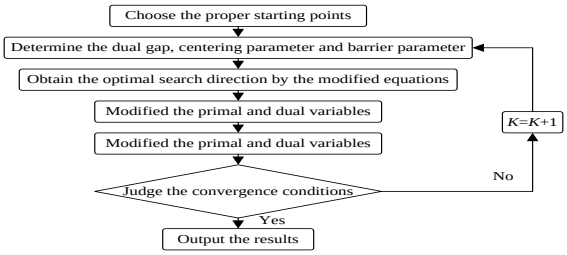

(9)

Where: .

From the above descriptions, it is obvious that the calculation amount of this method mainly lies in the modified (9). If (9) is calculated directly, much calculation time and computer memory will be wasted. To solve this problem, a method for the improvement of the modified equations is proposed here. The details of its realization are as follows:

First, (9) can be written as follows:

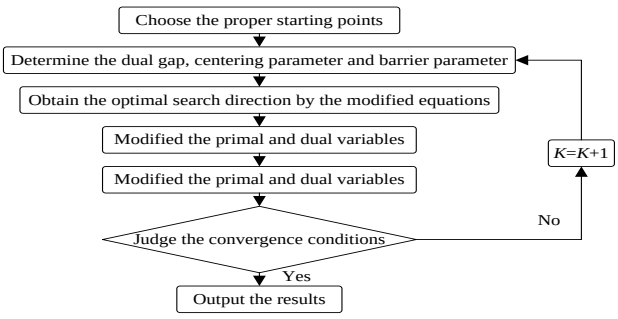

(10)

Simplifying the third and fourth items of (10):

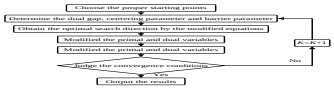

(11)

Substituting the first and second items of (11) into the first and second items in (10) yields

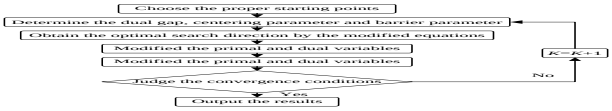

(12)

Substituting the second item of (12) into the fifth item of (11) yields

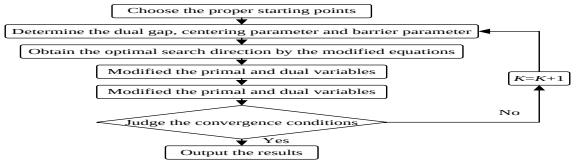

(13)

Combining the first item of (13) with the sixth item of (10), the simplified matrix of the modified equations could be obtained as follows:

(14)

Where: and can be calculated by (14). Then, , , and can be calculated by (11) and (12). Therefore, the calculation time can be reduced.

4.3 The Dual Gap, Centering Parameter and Barrier Parameter

The relational expression between the barrier parameter and the complementarity gap is as follows [F. Capitanescu et al, 2007]:

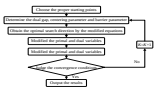

(15)

Where: 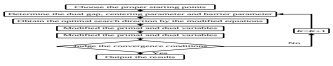 is the dual gap; 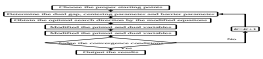 is the centering parameter and is the number of inequality constraints.

4.4 The Iteration Step

In the iteration procedure, the step length should be modified so as to guarantee the primal feasibility and dual feasibility of solutions. Meanwhile, to enhance the convergence speed, different kinds of variables employ different step lengths in this chapter. The step lengths are mathematically expressed as follows:

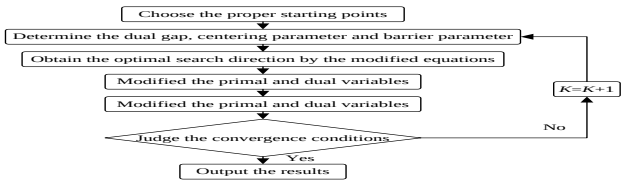

(16)

Where: is the step length of primal variables; is the step length of dual variables; is the safety factor.

The primal and dual variables can be modified according to the step length and optimal search direction. Then, the starting points of the next iteration are determined by:

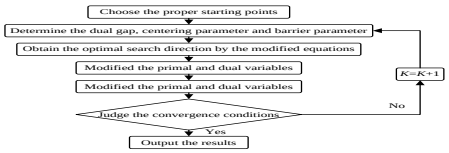

(17)

4.5 The Convergence Conditions

The convergence conditions of the MPDIPA must include the complementarity, primal feasibility, dual feasibility and optimality [Xihui Yan and V.H. Quintana, 1996]. Therefore, it can be expressed as follows in the form of inequality constraints:

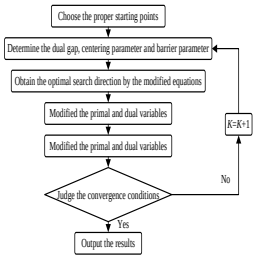

(18)

Where: , and are constants.

4.6 The Computational Procedure

Step 1: Set the iteration counter and specify the starting points.

Step 2: According to (15), determine the barrier parameter , dual gap and centering parameter .

Step 3: According to (14), (11) and (12), calculate the search directions of every variable.

Step 4: According to (16), determine the step length of primal variables and dual variables.

Step 5: According to (17), update the primal variables and dual variables.

Step 6: According to (18), judge whether the convergence condition is met. If yes, stop the calculation and output the results; otherwise, set the iteration counter , and then return to step 2.

The computational procedure is shown in Fig 4.1:

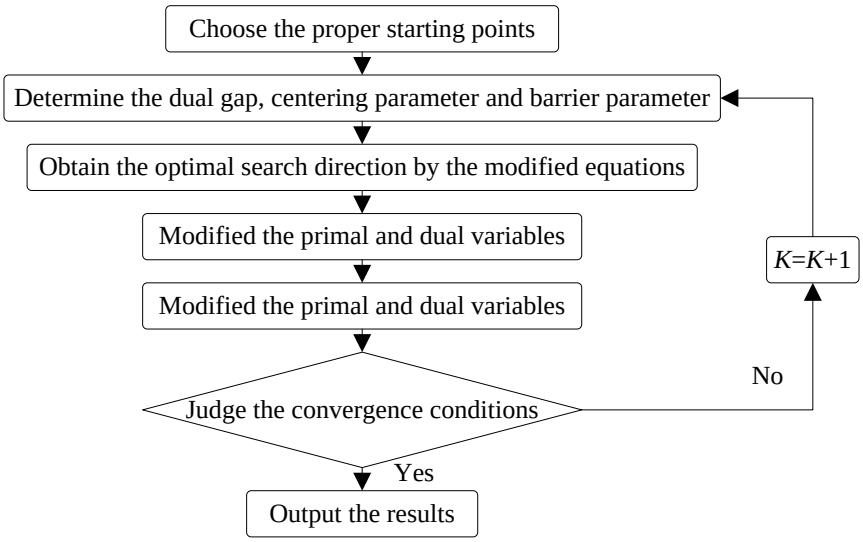

Fig 4.1 The computational procedure of the MPDIPA

5. Case studies

The IEEE 123-node test feeder [IEEE Distribution System Analysis Subcommittee, 2004], as shown in Fig 4.2, is used for testing the proposed method. In this test case, the states of three phase switches are shown in Table I. Suppose that the power of the load is constant, and the reference voltage is 1.00. In the environment of Visual C++ 6.0, a program is developed.

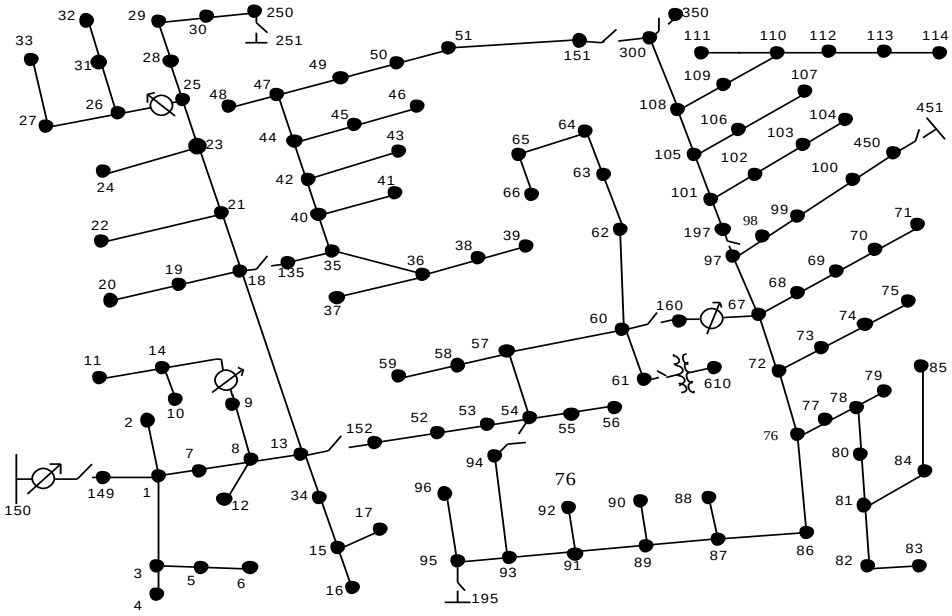

Fig 4.2 The diagram of the IEEE 123-node test feeder

Table 4.1 The states of three phase switches

Node A	Node B	Normal
13	152	closed
18	135	closed
60	160	closed
61	610	closed
97	197	closed
150	149	closed
250	251	open
450	451	open
54	94	open
151	300	open

First, the values of the loss sensitivity on every bus voltage are shown in Fig 4.3. It is obvious that the voltages at nodes 60, 37, 57 and 42 have great impacts on the network losses, and the values associated are listed in Table II. Therefore, if these four node voltages rise, the network losses will decrease dramatically. Therefore, the buses of 60, 37, 57 and 42 are the optimal sitings of DGs.

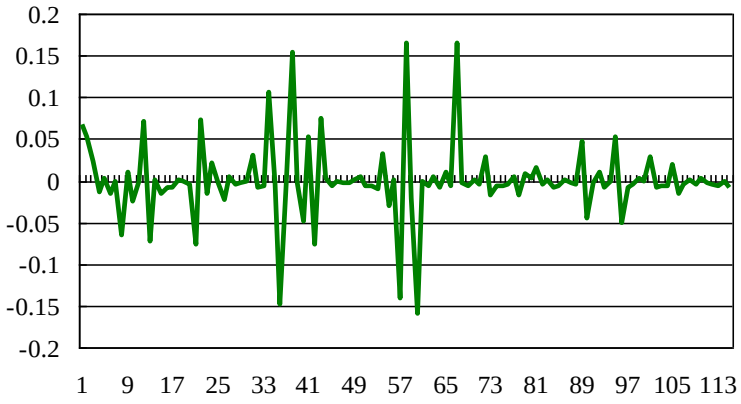

Fig 4.3 The loss sensitivity on the bus voltage in the IEEE 123-node test feeder

Table 4.2 The loss sensitivity on the bus voltage of the four buses in the IEEE 123-node test feeder

Bus	Bus voltage	The loss sensitivity on bus voltage
60	0.988	-0.160281
36	0.9951	-0.149043
57	0.9945	-0.141629
42	0.9929	-0.0773531

After the optimal siting of DGs is carried out, the MPDIPA is used to determine the sizing of DGs. The optimal siting and sizing of DGs are shown in Table III. From Fig 4.4, Fig 4.5 and Fig 4.6, it can be observed that the voltage profile at every bus has been greatly improved and the network loss also has been decreased dramatically. Moreover, every bus voltage concentrates on the reference voltage after the optimization.

Table 4.3 The siting and sizing of DGs after the optimization

The siting of DGs	The reactive power of DGs/KW	The real power of DGs/KVar	The network loss without DGs/KW	The network loss with DGs/KW	Iteration (times)
60	65.37	43.21	50.54	20.13	0.93
36	34.75	15.83			
57	12.17	8.52			
42	31.43	22.92			

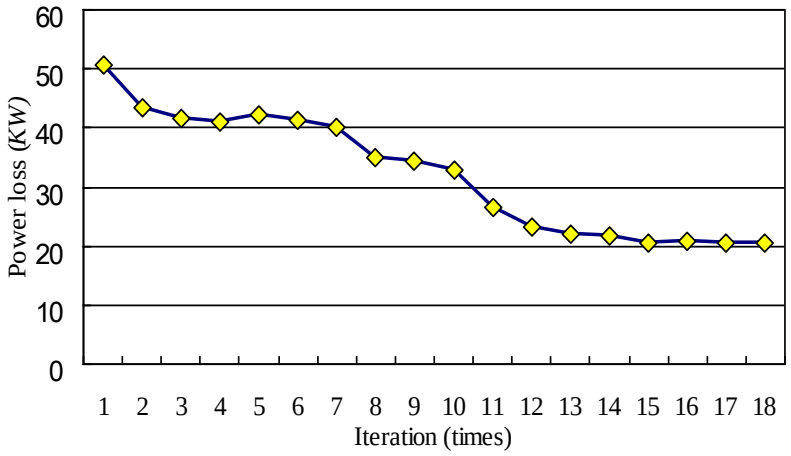

Fig 4.4 The variations of the network loss in the iteration process

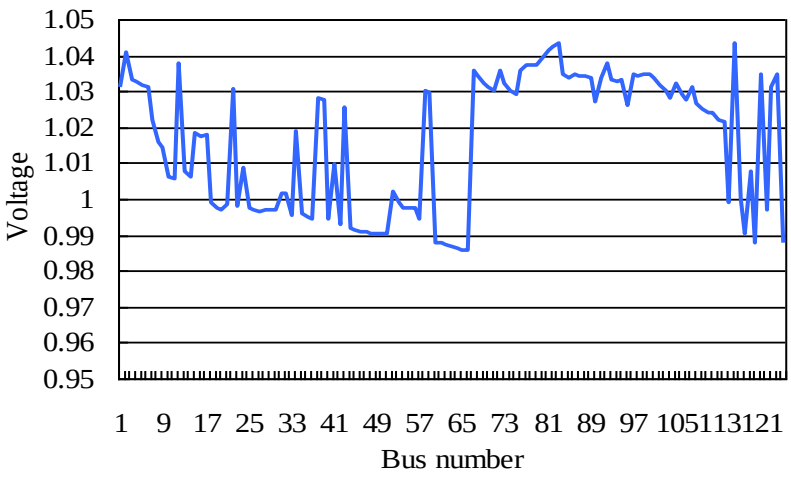

Fig 4.5 The voltage at every bus in the IEEE 123-node test feeder without DGs

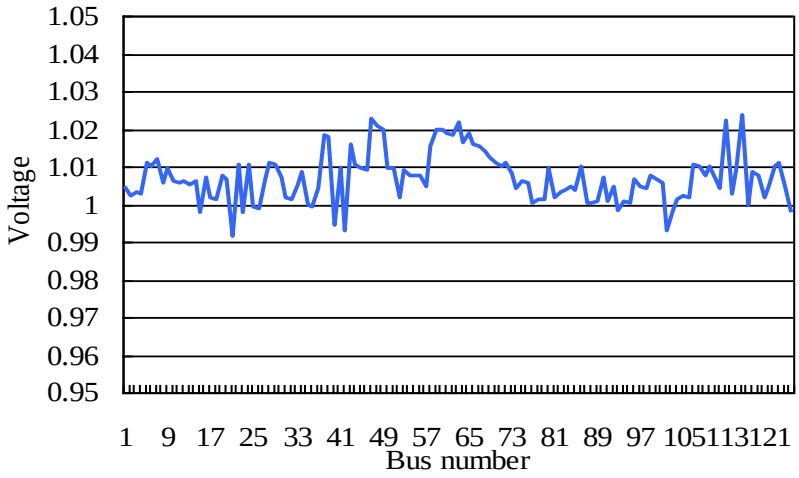

Fig 4.6 The voltage at every bus in the IEEE 123-node test feeder with DGs

It is an important sign of the MPDIM convergence that the dual gap tends to zero [G.L. Torres and V.H. Quintana, 1998]. The graph as shown in Fig 4.6 indicates that the dual gap tends to zero during the iteration process. This illustrates that the proposed algorithm has reliable convergence characteristics.

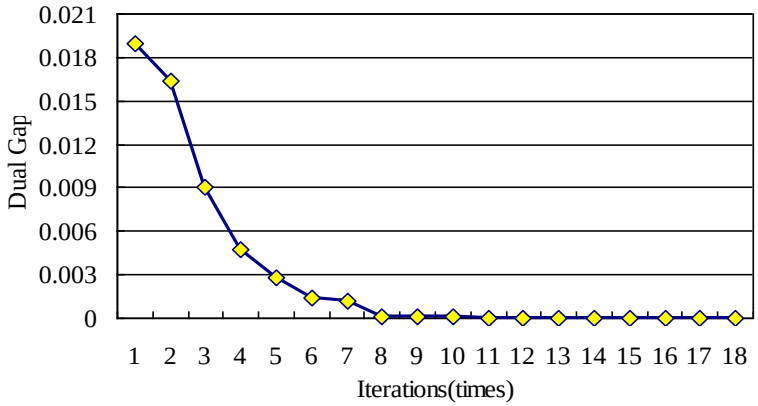

Fig 4.7 The dual gap in each iteration

6. Conclusions

In this chapter, a new approach combining the loss sensitivity on every bus voltage with the MPDIPA is presented for optimizing the siting and sizing of DGs. The former is used for the optimal siting of DGs so as to reduce the calculation time and optimization scale. The latter is used for the optimal sizing of DGs. Test results of the IEEE 123-node test feeder demonstrate that the developed method can determine the siting and sizing of DGs optimally, and as a result, the voltage profile can be significantly improved and the network loss obviously reduced.

References

Wang Chengshan, Chen Kai, Xie Yinghua, and Zheng Haifeng (2006). "Siting and sizing of distributed generation in distribution network expansion planning." *Automation of Electric Power Systems*, 30(3), 38-43.

N. Acharya, P. Mahat, and N. Mithulananthan (2006). "An analytical approach for DG allocation in primary distribution network." *Electric Power and Energy Systems*, 28(10), 669-678.

M. Gandomkar, M. Vakilian, and M. Ehsan (2005). "A genetic-based Tabu search algorithm for optimal distributed generation allocation in distribution networks." *Electrical Power and Components System*, 33(11), 1351-1362.

D. Singh, and K.S. Verma (2005). "GA based optimal sizing and placement of distributed generation for loss minimization." *International Journal of Intelligent Technology*, 2(4), 263-269.

Wang Zhiqun, Zhu Shouzhen, Zhou Shuangxi, Huang Renle, and Wang Lianguan (2005). "Study on location and penetration of distributed generations." in *Proceedings of the Chinese Society of Universities for Electric Power System and its Automation*, 17,(1) , 53-58.

G. Celli, E. Ghiani, S. Mocci, and F. Pilo (2005). "A multi-objective evolutionary algorithm for the sizing and siting for distributed generation." *IEEE Trans. on Power Systems*, 20(2), 750-757.

Yu-chi Wu, A.S. Debs, and R.E. Marsten (1994). "A direct nonlinear predictor-corrector primal-dual interior point algorithm for optimal power flows." *IEEE Trans. on Power Systems*, 2(9), 876-883.

F. Capitanescu, M. Glavic, D. Ernst, and L. Wehenkel (2007). "Interior-point based algorithms for the solution of optimal power flow problems." *Electric Power Systems Research*, 77(5-6), 508-517.

Xihui Yan and V.H. Quintana (1996). "An infeasible interior-point algorithm for optimal power flow problems." *Electrical Power and Energy Systems*, 39(1), 39-46.

IEEE Distribution System Analysis Subcommittee (2004, Nov. 05). *IEEE Radial Test Feeders*. [Online]. Available: http://www.ewh.ieee.org/soc/pes/dsacom/testfeeders.html.

G.L. Torres and V.H. Quintana (1998). "An interior-point method for nonlinear optimal power flow using voltage rectangular coordinates." *IEEE Trans. on Power System*s, 13(4), 1211-1218.

CHAPTER 5. OPTIMAL SITING AND SIZING OF DISTRIBUTED GENERATORS IN DISTRIBUTION SYSTEMS WITH PLUG-IN ELECTRIC VEHICLES

With the ever-increasing deployment of distributed generators (DGs) in modern power systems, the siting and sizing of DGs are becoming increasingly important in distribution system planning. Inappropriate siting and sizing of DGs could lead to many negative effects on the distribution systems concerned, such as the relay system configurations, voltage profiles and network losses. Another issue is that the rapid development of electric vehicles has imposed new challenges to power system planning and operation control. Some uncertainties such as the uncertain output power of a plug-in electric vehicle (PEV) due to its stochastic charging and discharging schedule, that of a wind generation unit due to stochastic wind speed, and that of a solar generating source due to the stochastic illumination intensity, volatile fuel prices and future uncertain load growth, could lead to some risk in determining the optimal siting and sizing of DGs in distribution systems. Given this background, under the chance constrained programming (CCP) framework, a new method is presented to handle these uncertainties in the optimal siting and sizing of DGs. First, a mathematical model of CCP is developed with the minimization of DGs' investment cost, operating cost and maintenance cost as well as the network loss cost as the objective, security limitations as constraints, the siting and sizing of DGs as optimization variables. Then, a Monte Carlo simulation embedded genetic algorithm based approach is developed to solve the developed CCP model. Finally, the IEEE 37-node test feeder is employed to verify the feasibility and effectiveness of the developed model and method, and test results have demonstrated that the voltage profile can be significantly improved and the network loss substantially reduced.

1. Introduction

With the progressing exhaustion of fossil energy, the limitation of available transmission corridors and the gradual increase in the global temperature, rapid development of Distributed Generators (DGs) has been observed around the world. Although the employment of DGs is helpful for postponing transmission investment, reducing primary energy consumption, decreasing the emission of greenhouse gases and hence alleviating global warming, the extensive penetration of DGs could lead to some risks to the secure and economic operation of power systems.

Due to the increasing penetration of DGs in distribution systems, the siting and sizing of DGs in distribution system planning is becoming increasingly important. Inappropriate siting and sizing of DGs could lead to many negative effects on the distribution systems concerned, such as the relay system configurations, voltage profiles and network losses. Another issue is more and more attention is being paid to the applications of plug-in electric vehicle (PEV) [S. Rahman, and G. B.

Shrestha, 1993; K. Clement-Nyns et al, 2010; P. Mitra and G. K. Venayagamoorthy, 2010]. However, some uncertainties such as the stochastic output power of a PEV due to its random charging and discharging schedule [P. T. Staats et al, 1997; J. G. Vlachogiannis, 2009; M. Etezadi-Amoli et al, 2010], that of a wind power unit due to the frequently variable wind speed, and that of a solar generating source due to the stochastic illumination intensity, volatile fuel prices and future uncertain load growth could lead to some risk in determining the optimal siting and sizing of DGs in distribution systems [M. R. Haghifam et al, 2008; D. Zhu et al, 2006]. Hence, the optimal siting and sizing of DGs need to be carefully considered in distribution system planning. In this chapter, for the simplicity of presentation, the load power of a PEV in the charging condition is regarded as the negative output power of the PEV and negative input power to the system concerned. Therefore, the load power of a PEV in both charging and discharging conditions is called "output power" of the PEV. Moreover, the PEV is regarded as a kind of DG with stochastic output power.

The objective of the distribution system planning with DGs considered is to find an optimal combination of a capacity expansion scheme such as the new feeders to be built, the expanded capacity of the substation, and the siting and sizing of DGs so as to minimize/maximize a given objective function, with the load growth constraints and some security constraints well respected [W El-Khattam et al, 2005].

At present, a large number of research publications are available on the subject of the optimal siting and sizing of DGs [C. S. Wang, and M. H. Nehrir, 2004; G. Carpinelli et al, 2005; A. Keane and M. O'Malley, 2005; K. H. Kim et al, 2008; R. K. Singh and S. K. Goswami, 2009; M. M. Elnashar et al, 2010; D. Gautam and N. Mithulananthan, 2007; S. Ghosh et al, 2010; T. Gözel and M. H. Hocaoglu, 2009]. However, most of them are based on deterministic methods. For example, in [C. S. Wang, and M. H. Nehrir, 2004], analytical methods are presented to determine the optimal location of a DG in radial as well as networked systems with the minimization of the network loss as the objective; in [K. H. Kim et al, 2008], the fuzzy goal programming is employed to determine the optimal placement of DGs for loss reduction and voltage improvement in distribution systems. A simple yet conventional iterative search technique is combined with the Newton-Raphson load flow method for finding the optimal sizing and placement of DGs in [S. Ghosh et al, 2010], and the modified IEEE 6-bus, IEEE 14-bus and IEEE 30-bus test systems are employed to demonstrate the developed method. In [T. Gözel and M. H. Hocaoglu, 2009], an equivalent current injection based loss sensitivity factor is used to determine the optimal locations and sizes of DGs by an analytical method with the minimization of the total power losses as the objective. A new approach is proposed in [M. M. Elnashar et al, 2010] to optimally determine the locations and sizes of DGs in a large mesh-connected system. Three indexes including the losses, voltage profile and short circuit level are used to determine the optimal locations and sizes of DGs. In these papers, some deterministic mathematical models are employed to formulate the optimal siting and sizing of DGs,

and generally the mathematical models such obtained are mixed-integer nonlinear programming ones with multiple variables and constraints included.

As already mentioned before, there are some uncertainties associated with the optimal siting and sizing of DGs in distribution system planning. Given this background, under the CCP framework, a new method is presented to handle the risks brought by these uncertainties in the optimal siting and sizing of DGs. First, a mathematical model of CCP is developed with the minimization of DGs' investment cost, operating cost and maintenance cost as well as the network loss cost as the objective, security limitations as constraints, the siting and sizing of DGs as optimization variables. Then, a Monte Carlo simulation embedded Genetic Algorithm approach is developed to solve the developed CCP model. Finally, the IEEE 37-node test feeder is employed to verify the feasibility and effectiveness of the developed model and method, and test results have demonstrated that the voltage profile can be significantly improved and the network loss substantially reduced.

The major components of the CCP based optimal siting and sizing of DGs in distribution system planning are outlined in Fig 5.1, and details associated will be clarified in the following sections.

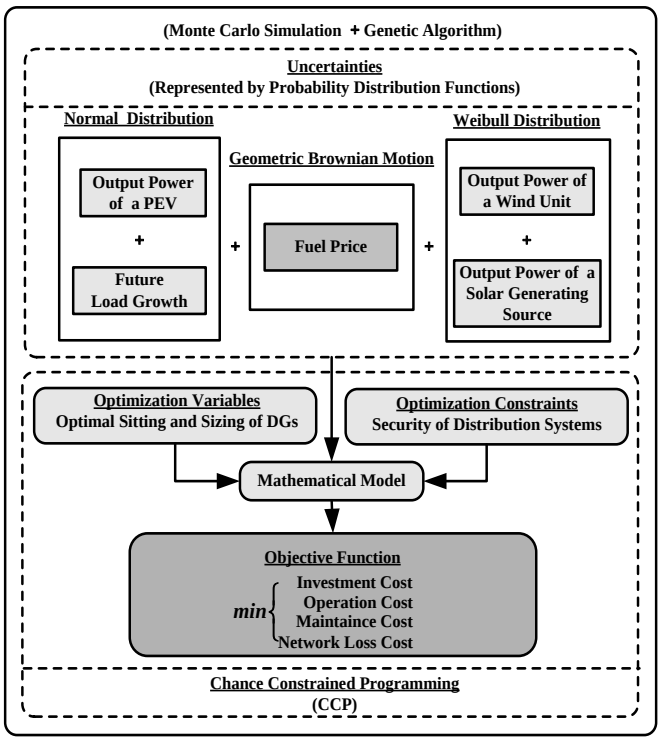

Fig 5.1 The flowchart of the developed CCP based method for optimal siting and sizing of DGs in Distribution Systems

2. Chance Constrained Programming

As a branch of stochastic programming methods, CCP can accommodate constraints with stochastic variables included, and makes decisions before stochastic variables are actually observed [N. Yang and F. S. Wen, 2005a]. Moreover, CCP allows that the decision-making procedure does not satisfy some constraints, but must satisfy the constraints with a given probability, i.e., the so-called confidence interval.

The general form of a CCP problem can be described as

$$\begin{cases} min & \overline{f} \\ s.t. & \\ & \Pr\ f(X,\xi) \le \overline{f}\ \ge \alpha \\ & \Pr\ g_j(X,\xi) \le 0\ \ge \beta\ \ (j=1,2,\cdots,n) \end{cases} \tag{1}$$

Where:

- X is a k-dimension decision-making vector;
- ξ is a set of stochastic variables with known probability distributions;
- $g_j(X,\xi) \le 0\ \ (j=1,2,\cdots,n)$ are stochastic constraints;
- $f(X,\xi)$ is the objective function;
- $\overline{f}$ is the optimal value of the objective function with the given confidence interval β;
- α and β are both the given confidence intervals;
- $\Pr\{\cdot\}$ represents the probability of the event included in $\{\cdot\}$.

A constraint represented by the probabilistic form is called a chance constraint. More details about CCP can be found in [N. Yang and F. S. Wen, 2005b] and [B. Liu, 1999].

3. Modeling of Uncertainties

3.1 The Output Power Uncertainty of PEVs

According to the charging-discharging characteristics of the PEV's battery, the recently established Vehicle to Grid (V2G) technology can make the battery release the stored electrical energy in peak load periods for mitigating the power supply shortage and absorb the electrical energy in off-peak especially valley periods so as to smoothing the load curve. Moreover, the negative effects of intermittent DGs such as wind units and solar generating sources on the secure and economic operation of power systems can be alleviated if the charging and discharging of PEVs could be

properly scheduled. To make the full use of the above advantages and reduce the impacts of the stochastic charging and discharging schedules of PEVs on power systems, a centralized dispatching mechanism for charging and discharging of PEVs could be very helpful.

Some recent simulation experiments have demonstrated that the output power of a PEV in the charging or discharging conditions approximately follows the normal distribution [J. H. Zhao et al, 2010]. Thus, in off-peak load periods, the output power of a charging PEV could be described as $-P_v(t) \sim N(\mu_v(t), \sigma_v^2(t))$; in peak load periods, the output power of a discharging PEV could be described as $P_v(t) \sim N(\mu_v(t), \sigma_v^2(t))$.

3.2 The Output Power Uncertainty of Wind Generating Units

A large number of experiments have demonstrated that the stochastic wind speed in most regions approximately follows the Weibull distribution, and this conclusion is employed in this chapter. Suppose that the stochastic wind speed v follows a Weibull distribution $\omega(k,c)$ with the probability density function [A. E. Fijoo et al, 1999]:

$$f(v) = \frac{k}{c^k} v^{(k-1)} e^{-(v/c)^k} \quad 0 \le v \le \infty \tag{2}$$

Where: k and c are respectively the shape index and the scale index of the Weibull distribution.

When the mean value of the wind speed samples in a given region is known, the scale index could be calculated by employing the following equation,

$$v_m = \int_0^\infty v f(v) dv = \int_0^\infty \frac{2v^2}{c^2} e^{-(v/c)^2} dv = \frac{\sqrt{\pi}}{2} c \tag{3}$$

Thus, the shape index of the Weibull distribution curve can be obtained as $c = \frac{2}{\sqrt{\pi}} v_m$.

Based on the known probability distribution function of the wind speed, the relationship between the output power of a wind generating unit and the wind speed can be formulated as [Y. M. Atwa et al, 2008]:

$$P_w = \begin{cases} 0 & 0 \le v \le v_{ci} \text{ or } v_{co} \le v \\ P_{w\_rated} \dfrac{(v - v_{ci})}{(v_r - v_{ci})} & v_{ci} \le v \le v_r \\ P_{w\_rated} & v_r \le v \le v_{co} \end{cases} \quad (4)$$

Where:

- v is the wind speed at hub high of the wind unit;
- v_{ci} is the cut-in wind speed;
- v_{co} is the cut-out wind speed;
- v_r is the rated wind speed;
- P_{w_rated} is the rated output power of the wind unit.

Thus, the relationship between the output power of a wind unit and the wind speed at hub high could be shown as Fig 5.2.

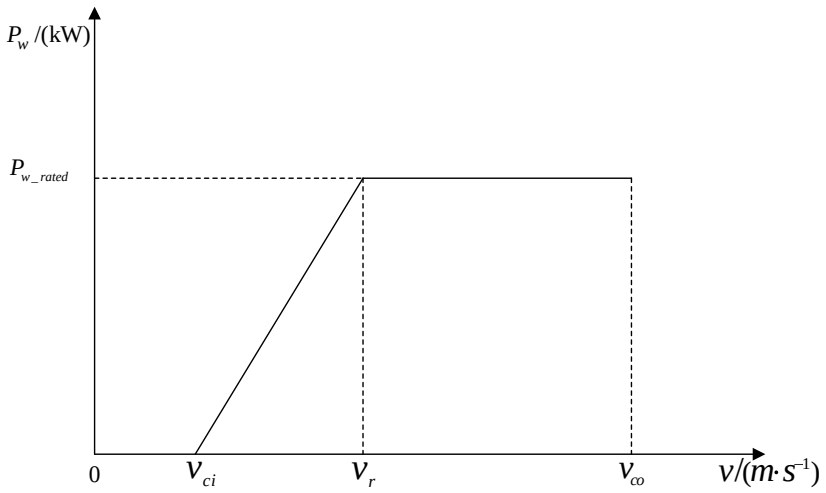

Fig 5.2 The relationship between a wind unit's output power and the wind speed

3.3 The Output Power Uncertainty of Solar Generating Sources

The output power of a solar generating source is affected by many factors such as the spectral distribution of the solar energy, the temperature of solar cells, and the illumination intensity. The illumination intensity is usually considered to be the dominant one [N. Mutoh et al, 2002]. To facilitate the presentation, only the relationship between the illumination intensity and the output power of the solar generating source is given here.

Suppose that the stochastic illumination intensity follows the Weibull distribution $\omega(k_s, c_s)$. Whereby, k and c are determined by the history data in the local area associated. Thus, suppose that the relationship between the illumination intensity and the output power of a solar generating source can be described as [N. Mutoh et al, 2002]

$$P_s = \begin{cases} P_{s\_rated} \dfrac{s}{s_r} & 0 \le s \le s_r \\ P_{s\_rated} & s_r \le s \end{cases} \tag{5}$$

Where:

- s is the illumination intensity;
- s_r is the rated value;
- P_{s_rated} is the rated output power of the solar cells.

Thus, the relationship between the output power of a solar generating source and the illumination intensity could be shown as Fig 5.3.

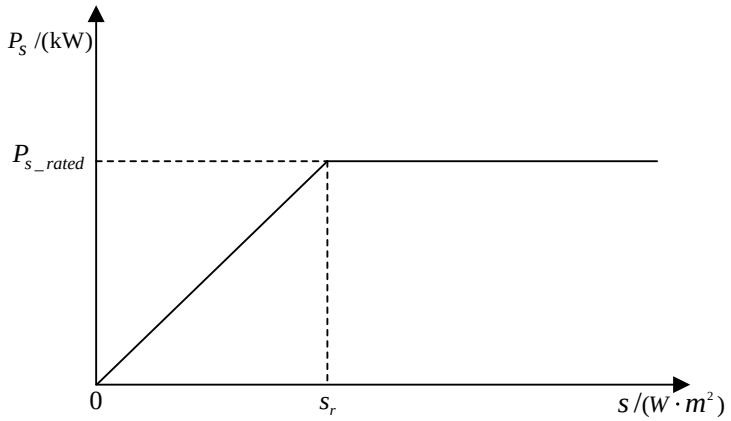

Fig 5.3 The relationship between the output power of a solar generating source and the illumination intensity

3.4 The Uncertainty of Future Load Growth

Suppose that the original load on node *i* is $P^*_{Li(0)}$, and the load growth at this node in the year *t* of the planning period is $\Delta P_{Li}(t)$ and follows the normal distribution, i.e. $\Delta P_{Li}(t) \sim N(\mu_i(t), \sigma_i^2(t))$ [E. Handschin et al, 2006]. Thus, the load on node *i* in year *t* is $P_{Li}(t) = P^*_{Li}(t) + \Delta P_{Li}(t)$.

3.5 The Uncertainty of Fuel Prices

For the fueled DGs such as micro turbines, the operating costs mainly consist of the fuel (coal, oil, gas etc.) costs. However, the fuel price in the future is affected by many factors, and could not be accurately forecasted.

Generally, the volatile fuel price is deemed to follow the Geometric Brownian Motion (GBM) [G. Z. Liu et al, 2009]:

$$\frac{dp_f(t)}{p_f(t)} = \mu_f dt + \sigma_f dW(t) \tag{6}$$

Where:

- $p_f(t)$ is the fuel price in year t;
- μ_f is the expected value of the variation of the fuel price during the planning period;
- σ_f is the standard deviation of the variation of the fuel price during the planning period;
- $W(t)$ is the standard Brownian Motion, $W(t) \sim N(0,t)$;
- dt is the time step length, and is specified to be one year in this chapter.

Hence, during the planning period, the fuel price in year t can be obtained as follows according to Eqn. (6):

$$p_f(t) = p_f(t-1) \cdot \exp\left[(\mu_f - \frac{1}{2}\sigma_f{}^2)t + \sigma_f W(t) \right] \tag{7}$$

Where: $p_f(t-1)$ is the fuel price in year t-1.

4. The Mathematical Model

4.1 The Objective Function

In this chapter, the objective function is defined to be the minimization of the total costs associated with the DGs to be planned, including investment cost, operating cost, maintenance cost and network loss cost, in the planning period [G. Celli et al, 2005]. The mathematical model is described below:

$$
\begin{aligned}
\min f &= \chi C^I + \gamma C^O + \tau C^M + \varsigma C^L \\
&= \sum_{t=1}^{T} \Bigg\{ \chi \sum_{i=1}^{N_{DG}} \Big[E_{DG_i}(t) C^I_{DG_i}(t) \ P^N_{DG_i}(t) - P^N_{DG_i}(t) \ \Big] \\
&+ \gamma \sum_{i=1}^{N_{DG}} \ E_{DG_i}(t) C^O_{DG_i}(t) T_{DG_i}(t) P^N_{DG_i}(t) \\
&+ \tau \sum_{i=1}^{N_{DG}} \ E_{DG_i}(t) C^M_{DG_i}(t) T_{DG_i}(t) P^N_{DG_i}(t) \ + \varsigma C^L(t) \Delta W_h(t) \Bigg\}
\end{aligned} \tag{8}
$$

Where:

- $\chi + \gamma + \tau + \varsigma = 1$;
- χ, γ, τ and ς are weighting coefficients;
- T is the total number of years in the planning period;
- C^I, C^M, C^O are respectively the investment cost, maintenance cost and operating cost of DGs, and C^L is the network loss cost, in the planning period;
- $E_{DG_i}(t)$ represents the optimization variable included in the planning scheme, $E_{DG_i(t)} = 0/1$ denotes that there will not be /there will be a DG built at node i in year t;
- $P^N_{DG_i}(t)$ and $P^N_{DG_i}(t-1)$ are the installed capacities of DGs at node i in year t and year $t-1$, respectively;
- $\Delta W_h(t)$ is the energy loss of the distribution system in year t;
- N_{DG} is the number of candidate DGs to be installed in the distribution system;
- $T_{DG_i}(t)$ is the equivalent generation hours of the DG at node i in year t;
- $C^I_{DG_i}(t)$ is the per unit capacity investment cost of the DG at node i in year t;
- $C^O_{DG_i}(t)$ is the per unit operating cost of the DG at node i in year t;
- $C^M_{DG_i}(t)$ is the per unit maintenance cost of the DG at node i in year t.

Specifically speaking, for a renewable DG, $C^O_{DG_i}(t) = 0$; for a fuel-based DG, its operating cost is mainly composed of the fuel cost, and $C^O_{DG_i}(t)$ can be obtained by Eqn. (7). For a PEV, its operating cost is determined by its charging and discharging cost. The per unit capacity operating cost of a PEV can be obtained as

$$
\begin{aligned}
C^O_{DG_i}(t) = &\frac{C^L(t) r^C_{DG_i}(t) T^C_{DG_i}(t) + C^L(t) r^{C^*}_{DG_i}(t) T^{C^*}_{DG_i}(t)}{T_{DG_i}(t)} \\
&- \frac{C^G(t) r^D_{DG_i}(t) T^D_{DG_i}(t) + C^G(t) r^{D^*}_{DG_i}(t) T^{D^*}_{DG_i}(t)}{T_{DG_i}(t)}
\end{aligned}
$$

Where:

- $T_{DG_i}(t) = T^C_{DG_i}(t) + T^{C^*}_{DG_i}(t) + T^D_{DG_i}(t) + T^{D^*}_{DG_i}(t)$;
- $T^C_{DG_i}(t)$ ($T^{C^*}_{DG_i}(t)$) is the charging time of the PEV at node i in year t at the valley load (other periods);

- $T_{DG_i}^{D}(t)$ ($T_{DG_i}^{D*}(t)$) is the discharging time of the PEV at node i in year t at the peak load (other periods);
- $C^{L}(t)$ ($C^{G}(t)$) is the retail price (on-grid price) in year t;
- $r_{DG_i}^{C}(t)$ ($r_{DG_i}^{C*}(t)$) is the electricity price adjustment coefficient for charging at the valley load (other periods) in year t;
- $r_{DG_i}^{D}(t)$ ($r_{DG_i}^{D*}(t)$) is the electricity price adjustment coefficient for discharging at the peak load (other periods) in year t.

To encourage the owners of electric vehicles to take part in the centralized dispatching, i.e. charging in valley/off-peak periods and discharging in peak periods, the electricity prices adjustment coefficients for charging and discharging as represented by $r_{DG_i}^{C}(t)$ ($r_{DG_i}^{C*}(t)$) and $r_{DG_i}^{D}(t)$ ($r_{DG_i}^{D*}(t)$) can be employed.

4.2 The Weighting Coefficients

Due to the multi-objective feature of Eqn. (8), an algorithm called Analytic Hierarchy Process (AHP) is employed here to determine the optimal weighting coefficient for each objective. AHP was proposed in 1970' and since then it has gradually become an algorithm with extensive applications in multi-objective comprehensive evaluations [J. Jeonghwan et al, 2010].

First, by comparing the importance of each two indices (in this chapter, indices refer to objectives), a pairwise comparison matrix is formed with the scale from 1 to 9. A larger scale value indicates that the index associated is more important. A pairwise comparison matrix can be expresses as

$$M = \begin{array}{c} \\ M_1 \\ M_2 \\ \vdots \\ M_n \end{array} \begin{array}{c} \begin{array}{cccc} M_1 & M_2 & \cdots & M_n \end{array} \\ \begin{bmatrix} m_{11} & m_{12} & \cdots & m_{1n} \\ m_{21} & m_{22} & \cdots & m_{2n} \\ \vdots & \vdots & \ddots & \vdots \\ m_{n1} & m_{n2} & \cdots & m_{nn} \end{bmatrix} \end{array} \tag{9}$$

Where:

- M_i represents index i and n is the number indices;
- $m_{ii} = 1\ (i = 1, 2, \cdots, n)$ represents the importance comparison result between the index M_i and itself;
- $m_{ij} = \dfrac{1}{m_{ji}} = \dfrac{m_{ik}}{m_{jk}}\ (i, j, k = 1, 2, \cdots, n)$ represents the importance comparison result between M_i and M_j.

Then, the weighting coefficient for each index can be calculated as

$$W_i = \frac{\sqrt[n]{\prod_{j=1}^{n} m_{ij}}}{\sum_{i=1}^{n} \sqrt[n]{\prod_{j=1}^{n} m_{ij}}} \quad (i = 1, 2, \cdots, n) \tag{10}$$

In a vector form, the weighting coefficients can be represented as $W = [W_1, W_2, \cdots, W_n]^{\mathrm{T}}$.

Finally, the consistency of the pairwise comparison matrix M is checked as follows:

$$F_{CR} = \frac{F_{CI}}{F_{RI}} = \frac{(\lambda_{max} - n)}{(n-1) \cdot F_{RI}} < 0.1 \tag{11}$$

Where:

- F_{CR} is the consistency ratio, if $F_{CR} < 0.1$, then the weighting coefficient of each index calculated by Eqn. (10) is reasonable;
- F_{CI} is the consistency index, $F_{CI} = \frac{\lambda_{max} - n}{n-1}$;
- F_{RI} is an random index is a random index, and for different index number *n* its values are given in [J. Jeonghwan et al, 2010];
- λ_{max} is the maximal eigenvalue of M and can be calculated by $MW = \lambda_{max} W$.

4.3 The Chance Constraints

To maintain the secure operation of a distribution system, the current in each feeder cannot exceed its limitation. However, this limitation is not a strict constraint and can be violated in a short time and to a certain degree. This can be properly handled by a chance constraint below:

$$\Pr \left| I_{ij}(t) \right| - I_{ijmax} \le 0 \ge \beta \quad (i, j = 1, 2, \cdots, N_B) \tag{12}$$

Where: $I_{ij}(t)$ is the current in the feeder between node i and node j in year t.

4.4 The Equality Constraints

The equality constraints are the well-known load flow equations as

$$\begin{cases} P_{DG_i}(t) - P_{Li}(t) - V_i(t)\sum_{j=1}^{N_B} V_j(t)\ \left[G_{ij}\cos\delta_{ij}(t) + B_{ij}\sin\delta_{ij}(t)\right] = 0 \\ Q_{DG_i}(t) - Q_{Li}(t) - V_i(t)\sum_{j=1}^{N_B} V_j(t)\ \left[G_{ij}\sin\delta_{ij}(t) - B_{ij}\cos\delta_{ij}(t)\right] = 0 \end{cases} \tag{13}$$

Where:

- $P_{DG_i}(t)/Q_{DG_i}(t)$ is the total active/reactive output power of the generators at node i (including the operating generators and the newly installed DGs) in year t;
- $P_{Li}(t)/Q_{Li}(t)$ is the active/reactive load power at node i in year t;
- $V_i(t)$ and $V_j(t)$ are the voltage amplitudes at node i and node j in year t, respectively;
- G_{ij}/B_{ij} is the conductance/susceptance between node i and node j;
- $\delta_{ij}(t)$ is the voltage angle between node i and node j in year t;
- N_B is the number of nodes in the distribution system.

4.5 The Inequality Constraints

The deterministic constraints considered here mainly include the upper and lower limits of active output power of DGs (i.e. $P_{DG_{imax}}$ and $P_{DG_{imin}}$), the upper and lower limits of reactive output power of DGs (i.e. $Q_{DG_{imax}}$ and $Q_{DG_{imin}}$), the given permitted penetration capacities of DGs in the distribution system (i.e. P_{DGmax}), the upper and lower voltage limits at each node (i.e. V_{imax} and V_{imin}). The inequality constraints considered here are formulated below:

$$\begin{cases} P_{DG_{imin}} \le P_{DG_i}(t) \le P_{DG_{imax}} & i = 1,2,\cdots,N_{DG} \\ Q_{DG_{imin}} \le Q_{DG_i}(t) \le Q_{DG_{imax}} & i = 1,2,\cdots,N_{DG} \\ \sum_{i=1}^{N_{DG}} P_{DG_i}(t) \le P_{DGmax} & i = 1,2,\cdots,N_{DG} \\ V_{imin} \le V_i(t) \le V_{imax} & i = 1,2,\cdots,N_B - 1 \end{cases} \tag{14}$$

Thus, the developed mathematical model of the CCP-based optimal siting and sizing of DGs can be formulated as

$$\begin{cases} \min \quad f(E_{DG}, P_{DG}) \\ s.t. \\ \quad \Pr \ \ f(E_{DG}, P_{DG}) \le \overline{f} \ \ge \alpha \\ \quad \Pr \ \ g_j(E_{DG}, P_{DG}) \le 0 \ \ge \beta \ \ (j = 1, 2, \cdots, N_L) \\ \quad G = 0 \\ \quad H_{min} \le H \le H_{max} \end{cases} \tag{15}$$

Where: N_L is the number of feeders in the distribution system.

It should be mentioned that the developed methodological framework in this chapter could accommodate other uncertainties and constraints as well.

5. Solving Strategies

5.1 Checking of Chance Constraints

In this chapter, the well-established Monte Carlo Simulation procedure is employed to check if chance constraints hold. Based on the probability distribution functions of associated stochastic variables, N_S samples could be generated by using random number generators. Suppose that among the N_S simulations, the number that chance constraints hold is N_F. Then, N_F / N_S could be used to estimate the probability that chance constraints hold. If and only if N_F / N_S is larger than or equal to the specified confidence interval, then the chance constraint holds [N. Yang and F. S. Wen, 2005a; N. Yang and F. S. Wen, 2005b].

5.2 Solving Steps

A Monte Carlo simulation embedded genetic algorithm approach is employed to solve the optimization problem described by Eqn. (15). First, the chance constraints are dealt with by the penalty function method. Secondly, the fitness function is formed by the objective function and penalty constraints together [G. Celli et al, 2005]. The detailed solving steps are as follows:

Step 1) Specify some parameters including N_S, and the ones associated with the genetic algorithm such as the population size N_P, crossover probability P_C, and mutation probability P_M, and the maximum permitted generation number N_C.

Step 2) Randomly generate N_P chromosomes and check their feasibilities by the Monte Carlo simulation.

Step 3) Update the N_P chromosomes by crossover and mutation operators according to the specified probabilities P_C and P_M, and check their feasibilities again by the Monte Carlo simulation.

Step 4) Calculate the objective function value of all chromosomes such produced.

Step 5) Calculate the fitness value of each chromosome in terms of the objective function value.

Step 6) Select the chromosomes in the current population by the roulette wheel method.

Step 7) Repeat Step 4 to Step 7 for N_C times.

Step 8) Select the best chromosome found in the above solving procedure as the optimal solution of the siting and sizing of DGs.

The flowchart of the GA-embedded Monte Carlo simulation procedure is shown in Fig 5.5.

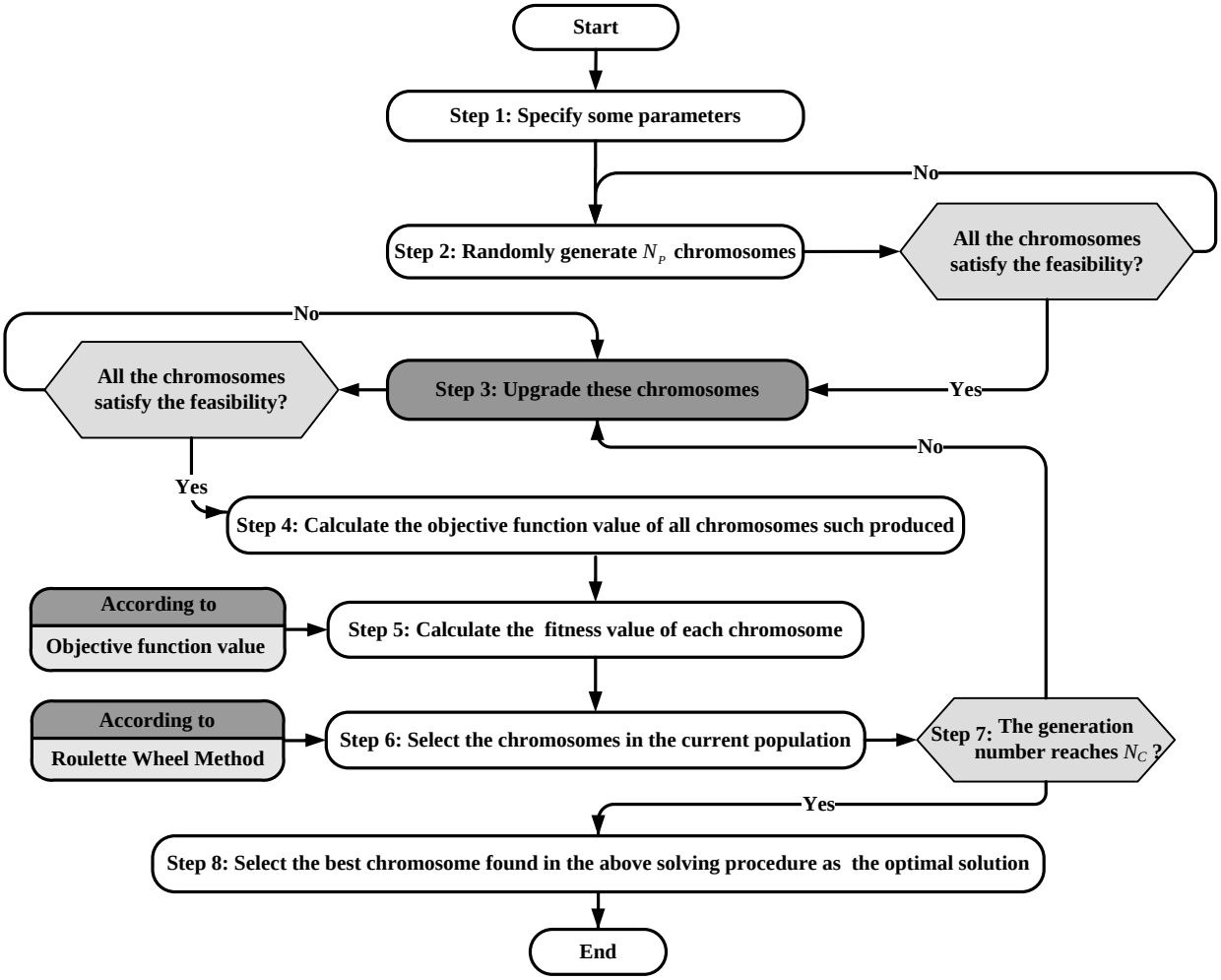

Fig 5.5 The flowchart of the GA-embedded Monte Carlo simulation procedure

6. Case studies

The IEEE 37-node test feeder [IEEE Distribution System Analysis Subcommittee, 2004], as shown in Fig 5.6, is used for demonstrating the developed model and method. In A computer program is developed in the Matlab 7 and Visual C++ 6.0 environment.

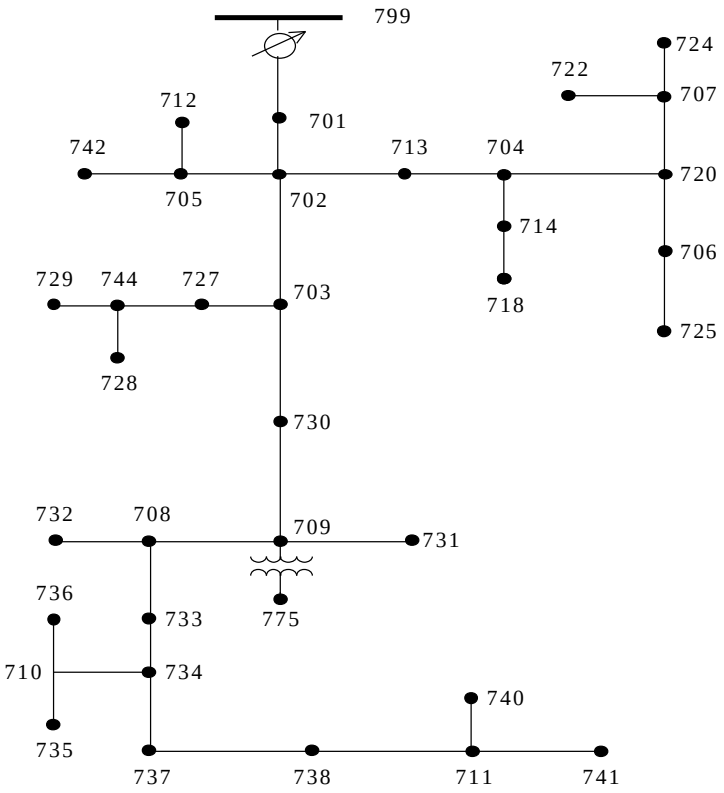

Fig 5.6 The IEEE 37-node test feeder

Some parameters are specified as follows:

1) The planning period: $T = 3$.
2) The reference voltage at the supply substation is 1.00.
3) The confidence levels: $\alpha = 0.95, \beta = 0.95$.
4) The parameters associated with the original loads and the probability distributions of the load growth are shown in Table 5.1 and Table 5.2, respectively.
5) According to Eqn. (10), the pairwise comparison matrix about the four indexes (investment cost, maintenance cost, operating cost and network loss cost) in Eqn. (8) is given as

$$M_f = \begin{array}{c} \\ C^I \\ C^F \\ C^O \\ C^L \end{array} \begin{array}{c} \begin{array}{cccc} C^I & C^O & C^M & C^L \end{array} \\ \left[\begin{array}{cccc} 1 & 1 & 3 & 4 \\ 1 & 1 & 3 & 4 \\ 1/3 & 1/3 & 1 & 1 \\ 1/4 & 1/4 & 1 & 1 \end{array}\right] \end{array}$$

Then, in terms of Eqn. (11), the optimal weighting coefficients of the four indexes are: $\chi = 0.39$, $\gamma = 0.39$, $\tau = 0.12$, $\varsigma = 0.10$, and the consistency ratio F_{CR} = 0.056 < 0.1.

6) For the wind generation, the cut-in, cut-out, and rated wind speeds are respective specified as $v_{ci} = 4\,m \cdot s^{-1}$, $v_{co} = 20\,m \cdot s^{-1}$, and $v_r = 15\,m \cdot s^{-1}$; the shape index is $k = 2.0$; the scale index is $c = 6.5$.
7) For the photovoltaic generation, the rated illumination intensity is $s_r = 1000\ W \cdot m^2$; the shape index is $k = 1.8$; the scale index is $c = 5.5$.
8) The candidate schemes for the types, siting and sizing of DGs are shown in Table 5.3. In each year of the planning period, the retail electricity price for consumers and on-grid prices for DGs are shown in Table 5.4. The investment and maintenance costs of a plug-in electric vehicle as well as the electricity price adjustment coefficients in the planning period are shown in Table 5.5. The investment and maintenance costs of renewable DGs and fueled DGs in the planning period are shown in Table 5.6 and Table 5.7, respectively.
9) In the Monte Carlo simulation embedded genetic algorithm approach, the parameters are specified as follows: $N_S = 5000$; $N_P = 30$; $P_C = 0.3$; $P_M = 0.2$; $N_C = 1000$.

Table 5.1 The original loads

Node	Load Model*	P_{Li}/(kW)	Q_{Li}/(kVar)
701	D-PQ	140.0	70.00
712	D-PQ	0.000	0.000
713	D-PQ	0.000	0.000
714	D-I	17.00	8.000
718	D-Z	85.00	40.00
720	D-PQ	0.000	0.000
722	D-I	0.000	0.000
724	D-Z	0.000	0.000
725	D-PQ	0.000	0.000
727	D-PQ	0.000	0.000
728	D-PQ	42.00	21.00
729	D-I	42.00	21.00
730	D-Z	0.000	0.000
731	D-Z	0.000	0.000
732	D-PQ	0.000	0.000
733	D-I	85.00	40.00
734	D-PQ	0.000	0.000
735	D-PQ	0.000	0.000
736	D-Z	0.000	0.000
737	D-I	140.0	70.00
738	D-PQ	126.0	62.00
740	D-PQ	0.000	0.000
741	D-I	0.000	0.000
742	D-Z	8.000	4.000
744	D-PQ	42.00	21.00

*Notes:

1) D-PQ: The load is assigned with the delta connection code and constant kW and kVar model;
2) D-I: The load is assigned with the delta connection code and constant current;

3) D-Z: The load is assigned with the delta connection code and constant impedance

Table 5.2 Probability distribution parameters of the load growth

Node	t = 1		t = 2		t = 3	
	$\mu_i(t)$/(kW)	$\sigma_i(t)$/(kW)	$\mu_i(t)$/(kW)	$\sigma_i(t)$/(kW)	$\mu_i(t)$/(kW)	$\sigma_i(t)$/(kW)
701	30.84	6.20	40.14	10.38	47.04	12.08
712	8.38	2.03	10.93	4.60	15.40	6.94
713	6.89	2.62	9.30	3.63	12.37	5.48
714	9.81	4.47	11.56	4.04	14.00	4.51
718	2.93	1.13	3.37	2.57	4.34	2.73
720	6.90	3.32	6.90	3.32	8.739	4.29
722	13.74	4.65	15.82	5.21	17.93	6.00
724	4.63	1.03	4.83	1.90	5.38	2.12
725	5.01	2.00	5.93	2.67	6.02	2.90
727	8.74	3.20	9.14	4.56	10.00	4.80
728	14.87	3.73	15.45	4.74	16.24	4.86
729	3.23	2.42	4.53	3.59	5.75	4.14
730	5.23	1.25	5.60	1.35	6.23	2.33
731	6.32	2.73	7.25	3.07	7.98	3.69
732	5.92	3.21	6.45	4.32	7.93	5.56
733	27.98	14.64	30.10	15.63	32.87	15.71
734	4.34	1.86	4.47	1.98	5.23	2.06
735	4.34	1.86	4.47	1.98	5.23	2.06
736	23.21	10.10	24.27	11.34	25.35	13.21
737	43.73	24.83	44.35	24.96	47.97	27.62
738	30.39	15.83	32.43	16.36	33.64	17.75
740	13.30	5.02	14.07	5.53	15.34	6.48
741	17.62	4.24	17.96	5.01	18.03	5.83
742	25.24	12.23	28.02	14.45	36.38	15.39
744	13.84	2.33	14.57	2.374	18.08	3.72

Note: $\mu_i(t)$ and $\sigma_i(t)$ are the mean value and standard deviation of load growth at node *i*, respectively.

Table 5.3 The candidate schemes for the types, siting and sizing of DGs

Siting of DGs	Sizing of DGs/(kW)	Types*
704	5.00, 10.00, 15.00	1, 2
705	5.00, 10.00, 15.00	1, 2
718	10.00, 15.00, 20.00	1, 2, 3
722	10.00, 15.00, 20.00	1, 2, 3
729	10.00, 15.00, 20.00	1, 2, 3
732	10.00, 20.00, 30.00	1, 2, 3, 4

736	10.00, 20.00, 30.00	1, 2, 3, 4
741	20.00, 30.00, 40.00	1, 2, 4
742	40.00, 50.00, 60.00	1, 2, 4

*Notes: 1-wind generation, 2-photovoltaic generation, 3-PEV, 4-fueled DGs

Table 5.4 The retail prices and on-grid prices in the planning period

Year	Retail prices	On-grid prices
	$C^{L}(t)/(\$\cdot\mathrm{kWh}^{-1})$	$C^{G}(t)/(\$\cdot\mathrm{kWh}^{-1})$
$t=1$	0.08	0.06
$t=2$	0.09	0.07
$t=3$	0.10	0.08

Table 5.5 The investment and maintenance costs of a plug-in EV as well as electricity price adjustment coefficients in the planning period

Year	$C^{I}_{DG_i}(t)/(\$\cdot\mathrm{kW}^{-1})$	$C^{M}_{DG_i}(t)/(\$\cdot\mathrm{kWh}^{-1})$	Electricity price adjustment coefficients for charging		Electricity price adjustment coefficients for discharging	
			$r^{C}_{DG_i}(t)$	$r^{C*}_{DG_i}(t)$	$r^{D}_{DG_i}(t)$	$r^{D*}_{DG_i}(t)$
			Off-peak periods (23:00-7:00)	Other periods (7:00-23:00)	On-peak periods (9:00-11:00, 19:00-23:00)	Other periods (23:00-9:00, 11:00-19:00)
$t=1$	1500.00	0.03	0.75	1.25	1.25	0.75
$t=2$	1250.00	0.02	0.80	1.20	1.20	0.80
$t=3$	1000.00	0.01	0.85	1.15	1.15	0.85

Table 5.6 The investment, maintenance and operating costs of renewable DGs in the planning period

Year	Wind generation			Photovoltaic generation		
	$C^{I}_{DG_i}(t)/(\$\cdot\mathrm{kW}^{-1})$	$C^{M}_{DG_i}(t)/(\$\cdot\mathrm{kWh}^{-1})$	$C^{O}_{DG_i}(t)/(\$\cdot\mathrm{kWh}^{-1})$	$C^{I}_{DG_i}(t)/(\$\cdot\mathrm{kW}^{-1})$	$C^{M}_{DG_i}(t)/(\$\cdot\mathrm{kWh}^{-1})$	$C^{O}_{DG_i}(t)/(\$\cdot\mathrm{kWh}^{-1})$
$t=1$	1,800.00	0.05	0.00	2,000.00	0.03	0.00
$t=2$	1,650.00	0.04	0.00	1,750.00	0.02	0.00
$t=3$	1,400.00	0.03	0.00	1,650.00	0.01	0.00

Table 5.7 The investment and maintenance costs of fueled DGs in the planning period

Year	Fueled DGs	
	$C^{I}_{DG_i}(t)/(\$\cdot \mathrm{kW}^{-1})$	$C^{M}_{DG_i}(t)/(\$\cdot \mathrm{kWh}^{-1})$
$t=1$	850.00	0.04
$t=2$	800.00	0.03
$t=3$	760.00	0.02

Table 5.8 Optimal siting and sizing of DGs in the planning period

$(\alpha = 0.95, \beta = 0.95)$

Types		Node	$P^{N}_{DG_i}(t)/(\mathrm{kW})$		
			$t=1$	$t=2$	$t=3$
Renewable DGs	Wind generation	718		10.00	20.00
		722	10.00	15.00	20.00
	Photovoltaic generation	729			10.00
Fueled DGs		732		10.00	10.00
		736	10.00	20.00	30.00
		741	30.00	30.00	40.00
		742	40.00	50.00	50.00
PEVs		718		10.00	15.00
		722	10.00	10.00	15.00
Network loss ratio/(%)			2.71	1.96	1.56

Table 5.9 The cost items in the planning period

Year	C^{I}/($)	C^{O}/($)	C^{M}/($)	C^{L}/($)
$t=1$	101,000.00	55,819.51	19,612.40	8,744.00
$t=2$	61,250.00	85,479.16	18,804.50	7,870.50
$t=3$	46,200.00	98,734.57	16,610.15	7,615.00

The optimal siting and sizing of DGs and the cost items in the planning period under the confidence levels of $\alpha = 0.95$ and $\beta = 0.95$ are shown in Table 5.8 and Table 5.9, respectively. With the load growth in the planning period, several new DGs are built in this test feeder each year. Moreover, the sizing of each kind of DGs follows an increasing trend as shown in Fig.7.

On the other hand, the network loss ratio has been decreased from 2.71% to 1.56% in the planning period, as shown in Table 5.8, and this represents a 42.44% reduction.

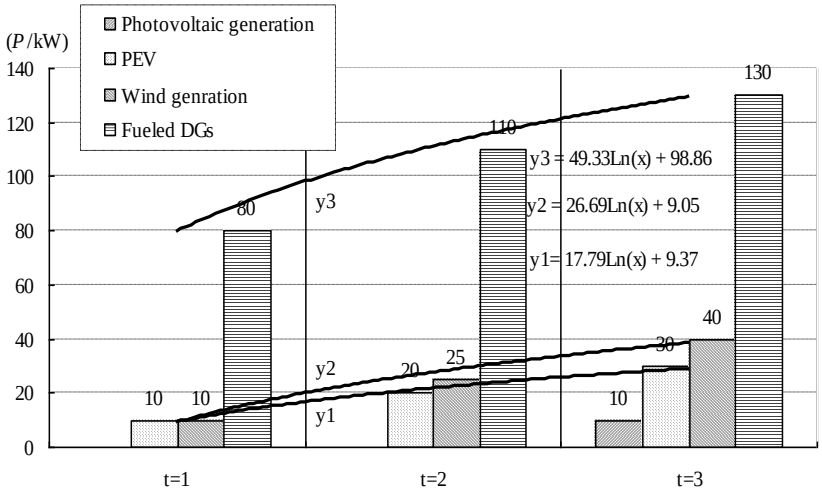

Fig 5.7 The optimal sizing of each kind of DGs in each year during the planning period

As shown in Fig 5.8, the numbers of PEVs and new renewable DGs are increasing more quickly in the planning period compared with fueled DGs. The total costs of PEVs and renewable DGs are declining gradually due to technology development, as shown in Table 5.5 and Table 5.6. It is 5.6nown from Table 5.7 and Table 5.9, although the investment and maintenance costs of fueled DGs are also decreasing, the growth of their operating costs caused by the increasing fueled price is much more than those of PEVs and renewable DGs. Therefore, in the long run, the fueled DGs will become less competitive.

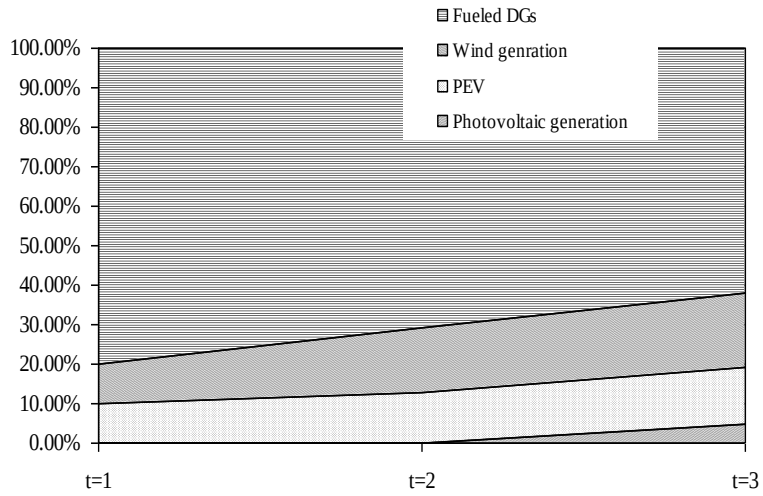

Fig 5.8 The proportion of the annually added capacity of each kind of DGs during the planning period

From Fig 5.9, it could be observed that in each year of the planning period with newly added DGs, the voltage profile at each node of the test feeder has been greatly improved.

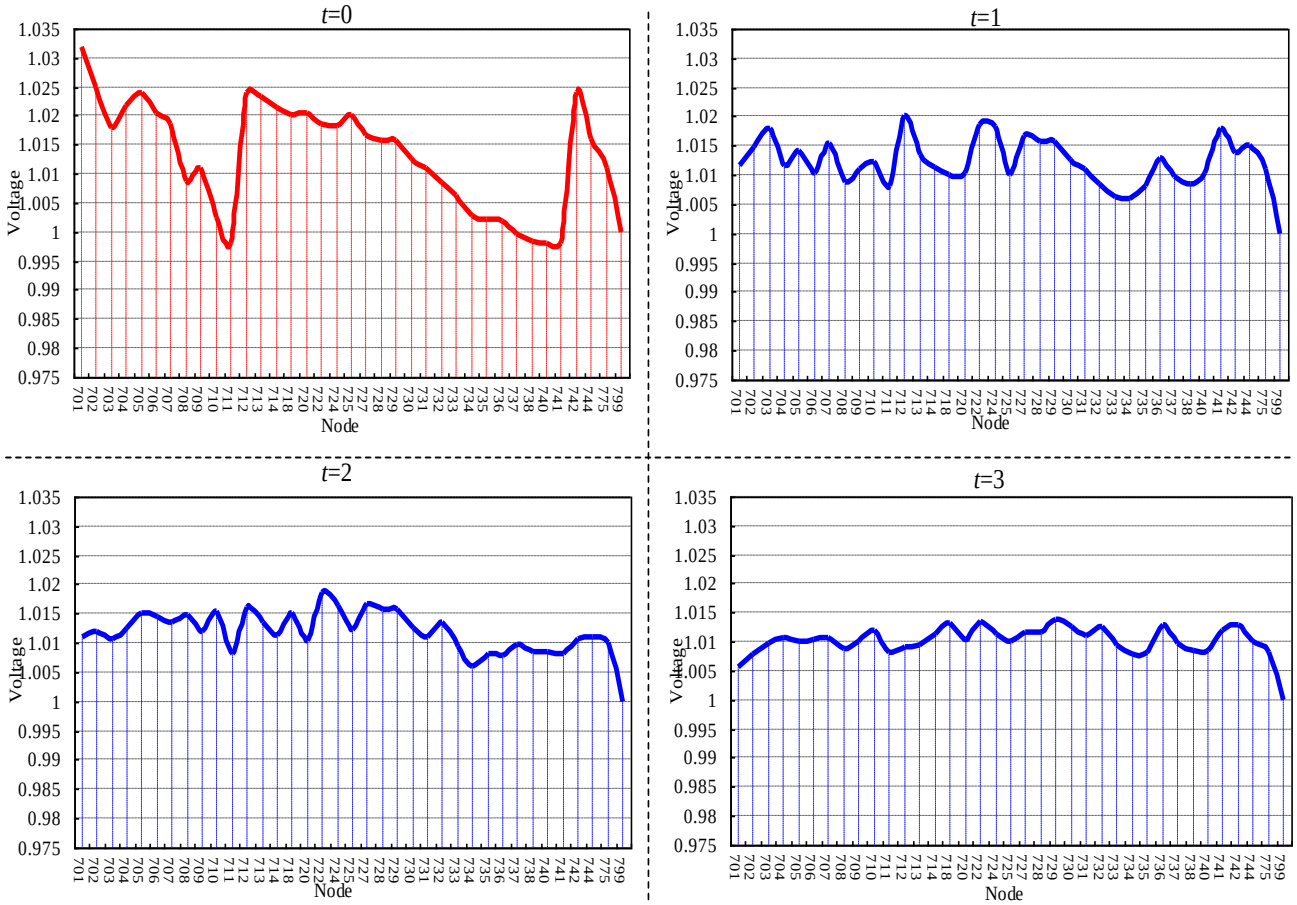

Fig 5.9 The voltage variations at each node of the test feeder with added DGs in the planning period

7. Conclusions

Under the chance constrained programming framework, a new mathematical model is developed to handle some uncertainties such as the stochastic output power of a PEV, that of a renewable DG, volatile fuel prices and future uncertain load growth in the optimal siting and sizing of DGs. Then, a Monte Carlo simulation embedded genetic algorithm approach is presented to solve the developed CCP model. Finally, the test results of the IEEE 37-node test feeder demonstrate the feasibility and effectiveness of the developed model and method.

References

S. Rahman and G. B. Shrestha (1993). "An investigation into the impact of electric vehicle load on the electric utility distribution system." *IEEE Transactions on Power Delivery*, 8(2), 591-597.

K. Clement-Nyns, E. Haesen, and J. Driesen (2010). "The impact of charging plug-in hybrid electric vehicles on a residential distribution grid." *IEEE Transactions on Power Systems*, 25(1), 371-380.

P. Mitra and G. K. Venayagamoorthy (2010). "Wide area control for improving stability of a power system with plug-in electric vehicles." *IET Generation, Transmission & Distribution*, 4(10), 1151-1163.

P. T. Staats, W. M. Grady, A. Arapostathis, and R. S. Thallam (1997). "A procedure for derating a substation transformer in the presence of wide spread electric vehicle battery charging." *IEEE Transactions on Power Delivery*, 12(4), 1562 - 1568.

J. G. Vlachogiannis (2009). "Probabilistic constrained load flow considering integration of wind power generation and electric vehicles." *IEEE Transactions on Power Systems*, 24(4), 1808-1817.

M. Etezadi-Amoli, K. Choma, and J. Stefani (2010). "Rapid-charge electric-vehicle stations." *IEEE Transactions on Power Delivery*, 25(3), 1883 - 1887.

M. R. Haghifam, H. Falaghi and O.P. Malik (2008). "Risk-based distributed generation placement." *IET Generation, Transmission and Distribution*, 2(2), 252-260.

D. Zhu, R. P. Broadwater, K. S. Tam, R. Seguin, and H. Asgeirsson (2006). "Impact of DG placement on reliability and efficiency with time-varying loads." *IEEE Transactions on Power Systems*, 21(1), 419 - 427.

W El-Khattam, Y. G. Hegazy, and M. M. A. Salama (2005). "An integrated distributed generation optimization model for distribution system planning." *IEEE Transactions on Power Systems*, 20(2), 1158 - 1165.

C. S. Wang, and M. H. Nehrir (2004). "Analytical approaches for optimal placement of distributed generation sources in power systems." *IEEE Transactions on Power Systems*, 19(4), 2068 - 2076 .

G. Carpinelli, G. Celli, S. Mocci, F. Pilo and A. Russo (2005). "Optimisation of embedded generation sizing and siting by using a double trade-off method." *IEE Proceedings: Generation, Transmission and Distribution*, 152(4), 503-513.

A. Keane, and M. O'Malley (2005), "Optimal allocation of embedded generation on distribution networks," *IEEE Transactions on Power Systems*, 20(3).

K. H. Kim, K. B. Song, S. K. Joo, Y. J. Lee, and J. O. Kim (2008). "Multiobjective distributed generation placement using fuzzy goal programming with genetic algorithm." *European Transactions on Electrical Power*, 18(3), 217-230.

R. K. Singh and S. K. Goswami (2009). "Optimum siting and sizing of distributed generations in radial and networked systems," *Electric Power Components and Systems*, 37(2), 127-145.

D. Gautam and N. Mithulananthan (2007). "Optimal DG placement in deregulated electricity market." *Electric Power Systems Research*, 77(12), 1627-1636.

S. Ghosh, S. P. Ghoshal, and S. Ghosh (2010). "Optimal sizing and placement of distributed generation in a network system." *Electrical Power and Energy Systems*, 32(8), 849-856.

T. Gözel and M. H. Hocaoglu (2009). "An analytical method for the sizing and siting of distributed generators in radial systems." *Electric Power Systems Research*, 79(6), 912-918.

M. M. Elnashar, R. E. Shatshat, and M. A. Salama (2010). "Optimum siting and sizing of a large distributed generator in a mesh connected system." *Electric Power Systems Research*, 80(6), 670-697.

N. Yang and F. S. Wen (2005). "A chance constrained programming approach to transmission system expansion planning." *Electric Power Systems Research*, 75(2-3), 171-177.

B. Liu (1999), Uncertain Programming, New York: Wiley.

J. H. Zhao, F. S. Wen, Y. S. Xue, Z. Y. Dong (2010). "Power system stochastic economic dispatch considering the uncertain outputs from plug-in electric vehicles and wind generators." *Automation of Electric Power Systems*, 34(20), 1-8.

A. E. Fijoo, J. Cidras, J.L.G. Dornelas (1999). "Wind speed simulation in wind farms for steady-state security assessment of electrical power systems." *IEEE Transactions on Energy Conversion*, 14(4), 1582-1588.

Y. M. Atwa, E. F. El-Saadany, R. Seethapathy, and M. M. A. Salama (2008). "Effect of wind-based DG seasonality and uncertainty on distribution system losses." *40th North American Power Symposium*, 1-6.

N. Mutoh, T. Matuo, K. Okada, M. Sakai (2002). "Prediction-data-based maximum-power-point-tracking method for photovoltaic power generation systems." *IEEE Annual Power Electronics Specialists Conference*, 1489-1494.

E. Handschin, F. Neise, H. Neumann, and R. Schultz (2006). "Optimal operation of dispersed generation under uncertainty using mathematical programming." *Electrical Power and Energy Systems*, 28(9) , 618-626.

G. Z. Liu, F. S. Wen, and Y. S. Xue (2009). "Generation investment decision-making under uncertain greenhouse gas emission mitigation policy." *Automation of Electric Power Systems*, 33(18), 17-22.

G. Celli, E. Ghiani, S. Mocci, and F. Pilo (2005). "A multiobjective evolutionary algorithm for the sizing and siting of distributed generation." *IEEE Transactions on Power Systems*, 20(2), 750-757.

J. Jeonghwan, L. Rothrock, P. L. Mcdermott, M. Barnes (2010). "Using the analytic hierarchy process to examine judgment consistency in a complex multiattribute task." *IEEE Transactions on Systems, Man and Cybernetics, Part A: Systems and Humans*, 40(5), 1105-1115.

N. Yang and F. S. Wen (2005). "Risk-constrained multiage transmission system expansion planning." *Automation of Electric Power Systems*, 29(4), 28-33.

IEEE Distribution System Analysis Subcommittee (2004, Nov. 05). *IEEE Radial Test Feeders*. [Online]. Available: http://www.ewh.ieee.org/soc/pes/dsacom/testfeeders.html.

CHAPTER 6. A HYBRID APPROACH FOR PLANNING DISTRIBUTED GENERATION EMPLOYING CHANCE CONSTRAINED PROGRAMMING

Siting and sizing of renewable energy distributed generation into existing distribution systems is essential to ensure the best benefits achievable from such resources while maintaining the secure and reliable operation of the distribution systems. In this chapter, a new methodology for planning embedded renewable energies within a distribution grid is developed. The new method minimizes various costs arising from the investment and running of the renewable energies, the network loss, as well as the costs due to the expected energy not supplied (EENS). To address the uncertainties associated with distribution systems containing distributed generation, the chance constrained programming (CCP) is applied to consider uncertain future in the planning horizon. A Monte-Carlo simulation embedded Harmony Search (HS) method is developed solve the proposed planning model. A case study has been carried out using the IEEE 37-node distribution network, and the results demonstrated the effectiveness of the proposed method.

NOMENCLATURES

C_I,	Annual equivalent capital cost for DG installation
C_O	Annual running (operating and maintenance) cost of DG
C_L	Annual network loss cost
C_R	Annual cost due to supply loss
n	The period taken into consideration in year
$N_{RE\text{-}DG}$	The number of installed DGs
$P_{RE-DG,k}$	The installed capacities of DG k.
$W_{RE-DG,k}$	The total generation output of DG k in a year
W_p	Annual network loss within the distribution system
R_a	Annual expected energy not supplied in MW
c_e, c_r, c_f and c_w	The per unit cost due to capital, running, network loss and supply loss down time constraint.
P_{Gi} , Q_{Gi}	Real and reactive power outputs of node i.
P_{Li} , Q_{Li}	Real and reactive demands at bus i.
V_i , V_j	Voltage magnitudes of node i and node j.
G_{ij} , B_{ij}	Conductance and susceptance between node i and node j
δ_{ij}	voltage angle between node i and node j
N_n	The number of nodes within the distribution system
P^i_{RE-DG}	The capacity of DG connected to node i.

$P_{RE-DG}^{i,\max}$	The maximum admitted capacity of DG at bus *i*.
ρ	Scale factor
I_m	Current magnitude of branch *m*.
$I_m^{\max}$	The maximum allowed current of branch *m*.
N_B	The number of branches
λ_q	The failure rate of component *q*.
s, *c*	The shape and scale indices of the Weibull distribution
v_{ci}	The cut-in wind speed.
v_{co}	The cut-out wind speed.
v_{rate}	The rated wind speed
P_{rated}	The rated output power of the wind unit
Γ	The set of system states sampled by MCS
$p(E)$	The probability of system state *E*
$P(E)$	The amount of load curtailment within state *E*, if exists.
ϕ_V , ϕ_I	The sets of nodes and branches which do not satisfy constraints.
$w(V_i)$, $w(I_m)$	The penalty factors.
X	A decision-making vector
ξ	A set of stochastic variables with known probability distributions.
$g_h(X,\xi) \le 0$ $(h=1,2,\cdots,N_c)$	Stochastic constraints
$f(X,\xi)$	The objective function
$\overline{f}$	The optimal value of the objective function.
α , β	The given confidence Levels.
$\Pr\{\cdot\}$	The probability of the event included in $\{\cdot\}$.
$V_i^{\min}$, $V_i^{\max}$	The maximum/minimum allowed voltage magnitudes at bus *i*.
$\alpha_{V,i}$	The confidence level for the nodal voltage of bus *i*.
$\alpha_{I,m}$	The confidence level for the current of branch *m*.

1. Introduction

Renewable Energy Distributed Generation (RE-DG) technique is receiving increased attention in recent years due to their environmental benefits and improved economy [E. J. COSTER et al, 2011]. Utilities may use the RE-DGs to relive network congestion, reduce network losses, minimize emissions, delay transmission investment and improve the reliability of electricity supply [E. J. COSTER et al, 2011; M. VARADARAJAN and K. P. UP, 2009; V. H. M. QUEZADA et al, 2006].

Although RE-DGs can bring significant benefits, they also impose new challenges to the secure and economical operation of power systems. Studies [E. J. COSTER et al, 2011; M. VARADARAJAN and K. P. UP, 2009; V. H. M. QUEZADA et al, 2006; C. S. WANG and M. NEHRIR, 2004; S. H. LEE and J. W. PARK, 2009; S. GHOSH et al, 2010; G. CELLI et al, 2005; Y. M. ATWA and E. F.

EI-SAADANY, 2009; G. GARPINELLI et al, 2011] have indicated that the beneficial effects from REs depend very much on the siting and sizing of such resources and unfavorable effects can be resulted if without appropriate planning. Hence, how to optimally plan the construction of RE-DGs to yield the maximum benefits without degrading the system security is a crucial issue. By far, lots of works [C. S. WANG and M. NEHRIR, 2004; S. H. LEE and J. W. PARK, 2009; S. GHOSH et al, 2010; G. CELLI et al, 2005; Y. M. ATWA and E. F. EI-SAADANY, 2009; G. GARPINELLI et al, 2011] has been reported to deal with the problem. Among them, the most used is the analytic model-based methods [S. GHOSH et al, 2010; G. CELLI et al, 2005; Y. M. ATWA and E. F. EI-SAADANY, 2009; G. GARPINELLI et al, 2011]. In this kind of approaches, an optimization objective, with a list of technical constraints, is formulated. Then an optimization method, such as the Genetic Algorithm (GA) or other Evolution Algorithms (EAs), is employed to search for an optimal solution which minimizes or maximizes the specified objective. In [S. GHOSH et al, 2010], the objective is defined to minimize the total related costs, such as capital cost, running cost, network loss cost and cost of energy losses, while satisfying the constraints, e.g. power balance, voltage limits, equipment capacity limits and maximum penetration limits of DG.

Since there is a high degree of uncertainty associated with the power system planning [Z. XU et al, 2006a; Z. XU et al, 2006b], e.g. the availabilities of components and fluctuation production of RE-DG, the voltage and power flow of the local system is likely to fluctuate, which may lead to over- or under-voltage at the customer's receiving point and overloading of other system components. Hence, how to reasonably account for the uncertainties, so as to maintain the secure and reliable operation of a power system, is a key issue in the decision-making procedure of siting and sizing of RE-DGs.

To cope with the uncertainties, probabilistic approaches, based on multi-scenario technique, have been extensively developed in [G. CELLI et al, 2005; Y. M. ATWA and E. F. EI-SAADANY, 2009; G. GARPINELLI et al, 2011]. Such approaches treat the uncertainty involved in a decision-making problem via a set of possible scenarios. For each scenario taken into account, an optimal planning scheme is obtained and then the best scheme is determined considering the scenarios with their probability. To accurately represent the most plausible realizations of the actual power system, the number of scenarios needed to be considered is generally very large, which may the complexities of planning analysis. In [G. CELLI et al, 2005; Y. M. ATWA and E. F. EI-SAADANY, 2009; G. GARPINELLI et al, 2011], only few representative scenarios are analyzed without considering the full spectrum of uncertainties involved.

In addition, to date, the potential of using embedded DGs to improve system reliability has not been efficiently addressed in the most established approaches. A major reason is that utilities normally do not permit islanding operations of distribution systems due to security issues. However, with the

increasing RE-DGs penetration, intentional islanding operation in some cases based on such resources becomes possible to improve local grid reliability [S. BAE and J. O. KIM, 2007].

Based on the previous works, a novel planning methodology, based on chance constrained programming (CCP), has been proposed for optimally planting RE-DG into the distribution systems so as to maximize the benefits. In this chapter, the RE-DG planning problem is formulated as a stochastic optimization problem subject to security limitations as chance constraints. The model to be developed could not only to yield the maximum benefits, but also maintain the performance of system under an uncertain environment. A new methodology is developed to evaluate the reliability of distribution systems with embedded RE-DGs, in which the intentional islanding operation of distribution grids in some cases is taken as an important way to improve system reliability and reduce outages. Based on the developed model and approach, the IEEE 37-node test system is employed to verify the effectiveness, and test results have demonstrated that the voltage profile and power flow can be significantly improved and the cost from loss of supply substantially reduced.

2. Overview of the planning method

RE-DG planning is a complex process that involves significant workloads. In general, the procedure should cover stages of reliability assessment, demand and fuel prices forecasts, security assessment, and cost and benefit analysis etc. For particularly RE planning, assessment of wind or solar resources is necessary.

The flowchart of the proposed planning method is given in Fig 6.1. The method consists of several stages including initialization, problem formulation, solving the model and the final security assessment.

1) Initialization

Utilities need to investigate the system and environment information, such as demand forecast and wind conditions, and then formulate candidate sites for DG installation.

2) Problem formulation

In this stage, the planning of DG problem is formulated as a mathematical model, with the objective to yield the maximum benefits of integration DG as well as various constraints assigned by human knowledge.

3) Solving the mathematical model

Some optimization algorithms are adopted to solve the developed mathematical model, which involves various costs and benefits evaluation for integration of DG, e.g. reliability improvement

and network loss reduction, and constraints check. A preferred option which maximizes the benefits of DG while satisfying the constraints is then obtained.

4) Final security assessment

The resultant optimal plan from the analytic model-based approach maybe, however, without considering some technique issues, e.g. conflicting to existing protection scheme and the increase of short-circuit current level. Therefore, the obtained scheme needs to be assessed by decision-makers with practical engineering and management concerns, so as to ensure the rationality for implementation.

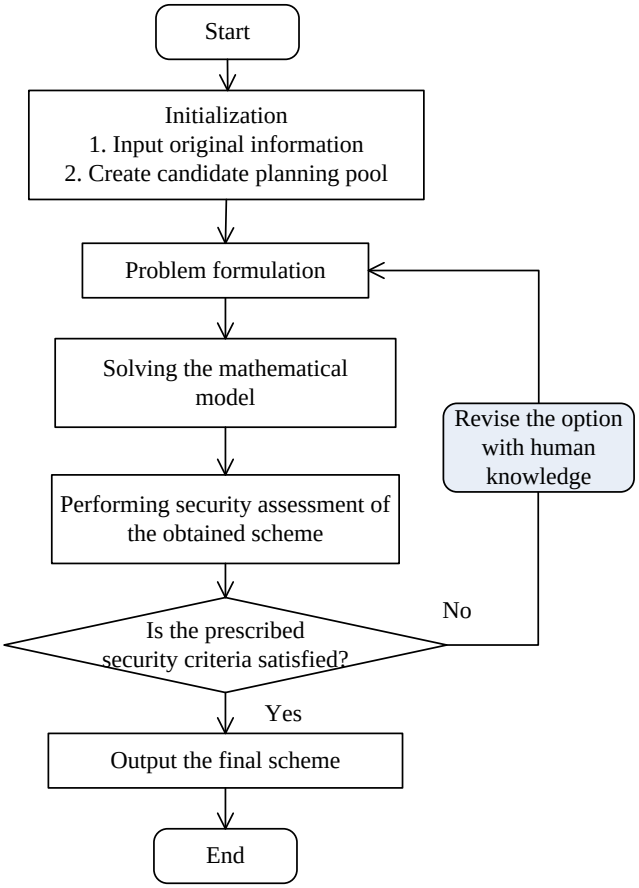

Fig 6.1 Flowchart of the hybrid planning scheme for DG

The main focus of this chapter is on a new planning approach considering uncertainties due to intermittent generations of RE-DGs and consequent impacts to the system reliability. Other works, such as demand forecasting, wind or solar resource assessment and security assessment will not be covered. The details associated will be clarified in the following sections

3. Problem formulation

3.1 Chance Constrained Programming

In a highly uncertain environment, the absolute reliability and security of power system can not be unconditionally guaranteed. To properly address uncertainties involved in RE-DG planning, the chance constrained programming (CCP) [N. YANG et al, 2007; N. YANG et al, 2005; J. WANG et al, 2004] provides a good means for solving this kind of problems. It is a stochastic programming method in which the constraints or objective function of an optimization problem contains stochastic parameters. CCP allows that the decision-making procedure does not strictly fulfil every constraint; rather the constraints are respected with a certain probability, called the confidence level, assigned by the system decision-maker, at the optimum solution point. A generalized CCP problem can be expressed as the following form.

$$\begin{cases} \min \quad \overline{f} \\ s.t. \\ \quad \Pr\ f(X,\xi) \le \overline{f}\ \ge \alpha \\ \quad \Pr\ g_h(X,\xi) \le 0\ \ge \beta\ \ (h=1,2,\cdots,N_c) \end{cases} \tag{1}$$

3.2 The Mathematical Model

1) Objective

The objective function is defined to be the minimizing of the equivalent annual total costs associated with the RE-DGs to be planned, including capital cost, running cost (operating and maintenance cost), network loss cost, and cost of supply lost, in the planning horizon. The mathematical objective is described below:

$$\begin{aligned} \min \quad & C = (C_I + C_O + C_L + C_R) = \\ \min \ \{ & \Big(\sum_{k=1}^{N_{RE-DG}} c_e P_{RE-DG,k} \Big) \Big[\frac{r(1+r)^n}{(1+r)^n - 1} \Big] + \\ & \sum_{k=1}^{N_{RE-DG}} (c_r W_{RE-DG,k}) + c_f W_P + c_w R_a \} \end{aligned} \tag{2}$$

2) Constraints

The physical constraints for RE-DGs planning are described below.

(1) Total power conservation

$$\begin{cases} P_{Gi} - P_{Li} = V_i \sum_{j=1}^{N_n} V_j (G_{ij} \cos\delta_{ij} + B_{ij} \sin\delta_{ij}) \\ Q_{Gi} - Q_{Li} = V_i \sum_{j=1}^{N_n} V_j (G_{ij} \sin\delta_{ij} - B_{ij} \cos\delta_{ij}) \end{cases} \tag{3}$$

(2) RE-DGs installed capacity constraint at each node

$$0 \le P^{i}_{RE-DG} \le P^{i,\max}_{RE-DG} \tag{4}$$

(3) Total RE-DGs installing capacity maximum penetration limit: the RE-DGs penetration should be smaller or equal to the specified amount.

$$\sum_{k=1}^{N_{RE-DG}} P_{RE-DG,k} \le \rho P^{\max}_{load} \tag{5}$$

Where ρ is usually to be 0.5.

(4) Bus voltage magnitude limit chance constraint

$$\mathrm{P_r}\{V_i^{\min} \le V_i \le V_i^{\max}\} \ge \alpha_{V,i} \quad i = 1,2,...,N_n \tag{6}$$

(5) Distribution feeder's thermal rating limit chance constraints

$$\mathrm{P_r}(|I_m| \le I_m^{\max}) \ge \alpha_{I,m} \qquad m = 1,2,...,N_B \tag{7}$$

It should be noted that depending on the market rules which guide the planning, slightly different cost and benefit evaluations may be required. The proposed approach, however, is a general approach and can be easily adapted to different situations/markets.

4. Modeling of uncertain factors

Among the uncertainties encountered in RE-DG planning, the availabilities of equipments and intermittent production are included in this chapter. However, it must be emphasized that the framework described in this chapter does not preclude the inclusion of other uncertainties.

1) Equipment availabilities

Due to unscheduled outages, the availabilities of equipments are random variables, i.e. the availability of component *q* can be expressed as:

$$p(X_q = x_j) = \begin{cases} 1-\lambda_q, & x_j = 1 \\ \lambda_q, & x_j = 0 \end{cases} \tag{8}$$

where $x_j = 1$ denotes that the component q is available, and $x_j = 0$ denotes the component is outage.

2) Output of distributed wind generator

As output from RE-DG is dependant upon the current environmental conditions, consequently, it is inherently intermittent.

Wind speed v is usually represented with Weibull distribution $\omega(s,c)$ with the probability density function [G. CELLI et al, 2005; Y. M. ATWA and E. F. EI-SAADANY, 2009; G. GARPINELLI et al, 2011]:

$$F(v) = f(V \le v) = 1 - e^{-(\frac{v}{c})^s} \tag{9}$$

The relationship between the output power of a wind generating unit and the wind speed can be formulated as [S. BAE and J. O. KIM, 2007]:

$$P = \begin{cases} 0 & 0 \le v < v_{ci} \\ P_{rate} \times \dfrac{v - v_{ci}}{v_{rate} - v_{ci}} & v_{ci} \le v < v_{rate} \\ P_{rate} & v_{rate} \le v < v_{co} \\ 0 & v > v_{co} \end{cases} \tag{10}$$

5. Solution method

5.1 Reliability Evaluation of Distribution System Containing RE-DG

Both analytical [G. CELLI et al, 2005] and simulation [S. BAE et al, 2004] techniques can be used to evaluate the reliability of an electric power system containing DGs. The analytical techniques are less time consuming, however, the uncertainties due to intermittent nature of DGs and other factors cannot be easily incorporated. Therefore, the simulation approach is used to accommodate uncertainties due to DGs in reliability evaluation of distribution networks in this chapter.

- Reliability indices

From system planning point of view, reliability indices such as the Loss of Load Probability (LOLP), Loss of Load Expectation (LOLE) and Expected Energy Not Supplied (EENS) or Expected Unserved Energy (EUE), are calculated to reflect the expected system performance on average. The most popular index is EENS, which is also adopted to assess the reliability of a distributed system with DGs in this chapter. Furthermore, the interruption cost is measured by the social production value of load loss, as described in (1).

- The main procedure

The procedure simulation based reliability assessment with DGs presence consists of the following steps.

1) System states generation

In this chapter, the non-sequential Monte Carlo Simulation (MCS) is employed to simulate the uncertainties due to equipment availabilities and intermittent DG productions. For simplicity, the operating statuses such as the unit availability and DG output are generated based on random seed variables without any chronological pattern. In addition, no correlations are considered for the operating state of each individual component.

2) Analysis of the generated states

When a system state is selected, the power system performance will be analyzed, and if necessary, corrective measures may be activated. Traditionally, all DGs are required to shut down due to security concerns e.g. when there is a fault. However, with technology advancements, DGs can now be a possible measure to improve system reliability, e.g. if islanding is allowed, DGs can continuously supply the un-faulted portions of a distribution network. Taking this into consideration, the detailed steps of system state evaluation are described in Fig 6.2.

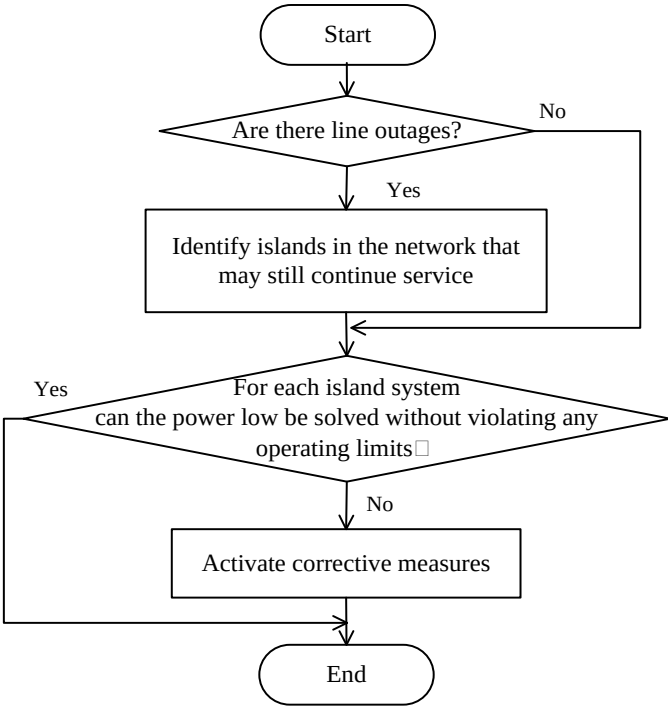

Fig 6.2 The flowchart of the system state analysis

For islanded distribution systems, the generation power must be sufficient to supply all loads while respecting various operation limitations. Otherwise, a likely consequence is the loss of at least some loads. To check this, the simplest approach here is for the operators to provide, in advance, a prioritized list of resources according to which loads shedding can be successively made until a balanced and feasible operation point is reached. However, it must be emphasized that the framework described in this chapter does not preclude other more advanced load shedding methods.

3) If the total simulation times are less than the specified maximum number, go to step 1); otherwise to step 4).

4) Computation of reliability indices. E.g., evaluate EENS using the following equation.

$$EENS / R_a = \sum_{E \in \Gamma} p(E)P(E)) \tag{11}$$

5.2 Constraints Check

When applying CCP to optimize the RE-DG planning, an important issue is to judge whether the planning scheme can fulfill the chance constraints of both the node voltage operation range and the thermal capacities of branches. In this work, the well-established Monte Carlo Simulation procedure is employed to check if chance constraints hold. MCS is a class of computational algorithm that relies on theory of probability and statistics, especially useful in studying systems with a large number of coupled degrees. The MCS algorithm has been very successfully applied in a wide variety of power system problems, such as reliability assessment and probabilistic stability analysis.

For any given planning decision, the procedure of use MCS to check the constraints is as follows [N. YANG et al, 2007]:

1) Specify the number of Monte Carlo simulations allowed, *N*.
2) Set counter *t*=0, violation times of voltage magnitude at bus *i*, $t_{V,i}=0(i=1,2,...,N_n)$, and violation times of current magnitude of branch *m*, $t_{I,m}=0(m=1,2,...,N_B)$.
3) Sample the RE-DG output.
4) Check whether if available generation and circuits are to satisfy the associated load without violating any operating limits. If "yes", go to step 5), otherwise go to step 3).
5) Calculate V_i and I_m.
6) If $V_i>V_i^{\max}$ or $V_i<V_i^{\min}$, $t_{V,i}=t_{V,i}+1$; if $|I_m|>I_m^{\max}$, $t_{I,m}=t_{I,m}+1$.
7) Set *t*=*t*+1.
8) If *t*<*K*, return to step 3), otherwise go to step 9).
9) If $(1-t_{V,i}/K)\geq\alpha_{V,i}$, the chance constraint (6) is satisfied; if $(1-t_{I,m}/K)\geq\alpha_{I,m}$, the chance constraint (7) is satisfied.

Generally, violations of constraints are handled using a penalty function approach. The penalty function is taken as (12).

$$\begin{cases} C_V=\sum_{i\in\phi_V}\sum_{t=1}^{t_{V,i}} w(V_i)(\Delta V_i)^2 \\ C_P=\sum_{m\in\phi_I}\sum_{t=1}^{t_{I,k}} w(I_m)(\Delta I_m)^2 \end{cases} \tag{12}$$

Where ΔV_i and ΔI_m are defined as follows:

$$\Delta V_i=\begin{cases} V_i-V_i^{\max} & V_i>V_i^{\max} \\ 0 & V_i^{\min}\leq V_i\leq V_i^{\max} \\ V_i^{\min}-V_i & V_i<V_i^{\min} \end{cases} \tag{13}$$

$$\Delta I_m=\begin{cases} |I_m|-I_m^{\max} & |I_m|>I_m^{\max} \\ 0 & |I_m|\leq I_m^{\max} \end{cases} \tag{14}$$

Finally, the fitness function is given below:

$$\min\ F=C_P+C_O+C_L+C_R+C_V+C_I \tag{15}$$

5.3 Harmony Search for Solving the CCP Model of RE-DG Planning

The Harmony Search (HS) algorithm [Z. W. GEEM et al, 2001; K. S. Lee and Z. W. Geem, 2005], a new meta-heuristic algorithm proposed by Z. W. Geem, has recently been developed to imitate the musical improvisation process of searching for a perfect state of harmony. The musical improvisation process seeking a pleasing harmony (a perfect state) as determined by an aesthetic standard is similar to the optimization process that seeks to search for a global solution (a perfect state) as determined by an objective function. By far, it has been successfully applied to various real-world problems like network planning [A. VERMA et al, 2010] and fault estimation [L. H. WEI et al, 2010], as its characteristics of simple in concept, less in parameters, and easy in implementation. As shown in Fig 6.3, the procedure of the HS algorithm is carried out by the following five steps:

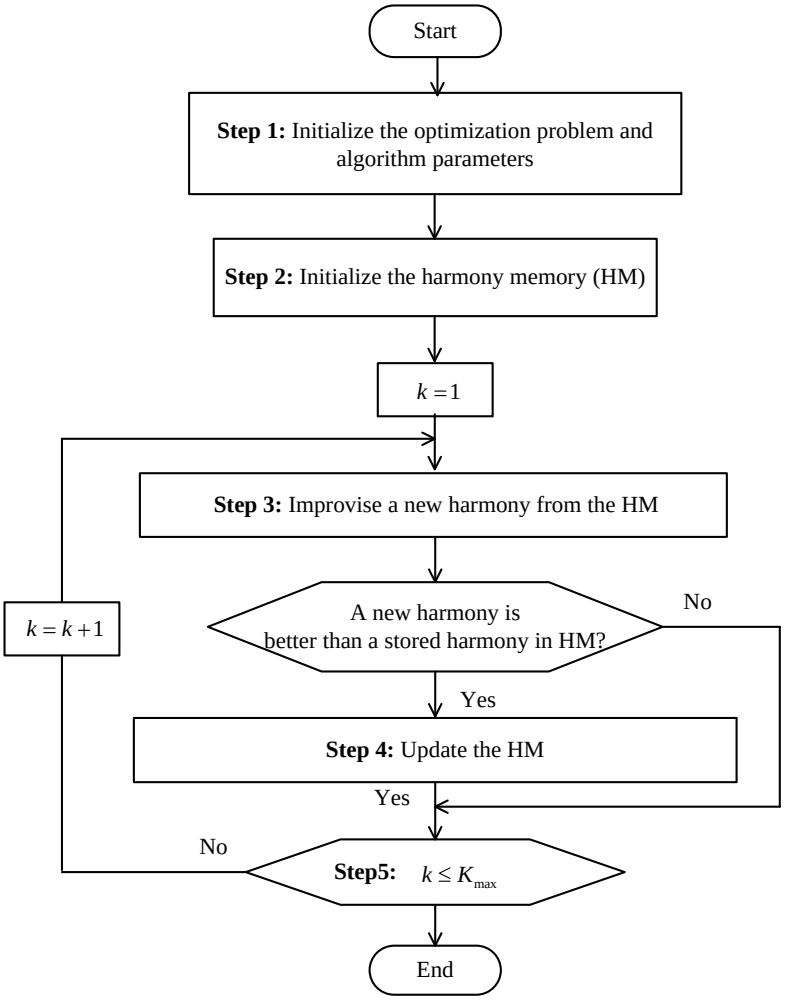

Fig 6.3 The flowchart of RE-DGs planning based on Harmony Search

It should be noted that other evolutionary computation algorithms such as DE or PSO can also be used here. The selection of a particular evolutionary algorithm is not the main focus of this chapter.

In general, the structure of solution vector for RE-DG planning problem is expressed as $\{x_1, x_2, ..., x_{N_n}\}$. "$x_i$" identifies the installed capacity within bus *i*, and $x_i = 0$ denotes that there will not be a DG built at bus *i*.

6. An application example

The modified IEEE-37, 4.8-kV system is employed to demonstrate the effectiveness of the proposed algorithm. The single line diagram of the system is shown in Fig 6.4.

For simplicity, suppose that the conditions for wind generation at each candidate installation site are the same: c=2 and s=6. The period taken into account for the planning study is 15 years long, and discount rate is 0.1. The per-unit power running cost is 200 $ /MWh. To evaluate economic loss of outage, the social production value of load loss is 25 times the per-unit power cost. The detailed parameters of candidate DGs are listed in Table 6.1. Finally, the presented methodology was developed in Visual Studio 2005.

Table 6.1 The parameters of candidate RE-DGs

Rated Capacity/kW	Operation parameters（m/s）			Associate cost		Power Factor
	v_{ci}	v_{rate}	v_{co}	c_e	c_r	
50	3	5.5	14	950	10	0.9
80	4	7	17	950	10	0.9

Table 6.2 Details of RE-DG planning schemes

Nodes		702	704	708	725	727	738	741	Total Capacity/kW
Installed Capacity /kW	Scheme A	0	130	0	80	130	50	150	540
	Scheme B	100	80	50	160	0	0	0	390

Table 6.3 Comparison of costs between scheme A and scheme B

cost （$/year）	Total annual cost	Annual installation cost	Annual cost of operation and maintenance	Annual cost of network loss	Annual cost of loss of supply
Scheme A	327696.601	67446.048	47222.663	49760.000	163267.890
Scheme B	351711.875	48711.034	27302.972	45119.999	230577.870

Table 6.4 The over-limitation of nodal voltage

Scheme A	Nodes	741	711	740	738	737	734	735	736	710	733	732	708
	Violation times	36	28	26	21	17	11	8	8	8	8	6	6
Scheme B	Nodes	720	707	722	724	706	725	713	704	710	714	701	702
	Violation times	6	4	3	3	3	3	3	2	2	2	2	2

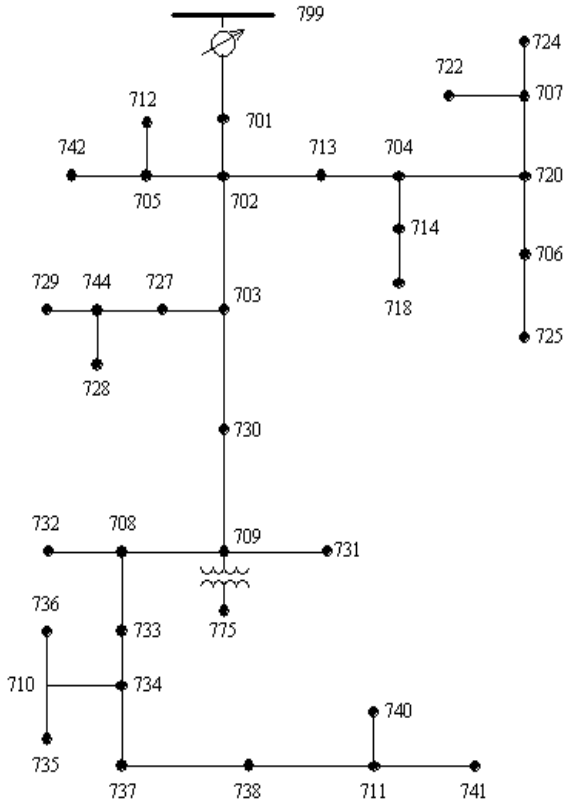

Fig 6.4 Single-line diagram of the IEEE 37-node test feeder

In what follows, two cases are analyzed in order to verify the performance of the approach developed.

Case 1): RE-DG planning when considering the cost due to loss of supply and the obtained planning scheme is called “Scheme A”.

Case 2): RE-DG planning without considering the cost due to loss of supply and the obtained planning scheme is called “Scheme B”.

Detailed planning results of Scheme A and Scheme B are listed in Table 6.2.

Comparisons of various cost for Scheme A and Scheme B are listed in Table 6.3.

The over-limitations of node voltage (the 12 worst nodes) within Scheme A and Scheme B are listed in Table 6.4.

The following can be observed from the planning results and comparisons.

1) As Table 6.3 and Fig 6.5 shown, compared to Scheme B, the cost due to energy not supplied for Scheme A is lower but annual cost due to network loss is higher. It indicates that the multiple objectives, involving issues of installation investment, network loss and reliability, may contradict each other. It is necessary for planners to give a compromise among the selected

objectives reasonably.

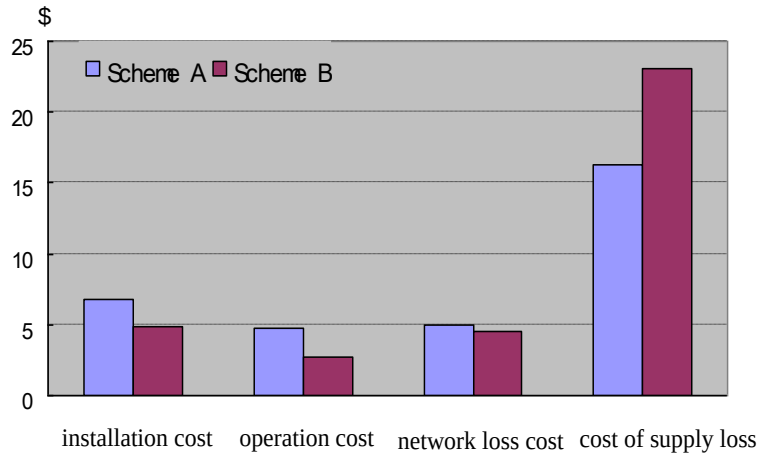

Fig 6.5 The cost comparison between scheme A and scheme B

2) From Table 6.4, it could be observed that the power flow of the local system is to fluctuate due to the uncertainty production of RE-DG and this fluctuation would cause overload on the components. And this phenomenon is getting worse gradually with an increasing penetration of DG. With the proposed method based on CCP in this chapter, the planner could manage the risk by specifying the confidence levels in advance.

7. Conclusions

Under the chance constrained programming framework, a new mathematical model is developed to handle some uncertainties, with the objective of minimizing the equivalent annual cost as well as the security limits as chance constraints. Then, an approach for assessing the reliability of distribution systems containing RE-DG, capturing the inherent uncertainty, is presented. Finally, a MCS embedded HS method is employed to solve the developed model. A case study is carried out to demonstrate the validity and essential features of the proposed model and methodology. The work presented in this work is at its initial stage of our continuous development of new planning techniques for DGs, in which we believe the hybrid CCP approach is an appropriate technique and has more potential in dealing with various uncertainties appeared with introduction of RE-DG. Further development of the proposed method is underway incorporate probabilistic indexes and additional realistic factor in DG planning, such as the transmission investment delay and emission reduction, into planning objective as well as more advanced reliability assessment.

References

E. J. COSTER, M. A. MYRZIK, and B. KRUIMER (2011). “Integration Issues of Distributed Generation in Distribution Grids.” *Proceeding of the IEEE*, 99, 28-38.

M. VARADARAJAN, K. P. UP (2009). “Assessing the Strategic Benefits of Distributed

Generation Ownership for DNOs." *IEE Proc. Generation, Transmission and Distribution*, 3, 225-236.

V. H. M. QUEZADA, J. R. ABBAD, and T. G. S. ROMAN (2006). "Assessment of Energy Distribution Losses for Increasing Penetration of Distributed Generation." *IEEE Trans. on Power Systems*, 21, 533-540.

C. S. WANG, M. NEHRIR (2004). "Analytical Approaches for Optimal Placement of Distributed Generation Sources in Power Systems." *IEEE Trans. on Power Systems*, 19, 2068-2076.

S. H. LEE, J. W. PARK (2009). "Selection of Optimal Location and Size of Multiple Distributed Generations by Using Kalman Filter Algorithm." *IEEE Trans. on Power Systems*, 24, 1393-1400.

S. GHOSH, S. P. GHOSHAL, and S. GHOSH (2010). "Optimal Sizing and Placement of Distributed Generation in a Network System." *Electrical Power and Energy Systems*, 32, 849-856.

G. CELLI, E. GHIANI, and S. MOCCI (2005), "A Multiobjective Evolutionary Algorithm for the Sizing and Siting of Distributed Generation." *IEEE Trans. on Power System*, 20, 750-757.

Y. M. ATWA, and E. F. EI-SAADANY (2009). "Probabilistic Approach for Optimal Allocation of Wind-based Distributed Generation in Distribution Systems." *IET Renew. Power Gener.*, 5, 79-88.

G. GARPINELLI, G. CELLI, and F. PILO (2001). "Distributed Generation Siting and Sizing under Uncertainty." *Pro. IEEE Porto Power Tech Conf.*

I. S. BAE, J. O. KIM (2007). "Reliability Evaluation of Distributed Generation Based on Operation Mode." *IEEE Trans. on Power Systems*, 22, 7785-790.

N. YANG, C. W. Yu, and F. S. WEN (2007). "An Investigation of Reactive Power Planning Based on Chance Constrained Programming." *International Journal of Electrical Power & Energy Systems*, 29, 650-656.

N. YANG, F. S. WEN (2005). "A Chance Constrained Programming Approach to Transmission System Expansion Planning." *Electric Power Systems Research*, 75, 171-177.

J. WANG, F. S. WEN, and R. G. YANG (2004). "Optimal Maintenance Strategy for Generation Companies Based on Chance-constrained Programming." *Automation of Electric Power Systems*, 28, 27-31.

I. S. BAE, J. O. KIM, and J. C. KIM (2004). "Optimal Operating Strategy for Distributed

Generation Considering Hourly Reliability Worth," *IEEE Trans. on Power Systems*, 19, 287-292.

Z. W. GEEM, J. H. KIM, and G. V. LOGANATHAN (2001). "A New Heuristic Optimization Algorithm: Harmony Search." *Simulation*, 76, 60-68.

K. S. Lee, Z. W. Geem (2005). "A New Meta-Heuristic Algorithm for Continuous Engineering Optimization: Harmony Search Theory and Practice." *Computer Methods in Applied Mechanics and Engineering*, 194, 3902-3933.

A. VERMA, B. K. PANIGRAHI, and P. R. BIJWE (2010). "Harmony Search Algorithm for Transmission Network Expansion Planning." *IET Proc. Generation, Transmission & Distribution*, 4, 663-673.

L. H. WEI, W. X. GUO, F. S. WEN, et al (2010). "Waveform Matching Approach for Fault Diagnosis of A High-voltage Transmission Line Employing Harmony Search Algorithm." *IET Generation, Transmission & Distribution*, 4, 801-809.

Z. XU, Z. Y. DONG, and K. P. WONG (2006). "Transmission Planning in a Deregulated Environment." *IEE Proc. Generation, Transmission and Distribution*, 153, 326-334.

Z. XU, Z. Y. DONG, and K. P. WONG (2006). "A Hybrid Planning Method for Transmission Network in Deregulation Environment." *IEEE Trans. on Power System*, 21, 925-932.

CHAPTER 7. RISK CONTROL IN TRANSMISSION SYSTEM PLANNING WITH WIND GENERATORS

1. Background

Wind power generation has drawn much more attention than ever before due to the urgent need for environmental protection and the continuous development of new technologies. For example, China, as a country with abundant wind power resources, has experienced rapid development in recent years in terms of exploiting wind energy for power generation. A large number of wind power bases with capacities of 10000 MW has been planned and constructed. It is expected that increasing numbers of large-scale wind farms will be connected to the power grids of China.

Although wind power is clean and renewable, wind farms can bring about significant unfavourable impacts on power systems due to their stochastic, intermittent and uncontrollable characteristics. With the expansion of wind power generation and thus the increasing quota of wind energy in power systems, these adverse influences could become technical barriers to wind power integration, resulting in new challenges to transmission system planning (TSP) and operation (Salehi-Dobakhshari and Fotuhi-Firuzabad, 1996; Sayas and Allan, 1996). To address these challenges, new approaches should be applied in TSP to facilitate the integration of wind energy through increasing the power system's ability to defend against the influence.

Till now, research on TSP including large-scale wind farms is still at its early stage. When taking into account the uncertainties associated with wind power generation, existing methods only evaluate the system reliability and various investment schemes (Billinton and Wangdee, 2007). A chance constrained method was proposed to resolve the uncertainties of transmission system expansion planning with wind generators. Nevertheless, the cost of computation using the convolution integral to calculate the probabilistic power flow was heavy. Accuracy of the model was also not assured due to the assumption of the normal distribution of wind power generation. Furthermore, the "N-1" reliability constraint was not considered in the planning model (Yu *et al.*, 2009). A flexible planning method based on multi-scenario probability was proposed in (Yuan *et al.*, 2009) to match the transmission system which contains large-scale wind farms. With this method, however, the simulation for the operation of a wind farm was only performed using the rating power or the zero power of wind generators and is hence unable to accurately describe the actual wind power generation.

2. The developed method

To overcome the shortcomings discussed above, this chapter presents a probabilistic model for the power output of wind generators. The DC probabilistic power flow is calculated with the combined use of cumulants and Gram-Charlier series. Three risk-controlling strategies are then introduced to enhance the system defense against security risks in allusion to the uncertain factors in TSP, and they are: probability of not violating each branch power flow limit (PBL), probability of not violating system power flow limit (PSL), probability for the security margin of system power flow (PSM).

Based on the above work, a TSP model with risk-controlling strategies is developed for power system containing wind generators. A cost-benefit method is utilized to evaluate the planning schemes in order to maximize the overall benefit.

3. Case study

The feasibility and effectiveness of the proposed TSP model is illustrated in the case study using two typical test systems: an 18-bus system and a 46-bus system, shown in Figures A1 and B1 in the appendix (A and B). The parameters of the two test systems are listed in Tables A1 and A2 as well as Tables B1 and B2, also included in the appendix. The load and the power generation of the two study systems are assumed to follow the normal distribution. The mean values of the power generation and the load are assumed to be equal to the expected values and the standard deviation equal to 4% of the mean values. These assumptions describe the uncertainties of the power generation and load demands.

Suppose that the investment cost of each line is 1.0 million RMB Yuan/km, the outage rate per unit length per year is 0.05 times/km for each line, and that the fixing rate of the line is 9.13×10^{-4} year per line for each repair. The lower limit $\underline{r_l}$ of the probability for not violating the branch power flow limit is set as 0.7. Both the base mode and the “N-1” operation status are investigated in the case study.

3.1 The 18-bus system

Currently the power system contains ten nodes and nine lines as shown in Fig 7.1 In future, the system is planned to expand to 18 nodes, composing 7 generator nodes and 17 load nodes. With the added generator nodes 11, 14, 16 and 18, the total load capacity will reach 35870 MW. The capacity of generators and loads are listed in Table A1, and the data for all branches are listed in Table A2. Suppose that the wind generators are connected to node 2 and their capacity is about 10% of that of the system.

a) Analysis of planning results

The computation time of the planning is 2 minutes and 25 seconds on a PC with Intel Core i3 CPU. Three optimal schemes are obtained as listed in Table 7.1, where the numbers enclosed by parentheses in the second column denote the numbers of the candidate lines. For example, 1-2(2) means two extra lines are to be added to the right-of-way of Line 1-2.

Table 7.1 Comparisons of the three planning schemes for the 18-bus system

Scheme	Added candidate lines	Investment cost (10^6 RMB Yuan)	R	R/C ($\times 10^{-6}$)
A	1-2 (2), 1-11 (2), 4-16 (1), 5-11 (1), 5-12 (1), 6-13 (1), 6-14 (3),7-8 (2), 7-9 (1), 7-13 (2), 8-9 (3), 9-10 (3), 9-16 (2), 10-18 (2), 11-12 (1), 11-13 (1), 12-13 (1), 14-15 (3), 16-17 (1), 17-18 (4)	389600.00	1.1510	2.9543
B	1-2 (2), 1-11 (2), 2-3 (1), 3-4 (1), 4-16 (2), 5-12 (2), 6-13 (1), 6-14 (3), 7-8 (2), 7-9 (1), 7-13 (1), 8-9 (2), 9-10 (4), 9-16 (1), 10-18 (1), 11-12 (1), 11-13 (1), 14-15 (3), 16-17 (2), 17-18 (3)	412400.00	1.1678	2.8317
C	1-2 (2), 1-11 (2), 4-16 (1), 5-12 (1), 6-13 (2), 6-14 (3), 7-8 (2), 7-9 (1), 7-13 (2), 8-9 (3), 9-10 (3), 9-16 (2), 10-18 (2), 11-12 (1), 11-13 (1), 12-13 (1), 14-15 (3), 16-17 (1), 17-18 (3)	383100.00	1.0755	2.8074

Table 7.1 shows that the investment cost of Scheme A is 1.70% more than that of Scheme C, while the security risk index R of the former is 7.02% more than that of the latter. Therefore, the cost-benefit index R/C of Scheme A is higher than that of Scheme C. The investment cost of Scheme B is the highest among the three. Compared to Scheme A, the investment of Scheme B is 5.85%

higher, whereas its security risk index is only improved by 1.46%. The higher investment cost of Scheme B does not lead to the expected level of security and reliability. In light of the above comparisons, Scheme A appears to be the optimal one due to its highest cost-benefit index and the best composite beneficial results.

To further verify the validity of the security risk index, the mean power values of generators and loads are increased by 7%. The performance of the above three schemes are assessed and compared again. The PABL of the three schemes are 78.75 %, 77.87 % and 68.92% respectively. Obviously, the lower limit of PABL in Scheme C is violated due to its weak security risk index. As a consequence, even a small load fluctuation can cause the system employing Scheme C to violate the security/reliability requirements. On the contrary, the higher security risk indexes of Scheme A and Scheme B can protect the system against the security risk.

b) Performance comparison with conventional optimal planning schemes

To verify the feasibility of the proposed TSP model, Scheme A is compared with Scheme D based on the investment minimization model. The comparison is shown in Table 7.2, where the minimum PBL represents the highest risk of violating the branch power flow limit.

Table 7.2 Comparisons of the optimal planning schemes using the developed model and the investment minimization model for the 18-bus system

Scheme	Added candidate lines	Investment cost (10^6 RMB Yuan)	minimum PBL
A	1-2 (2), 1-11 (2), 4-16 (1), 5-11 (1), 5-12 (1), 6-13 (1), 6-14 (3),7-8 (2), 7-9 (1), 7-13 (2), 8-9 (3), 9-10 (3), 9-16 (2), 10-18 (2), 11-12 (1), 11-13 (1), 12-13 (1), 14-15 (3), 16-17 (1), 17-18 (4)	389600.00	0.8797
D	1-2 (2), 1-11 (2), 4-16 (1), 5-12 (1), 6-14 (2), 7-8 (2), 7-13 (2), 7-15 (1), 8-9 (2), 9-10 (3), 10-18 (1), 11-12 (1), 14-15 (2), 16-17 (2), 17-18 (1)	257300.00	0.2616

As shown in Table 7.2, the minimum PBL of Scheme D is only 0.2616, far less than the required lower limit (0.70). Compared with Scheme A, scheme D is much less capable of defending against the security risk due to neglect of the uncertainties, in spite of its lower investment cost.

c) Power flow analysis with different wind farm characteristics

To analyse the influence of characteristics of wind farms on the system power flow, five parameters reflecting the characteristics of wind farms are adjusted respectively, with each parameter varying

in the range of $\pm 20\%$. The parameter adjustment and the influence to Scheme A are shown in Table 7.3.

Table 7.3 The probability of not violating branch power flow limits

Characteristics of wind farm		Minimum PBL	
Parameter	Adjust range	Variation	Change range
v_{ci}	-20% ~ 20%	0.9071 ~ 0.8507	3.12% ~ -3.29%

It is observed that the influence of parameter v_{ci}, c and k on power flow is significantly greater than that of the other two parameters. According to Table 3, the PBL only fluctuates slightly and still meets the specified requirement when the characteristics of wind farms change significantly, demonstrating the robust performance of the developed model.

3.2 The 46-bus system

To further verify the feasibility and effectiveness of the proposed model, a 46-bus system is adopted in the simulation of the developed model and the investment minimization model. The test system represents the southern part of the Brazilian interconnected network, which has 35 nodes and 62 rights-of-ways as shown in Fig. B1. The system is planned to expand to 46 nodes, including 12 generator nodes and 19 load nodes. With the added generator nodes 16, 28 and 31, the total load capacity will reach 6880.00MW. The capacity of generators and loads are listed in Table B1, and the data for all branches are listed in Table B2. In [ROMERO, R., MONTICELLI, A., GARCIA, A. (2002)], more detailed data and further explanations for the original system are available. Assume that only wind generators are connected to Node 17 and Node 34, and that the capacity of wind power generation is about 17.7% of the total capacity of the system. Other characteristics of the wind farm are all similar to that of the 18-bus system. The genetic algorithm is adopted and the computing time is 23 minutes and 43 seconds with the same PC. The planning results are shown in Table 7.4.

Table 7.4 Comparisons of the optimal planning schemes using the developed model and the investment minimization model for the 46-bus system

Scheme	Added candidate lines	Investment cost (10^3 dollar)	minimum PBL
E	12-14 (2), 19-21 (1), 17-19 (1), 14-22 (1), 22-26 (1), 24-33 (1), 37-39 (1), 32-43 (1), 42-44 (1), 44-45 (1), 20-21 (3), 42-43 (3), 14-15 (3), 46-10 (1), 05-11 (3), 46-06 (1), 46-03 (1), 21-25 (1), 25-32 (1), 31-32 (2), 28-31 (1), 28-30 (1), 26-29 (1), 28-41 (1), 46-11 (1), 24-25 (3), 29-30 (1), 40-41 (1), 02-03 (1), 05-06 (1), 09-10 (1)	462920.00	0.9659
F	12-14 (1), 19-21 (1), 17-19 (1), 14-22 (1), 20-21 (2), 42-43 (3), 14-15 (2), 46-10 (1), 05-11 (2), 46-06 (1), 46-03 (1), 21-25 (1), 25-32 (1), 31-32 (1), 28-31 (1), 28-30 (1), 26-29 (1), 28-43 (1), 31-41 (1), 40-45 (1), 46-11 (1), 24-25 (3), 29-30 (1), 40-41 (1), 02-03 (1), 05-06 (1), 09-10 (1)	414625.00	0.2526

Scheme E and Scheme F are the optimal planning schemes obtained using the developed model and the investment minimization model. It is observed from the table that the investment cost of Scheme E is 11.6% higher than that of Scheme F, whereas the minimum PBL of the former is 280% higher than that of the latter. Again, the proposed method is much more cost-effective compared to its conventional counterparts. As aforementioned, the low cost of the conventional methods is due to their negligence of the uncertainties and lack of risk-controlling strategies.

4. Conclusions

This chapter presents a probability model to simulate the uncertainties associated with the power output of wind generators integrated into a power system. The probability distribution of the branching power flow is obtained by the combined use of cumulants and Gram-Charlier series. This analytical approach has the advantages of low computation cost, efficiency and flexibility.

The two case studies demonstrate that it is possible to achieve a good trade-off among the security, reliability and economics of TSP schemes by employing risk-controlling strategies. Consequently, the security risks of a system associated with the uncertainties due to wind generators can be controlled using the developed TSP model.

References

BILLINTON, R., WANGDEE, W. (2007): 'Reliability-based transmission reinforcement planning associated with large-scale wind farms', *IEEE Trans. on Power Syst.*, 22, (1), pp. 34-41

ROMERO, R., MONTICELLI, A., GARCIA, A. (2002): Test systems and mathematical models for transmission network expansion planning. *IEE Proc. Gener. Transm. Distrib.*, 149, (1), PP. 27-36

SALEHI-DOBAKHSHARI, A., FOTUHI-FIRUZABAD, M. (2011): 'Integration of large-scale wind farm projects including system reliability analysis', *IET Renew. Power Gener.*, 5, (1), pp. 89-98

SAYAS, F.C., ALLAN, R.N. (1996): 'Generation availability assessment of wind farms', *IEE Proc. Gener. Transm. Distrib.*, 143, (5), pp. 507–518

YU, H., CHUNG, C. Y., WONG, K. P., et al. (2009): 'A chance constrained transmission network expansion planning method with consideration of load and wind farm uncertainties', *IEEE Trans. on Power Syst.*, 2009, 24, (3), pp. 1568-1576

YUAN, Y., WU, B. W., LI, Z. J., et al. (2009): 'Flexible planning of transmission system with large wind farm based on multi-scenario probability'. *Electric Power Automation Equipment*, 29, (10), pp. 8-12

CHAPTER 8. GENERATION SCHEDULING WITH FLUCTUATING WIND POWER

A stochastic optimization approach is proposed for the unit commitment problem with the uncertainty of wind power generation taken into account, based on mixed-integer linear programming (MILP). The problem is formulated to minimize the total operating cost of thermal units. In considering wind power generation, scenarios are generated by time series model ARMA and Latin Hypercube sampling (LHS) and the stochastic optimization problem is then transformed to a deterministic one. A large number of scenarios lead to computing complexity. Scenario reduction technology is introduced to decrease scenario number in order to reduce computing cost. The proposed formulation is tested on a ten-unit system and a 100-unit system. Simulation results show that the varying wind power generally leads to the increase of the total cost. In addition, the ramping rates of non-wind generators and the prediction precision of wind power are significant in making generation scheduling with volatile wind power generation. Moreover, the system operation cost decreases significantly if wind power is considered a spinning reserve resource.

Nomenclatures

A. Indices

S	The set of the wind power generation scenarios.
T	The set of the time periods.

B. Parameters

A_i	The coefficient of the piecewise linear production cost function of unit i
a_i , b_i , c_i	The coefficients of the quadratic production cost function of unit i.
$C_{i,hot}$, $C_{i,cold}$, t_i^{cold}	The coefficients of the startup cost function of unit i.
C_i^{sd}	The shutdown cost of unit i.
$D(t)$	The load demand in period t.
DT_i	The minimum down time of unit i.
$DT_i(0)$	The number of periods unit i has been offline prior to the first period of the time span (end of period 0).
$F_{l,i}(t)$	The slope of block of the piecewise linear production cost function of unit i.
G_i	The number of periods unit i must be initially online due to its minimum up time constraint.
K_i t	The cost of the interval t of the stairwise startup cost function of unit i.
L_i	The number of periods unit i must be initially offline due to its minimum down time constraint.
NG	The number of non-wind units.
NT	The number of periods under study (24 h).
NW	The number of wind power units.
ND_i	The number of intervals of the stairwise startup cost function of unit i.

NL_i	The number of segments of the piecewise linear production cost function of unit *i*.
$P_{i,\max}$	The active capacity of unit *i*.
$P_{i,\min}$	The minimum active power output of unit *i*.
$P_i^s(t)$	The simulated generation of power unit at time *t* in scenario s.
$P_i^{W,f}(t)$	The forecasted generation of wind power unit at time *t*.
$P_i^{W,s}(t)$	The simulated generation of wind power unit at time *t* in scenario *s*.
$R(t)$	The spinning reserve requirement in period *t*.
RD_i	The ramp-down limit of unit *i*.
RU_i	The ramp-up limit of unit *i*.
SD_i	The shutdown ramp constraint of unit *i*.
SU_i	The startup ramp limit of unit *i*.
$\lambda_{l,i}$	The upper limit of block of the piecewise linear production cost function of unit *i*.
UT_i	The minimum up time of unit *i*.
$UT_i(0)$	The number of periods unit *i* has been online prior to the first period of the time span (end of period 0).
$u_i(0)$	The initial commitment state of unit *i* (1 if it is online, 0 otherwise).
Δ_i	The permissible active power adjustment of unit *i*.

C. Variables

$C_i^d \ t$	The shutdown cost of unit *i* in period *t*.
$C_i^p \ t$	The production cost of unit *i* in period *t*.
$C_i^u \ t$	The startup cost of unit *i* in period *t*.
$p_i(t)$	The power output of unit *i* in period *t*.
$\bar{P}_i(t)$	The maximum available power output of unit *i* in period *t*.
$t_i^{off}(t)$	The number of periods in which unit *i* has been offline prior to the startup in period *k*.
$u_i(t)$	The binary variable that is equal to 1 if unit *i* is online in period t and 0 otherwise.
$\delta_{l,i}(t)$	The power generated in block of the piecewise linear production cost function of unit *i* in period *t*.

1. Introduction

Mitigating emissions of greenhouse gases causing global warming is currently one of the most pressing issues facing the electricity generation sector in industrialized countries. To that end, several continental European countries, most notably Denmark, Germany, and Spain, are increasing the level of penetration of renewable and low carbon electricity generation resources, and wind power generation (WPG) is the primary resource of this kind. The United Kingdom, although lagging its continental counterparts, is committed to cover 10% of its electricity demand from renewable resources by 2010 and reach the 20% mark by 2020 (Department of Trade and Industry of UK, 2003). In North America, although federal authorities in both the United States and Canada have been less proactive in the reduction of greenhouse gas emissions (Congress of the United

States of America, 2005, Government of Canada), several state and provincial jurisdictions have taken steps to increase the penetration of WPG and other renewable generation technologies (Bouffard and Galiana, 2008).

Wind power forecasting and associated forecasting accuracy issues are important in analyzing the impact of wind power on power system operations. Several investigations have looked at the prediction of wind speed for use in determining the available wind power. These investigations have been based on foundations such as fuzzy logic, neural networks, and time series (Hetzer et al., 2008). Although many prediction techniques are used to promote prediction accuracy, it cannot be forecasted without any error. Hence, the variation of wind power cannot be neglected.

Current generation scheduling cannot fully integrate the most essential features of non-dispatchable generation technologies like wind power. This limitation is becoming an issue for grid operators as there is increasing public and political pressure to increase the penetration of renewable generation technologies, which depend on randomly-varying weather conditions. Existing generation scheduling is however generally based on deterministic models and usually ignores the likelihood and the potential consequences of the random contingencies. Because of this limitation, this chapter proposes a generation scheduling suitable for fluctuating wind power, which is also applicable to other forms of renewable power generation.

The probabilistic approach is suitable for the modelling and prediction of varying wind power generation. In (Carpentier et al., 1996, Samer et al., 1996), scenario trees are developed to solve unit commitment problems when demand is not certain. In (Ummels et al., 2007), a simulation method, which was based on wind speed time series for dealing with volatile wind generation, employed the security-constrained economic dispatch algorithm which was further developed to investigate the impact of wind power on thermal generation unit commitment and dispatch. A stochastic model was introduced in (Barth et al., 2006) for evaluating the impact of integration of large amounts of intermittent wind power. However, the approach assumed that the generation unit status was already known. A security-constrained unit commitment algorithm which took the intermittency and volatility of wind power generation into account was presented in (Wang et al., 2008).. However, the algorithm requires a very high level of computing time and it seems that there is no practical application value for this algorithm.

The stochastic unit commitment problem is usually solved using the deterministic unit commitment algorithms. Due to developments in the last several decades, some solution techniques such as heuristics, dynamic programming, mixed-integer linear programming (MILP), Lagrangian relaxation (LR), simulated annealing, and evolution-inspired approaches (Carrión and Arroyo,

2006) have been proposed. A recent extensive literature survey on unit commitment can be found in (Padhy, 2004). MILP and LR are the most widely used. However, the benefits of the MIP formulation compared to the LR include: 1) Global optimality, 2) a more accurate measure of optimality, 3) improved modelling of security constraints, and 4) enhanced modelling capabilities and adaptability. Use of the MIP formulation to solve the Unit Commitment problem opens up many opportunities to deal directly with a number of constraints and models that tend to be very difficult to implement with the LR formulation. These include modelling of combined cycle plants, hydro unit commitment, forbidden zones, multi-area and zonal constraints, ancillary service markets, and many more (Streiffert et al., 2005). Hence, the MIP is utilized to solve the proposed optimization problem.

The rest of this chapter is organized as follows. Section 2 provides the basic mathematical model of MILP-UC. Section 3 presents the scenario generation and reduction. Section 4 proposes the formulation of UC with wind power. Two UC models considering varying wind power are detailed in section 5. The conclusions are clarified in section 6.

2. The MILP-UC Formulation

In this section, a mixed-integer linear formulation for cost-based unit commitment problem is described, which was initially proposed in (CARRIÓN and ARROYO, 2006).

2.1 The Objective Function

$$Minnimize \quad \sum_{i=1}^{NG}\sum_{t=1}^{NT}\left[C_i^p\ t\ + C_i^u\ t\ + C_i^d\ t\ \right] \tag{1}$$

The three components in Eqn. (1) are explained in the following.

1) The production cost

The quadratic generation production cost function typically used in scheduling problems can be formulated as

$$C_i^p\ t\ = a_i u_i(t) + b_i P_i(t) + c_i P_i^2(t) \tag{2}$$

As shown in Fig 8.1, the quadratic function can be approximated by a set of piecewise blocks.

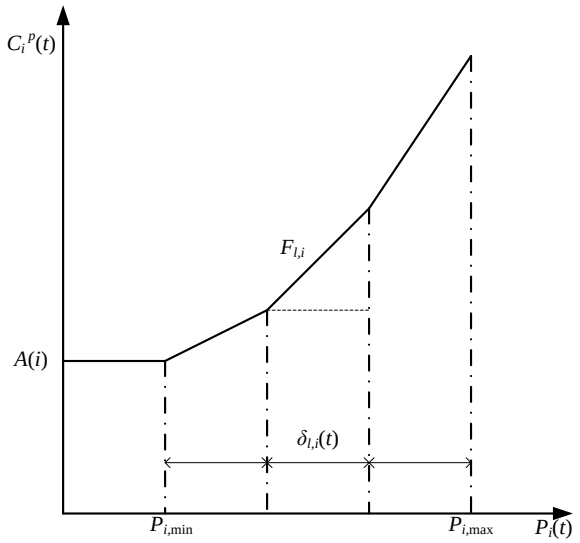

Fig 8.1 The piecewise linear energy cost function

$$C_i^p\ t\ = \mathrm{A}_i\, u_i(t) + \sum_{l=1}^{NL_i} F_{l,i}(t)\delta_{l,i}(t) \tag{3}$$

Where $\mathrm{A}_i = a_i + b_i P_{i,\min} + c_i P_{i,\min}^2$

$$P_i(t) = P_{i,\min} u_i(t) + \sum_{l=1}^{NL_i} \delta_{l,i}(t) \tag{4}$$

$$\delta_{1,i}(t) \le \lambda_{1,i} - P_{i,\min} \tag{5}$$

$$\delta_{l,i}(t) \le \lambda_{l,i} - \lambda_{l-1,i} \tag{6}$$

$$\delta_{NL_i,i}(t) \le P_{i,\max}(t) - \lambda_{NL_i-1,i} \tag{7}$$

$$\delta_{l,i}(t) \ge 0 \tag{8}$$

2) The startup cost

The discrete startup cost can be modelled as a stairwise function.

$$C_i^u\ t\ = \begin{cases} C_{i,hot}, & if \quad t_i^{off}(t) \le t_i^{cold} + DT_i \\ C_{i,cold}, & if \quad t_i^{off}(t) > t_i^{cold} + DT_i \end{cases}$$

In this work, only two situations, i.e. cold start and hot start, are considered.

$$C_i^u\ t\ \ge K_i\ k\ \cdot [u_i\ t\ - \sum_{n=1}^{k} u_i\ t-n\ ] \tag{9}$$

$$C_i^u\ t\ \ge 0 \tag{10}$$

Where $K_i\ k\ = \begin{cases} C_{i,hot}, & if \quad k = 1,\cdots, t_i^{cold} + DT_i \\ C_{i,cold}, & if \quad k = t_i^{cold} + DT_i + 1,\cdots, ND_i \end{cases}$

3) The shutdown cost

The shutdown cost is typically formulated as a constant. Similar to the startup cost, it can be modelled as follows:

$$C_i^d \quad t \quad \geq C_i^{sd}[u_i(t-1)-u_i(t)] \tag{11}$$

$$C_i^d \quad t \quad \geq 0 \tag{12}$$

2.2 The Operating Constraints of Units

1) Generation limits and ramping constraints

The generation limits of each unit in each period are set as follows:

$$P_{i,\min}u_i(t) \leq P_i(t) \leq \bar{P}_i(t) \tag{13}$$

$$0 \leq P_i(t) \leq P_{i,\max}u_i(t) \tag{14}$$

The ramp-up and startup ramp rates are limited by the following:

$$\begin{aligned}\bar{P}_i(t) \leq P_i(t-1) + RU_i \cdot u_i(t-1) + SU_i \cdot [u_i(t)-u_i(t-1)] \\ + P_{i,\max}[1-u_i(t)]\end{aligned} \tag{15}$$

$$\bar{P}_i(t-1) \leq SD_i \cdot [u_i(t-1)-u_i(t)] + P_{i,\max}u_i(t) \tag{16}$$

The ramp-down limits are imposed on the power output:

$$\begin{aligned}P_i(t-1) - P_i(t) \leq RD_i \cdot u_i(t) + SD_i \cdot [u_i(t-1)-u_i(t)] \\ + P_{i,\max}[1-u_i(t-1)]\end{aligned} \tag{17}$$

2) The minimum up and down time constraints

The minimum up and down time constraints:

$$\sum_{t=1}^{G_i}[1-u_i(t)] = 0 \tag{18}$$

$$\sum_{n=t}^{t+UT_i-1} u_i(n) \geq UT_i[u_i(t)-u_i(t-1)] \tag{19}$$

$$\sum_{n=t}^{NT}[u_i(n)-u_i(t)+u_i(t-1)] \geq 0 \tag{20}$$

Where $G_i = \min \quad NT, [UT_i - UT_i \quad 0 \;]u_i \quad 0$

The minimum up and down time constraints:

$$\sum_{t=1}^{L_i} u_i(t) = 0 \tag{21}$$

$$\sum_{n=t}^{t+DT_i-1}[1-u_i(n)] \geq DT_i[u_i(t-1)-u_i(t)] \tag{22}$$

$$\sum_{n=t}^{NT}[1-u_i(n)+u_i(t)-u_i(t-1)] \geq 0 \tag{23}$$

Where $L_i = \min\ NT,[DT_i - DT_i(0)][1-u_i\ \ 0\ ]$

2.3 The Power Balance Constraints

The active power balance or system equality constraint can be expressed as

$$\sum_{i=1}^{NG} P_i(t) = D(t) \tag{24}$$

2.4 The Spinning Reserve Constraints

$$\sum_{i=1}^{NG} P_{i,\max}(t) \geq D(t) + R(t) \tag{25}$$

Note that there is only one type of binary variables in this model, namely state variables used to describe the on/off state of units. This is the key point that is different from other MILP-UC algorithms and the major reason why this algorithm can decrease the computing time.

3. Scenario Generation and Reduction

3.1 The Wind Power Prediction

Wind power depends on weather condition and always fluctuates. Therefore, it is necessary to predict the electricity generated and demanded for the next hours to days ahead accurately and reliably for the integration of large amounts of wind power into the electricity supply system. For power plant scheduling and electricity trading the “day-ahead” prediction of demand is used; for grid operation, short-term forecasts are crucial (Pappala et al., 2009). In (Yan et al., 2009), the impact of the prediction error of wind power on unit commitment has been researched. Similar results will be illustrated in this chapter.

In (Giebel, 2003), the use of wind speed forecast with subsequent conversion to power offers no advantage over direct wind power prediction. It is found that two-stage modelling (conversion of wind speed predictions to wind power in which correlation structure in power measurements is disregarded) is inferior to models that take the power correlation into account (Giebel, 2003). Thus using direct wind power prediction might be more advantageous as it leads to higher forecast

accuracy. Moreover, the level of error would be notably lower if we were considering an aggregation of wind farms, or a complete region, thanks to smoothing effects (Focken et al., 2001).

The autoregressive moving average ARMA approach is selected here because it is a powerful, well-known time-series technique and has been used by the California Independent System Operator in some of its forecasting work (Milligan et al., 2003). Interested readers can consult (Box and Jenkins, 1976) for details. The ARMA model can be described as follows:

$$X_t - \phi_1 X_{t-1} - \cdots - \phi_1 X_{t-p} = \varepsilon_t + \theta_1 \varepsilon_{t-1} + \cdots + \theta_q \varepsilon_{t-q}$$

where p is the order of the autoregressive process of X on itself, and q is the order of the moving-average error term. The equation states that a realization of the time-series X at time t depends on a linear combination of past observations of X plus a moving average of series ε, which is the white noise process $N \sim 0, \sigma^2$ with zero mean and variance σ^2. Parameters of ARMA can be estimated from historical data.

3.2 The Sampling Technology

The well-established Monte Carlo method usually generates a large number of scenarios subject to a normal distribution as well as other distributions. Due to the large number of samples typically required, Monte Carlo simulation and optimization is often time consuming. There have been several efforts to reduce the number of samples required. One popular method is Latin Hypercube sampling, which was initially proposed by (Mckay et al., 1979).

The improvement offered by LHS over Monte Carlo can be easily demonstrated. Fig 8.2 above compares the results obtained by sampling from a normal distribution N ~ (100,100) with LHS and Monte Carlo sampling (Wang et al., 2008). Both simulations are conducted for 3000 samples. As shown in Fig 8.2, LHS can approximate the required normal distribution much better than the simple Monte Carlo method (Wang et al., 2008). It should be noted that LHS yields a stratified sample of the data, so the variance of a sample from this technique is considered smaller than that from MC (Jirutitijaroen and Singh, 2008). The detailed simulation results can be found in (http://www.vosesoftware.com/ModelRiskHelp/index.htm#Monte_Carlo_simulation/Latin_Hypercube_sampling.htm.).

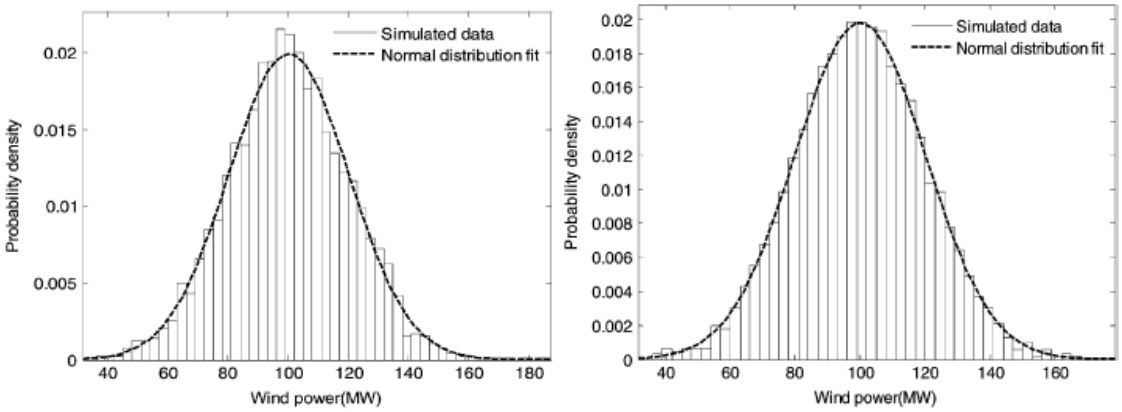

MCS LHS

Fig 8.2 The normal distribution fit by simple MCS and LHS

3.3 The Scenario Generation

Each scenario is assigned a probability, that is, one divided by the number of generated scenarios. In each scenario, an hourly random wind power generation is considered which is based on the forecasted wind power generation. (Kaut and Wallace, 2007) listed different scenario generation and reduction algorithms. In (Domenica et al., 2007) the general steps to generate scenarios can be found. The definition, goals methods of scenario generation and measuring quality of scenario trees are introduced in (Kaut, 2006).

As the focus of this chapter is not on the wind power forecasting, a wind power forecast is assumed to be available and ARMA(1, 1) model for wind power forecast error developed, which is used to predict wind speed in (Söder, 2004).

The white noise is generated by LHS, then the set of wind power forecast error scenarios can be generated by the ARMA(1, 1) model. A scenario fan is generated based on this model, and the process is shown in Fig 8.3.

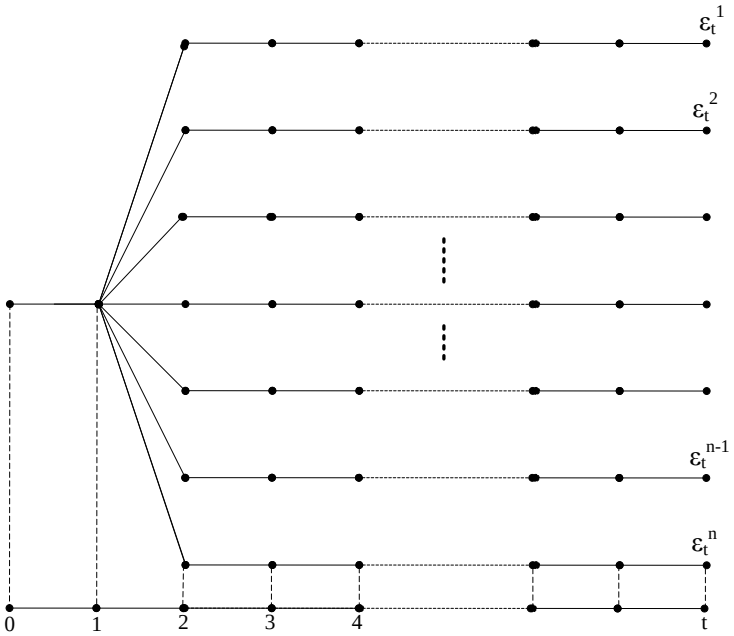

Fig 8.3 The schematic depiction of the generation of a scenario fan

3.4 The Scenario Reduction

The total number of scenarios has a double exponential dependency in the sense that a model with m stages, and n scenarios at each stage leads to a model with a total of n^m scenarios. Due to the computational complexity, it is necessary to reduce the scenarios such that its stochastic properties are not changed significantly. There are two main methods to reduce scenarios, namely moment matching (Hoyland and Wallace, 2001, Hoyland et al., 2003) and scenario reduction (Gröwe-kuska et al., 2003, Römisch and Heitsch, 2003, Dupačová, 2003). If the model demands small scenario tree sizes, moment matching then leads to better results, while for larger tree sizes, scenario reduction is more promising (Hasche, 2008).

In view of the computing expense of large-scale UC formulation, the scenario size must be very small. Hence, moment matching is used to reduce scenarios. Moment matching is based on the following parameters: mean values, standard deviations, skewness, kurtosis.

These four moments are examined for each scenario. If the four moments of a scenario match the corresponding four moments for the historical data, the scenario is accepted as a valid scenario; otherwise, it is deleted. In this way, the collection of all generated scenarios can be reduced to a practical manageable size (Zhou et al., 2009).

4. Generation Scheduling with Wind Power

Assume that the wind power is dispatched, no matter how much and when the wind power is generated. In this chapter, the variance of demand prediction is not taken into account.

There are two methods to incorporate the wind power into unit commitment. One is to take into account the wind power as a constant. In other words, the wind power can be forecasted without errors. The other one is the stochastic approach. The two strategies are presented as follows. Uncertainties are observed in wind power generation and a stochastic approach is most suitable for the modeling of generation. It is natural to transform a stochastic approach to a deterministic problem in the solving process.

4.1 The Deterministic Model

The wind power is taken as a constant in this strategy. In this case, the only difference from the traditional UC model is the power balance constraints.

$$\sum_{i=1}^{NG} P_i(t) + \sum_{i=1}^{NW} P_i^{W,f}(t) = D(t) \tag{26}$$

In this case, Eqn. (24) are replaced by Eqn. (26). The basic assumption in the deterministic model is that wind power is predicted without any error.

4.2 The Stochastic Model

Fig 8.4 shows the framework of the stochastic unit commitment. Historical data is used to estimate the parameters in the ARMA model and it is the so called preprocessed process. Scenarios generated by the ARMA approach, LHS introduced in section 2 and scenario reduction technology are also used to reduce the scenario number with the consideration of the computing complexity. Integrating the scenario data to MIP UC model is a key step to optimize the solution, because the solution must satisfy all the constraints involving any scenario data.

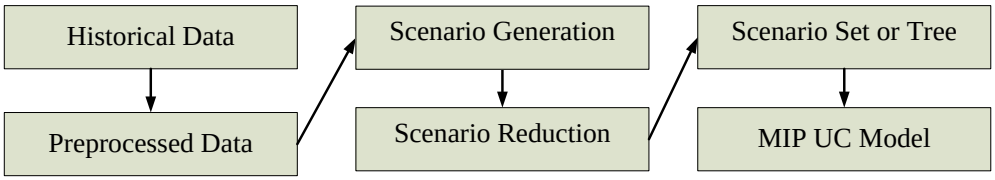

Fig 8.4 The Framework of the Stochastic Unit Commitment

Eqn. (24) is replaced by Eqn. (28). In each scenario, the simulated wind power takes in the place of the forecasted wind power. Eqn. (29) represents extra ramping constraints, which are the significant differences between the stochastic model and the deterministic model.

$$\sum_{i=1}^{NG} P_i^s(t) + \sum_{i=1}^{NW} P_i^{W,s}(t) = D(t) \tag{27}$$

$$P_{i,\min} u_i(t) \le P_i^s(t) \le P_{i,\max} u_i(t) \tag{28}$$

$$-\Delta_i \le P_i(t) - P_i^s(t) \le \Delta_i \tag{29}$$

In the day-ahead unit commitment the solutions are produced in the deterministic model based on the mean wind power in each hour. In an hour, the wind power is likely to fluctuate rather than keep constant. In order to keep the system stable, real time dispatch acts. However, the generation scheduling results, obtained by the day-ahead unit commitment, may be impossible to correct with the real time dispatch for the ramping limits of non-wind units. Hence, the constraints (29) are added in the stochastic model to make sure that the fluctuation of wind power can be made up by non-wind units. In this chapter, permissible real power adjustment Δ_i denotes 10 minutes ramping of unit *i*.

5. Case Studies

A ten-unit system and a 100-unit system are used for testing the proposed algorithm considering the uncertainty of wind power generation. The impact of large-scale integration of wind power to power system is analyzed based on economic indices such as operation costs and system security.

Table 8.1 System Data 1

Units	Pmax (MW)	Pmin (MW)	Ton (h)	Toff (h)	IniState (h)
1	455	150	8	8	8
2	455	150	8	8	8

3	130	20	5	5	-5
4	130	20	5	5	-5
5	162	25	6	6	-6
6	80	20	3	3	-3
7	85	25	3	3	-3
8	55	10	1	1	-1
9	55	10	1	1	-1
10	55	10	1	1	-1

5.1 A 10-unit System

In this study, a 10-generator system was used for test purposes. The data of the ten-unit system of (Barth et al., 2006) is provided in Tables 8.1-8.3. Without the consideration of transmission constraints, a single wind unit can represent all the wind generators and the forecasted wind power is shown in Table 8.3. A spinning reserve requirement of 10% of the load demand has to be met in each of the 24 hourly periods in which the time span is divided. The ramping of all non-wind units is assumed to be the same at180 MW/hour.

Table 8.2 System Data 2

Units	a ($/h)	b ($/MWh)	c ($/MW^{2}h)	hc ($/h)	cc ($/h)	t_{cold} (h)
1	1000	16.19	0.00048	4500	9000	5
2	970	17.26	0.00031	5000	10000	5
3	700	16.6	0.00200	550	1100	4
4	680	16.5	0.00211	560	1120	4
5	450	19.7	0.00398	900	1800	4
6	370	22.26	0.00712	170	340	2
7	480	27.74	0.00079	260	520	2
8	660	25.92	0.00413	30	60	0
9	665	27.27	0.00222	30	60	0
10	670	27.79	0.00173	30	60	0

Table 8.3 System Data 3

Hour	Load (MW)	$P^{w,f}$ (MW)	Hour	Load (MW)	$P^{w,f}$ (MW)
1	700	190	13	1400	390
2	750	300	14	1300	340
3	850	330	15	1200	320
4	950	360	16	1050	120
5	1000	350	17	1000	10
6	1100	370	18	1100	40

7	1150	440	19	1200	50
8	1200	460	20	1400	20
9	1300	350	21	1300	5
10	1400	250	22	1100	250
11	1450	420	23	900	350
12	1500	380	24	800	240

The model has been implemented on a PC with the AMD Sempron 2800+ and 512 MB of RAM memory using CPLEX 10.1 to solve the proposed formulation.

Table 8.4 Generation Scheduling with Forecasted Wind Power

Hour	Units									
	1	2	3	4	5	6	7	8	9	10
1	180	150	69	86	25	0	0	0	0	0
2	235	150	20	20	25	0	0	0	0	0
3	305	150	20	20	25	0	0	0	0	0
4	375	150	20	20	25	0	0	0	0	0
5	432	153	20	20	25	0	0	0	0	0
6	449.67	208	20	27.333	25	0	0	0	0	0
7	382	263	20	20	25	0	0	0	0	0
8	455	208	20	32	25	0	0	0	0	0
9	455	263	71.333	90.667	25	20	25	0	0	0
10	455	355	130	130	25	20	25	10	0	0
11	455	263	100.67	121.33	25	20	25	10	10	0
12	455	305	130	130	25	20	25	10	10	10
13	455	258	89	108	25	20	25	10	10	10
14	455	243	81.333	100.67	25	20	25	10	0	0
15	455	150	107.33	122.67	25	20	0	0	0	0
16	455	190	130	130	25	0	0	0	0	0
17	455	250	130	130	25	0	0	0	0	0
18	455	320	130	130	25	0	0	0	0	0
19	455	410	130	130	25	0	0	0	0	0
20	455	455	130	130	155	20	25	10	0	0
21	455	455	130	130	70	20	25	10	0	0
22	455	285	20	20	25	20	25	0	0	0
23	340	165	0	0	25	20	0	0	0	0
24	390	150	0	0	0	20	0	0	0	0

1) The Deterministic Model

In this case, wind power is assumed to be forecasted without error. Hence, this is equivalent to the situation that the actual load demand subtracts a certain amount of wind power. Eqns. (1)–(23) and (26) constitute the deterministic MILP-UC model, whose results are given in Table 8.4. The

cheapest Unit 1 , Unit 2 are committed during this decision period without any doubt. Unit 5 is also very cheap and not committed in the last hour. Unit 3 and Unit 4 are both committed between hour 1 and hour 23. Unit 8 – Unit 10 are the most expensive units, so they are committed only for a few hours. The total operation cost is $470586.04. The model contains 9845 constraints, 5041 variables, 240 binary variables and the solving time is 2.09 seconds.

2) The Stochastic Model

In this case, it is supposed that the white noise process of ARMA(1,1) model proposed in section 4.3 obeys a normal distribution with the standard deviation of 10%. According to scenario reduction technology, 1000 scenarios are generated for each hourly wind power by LHS introduced in section IV. Only ten scenarios remain after moment matching, as shown in Table 8.5.

Eqns. (1)-(25), (27)-(29) constitute the stochastic MILP-UC model, whose results are given in Table 8.6. According to Table 8.5 and Table 8.6, the generation scheduling results of most non-wind units keep steady. The outputs of non-wind units, which are different from those of the deterministic model, are marked in shadow.

Table 8.5 Scenarios Generated

Hour	Wind power scenarios									
	1	2	3	4	5	6	7	8	9	10
1	182.07	167.39	206.13	197.64	175.03	203.44	160.13	215.57	188.35	190.91
2	315.78	286.13	341.13	329.1	281.87	313.69	269.84	303.03	252.85	294.19
3	329.79	361.58	332.04	288.57	343.73	286.63	318.39	379.77	350.21	311.83
4	369.61	322.15	274.8	366.26	333.11	385.62	408.29	359.38	348.39	395.44
5	402.17	371.06	341.74	288.12	382.87	324.87	357.33	316.98	360.58	337.42
6	354.13	315.78	323.39	394.07	418.13	344.88	371.26	387.04	367.74	402.5
7	466.84	403.36	395.15	454.12	443.66	382.86	488.53	439.09	550.32	419.91
8	464.3	382.94	421.46	480.2	514.5	441.41	537.2	414.4	498.27	456.06
9	305.61	405.11	370.71	324.98	334.28	392.02	355.15	367.66	342.18	275.63
10	248.02	192.02	238.63	255.35	258.19	264.26	230.83	217.99	275	294.95
11	494.84	384.84	457.07	439.81	380.84	417.4	407.46	450.56	426.27	345.28
12	361.18	337.57	388.34	318.47	400.28	375.24	446.66	389.74	415.25	348.25
13	334.15	350.13	422.33	426.64	359.23	453.53	398.44	402.15	385.62	378.44
14	346.37	351.02	330.85	294.13	387.44	317.48	369.74	358.85	308.79	332.49
15	300.99	350.73	337.15	332.97	310.44	316.81	367.93	324.14	270.71	285.95
16	121.54	116.48	106.76	96.936	119.99	130.49	138.06	129.89	112.09	125.73
17	9.6226	10.044	7.8299	11.302	10.579	11.143	9.9483	10.271	9.3587	9.1359
18	36.571	52.929	39.175	37.999	36.989	34.369	44.632	42.215	41.235	40.825

19	55.17	52.535	61.054	43.528	43.947	53.195	49.574	50.394	47.06	48.431
20	18.687	19.318	21.5	20.123	19.791	20.532	15.728	21.759	18.127	23.249
21	4.8292	5.3131	4.6791	6.1619	5.0676	4.93	5.2196	5.4909	4.4765	4.2588
22	259.88	249.17	200.52	280.2	233.68	250.88	291.94	268.58	228.37	239.3
23	353.25	382.96	332.1	412.56	367.66	322.17	298.49	312.91	343.09	378.59
24	229.88	227.13	270.43	275.03	240.69	210.08	234.39	247.61	257.13	188.88

The total operation cost increases 0.01% to $470633.3167. It is shown by simulation results that the expected schedule cost under stochastic programming is generally more than that under the deterministic model. The difference in operating costs between the stochastic model and the deterministic model ($470633.3167–$470586.0391= $47.2776) is the cost of maintaining the system security when considering the variation of wind power. Compared to the security of the system, the extra cost is insignificant, since the cost can be easily compensated for by the benefit brought by the security of system and policy inclination. The stochastic model contains 19685 constraints, 7441 variables, 240 binary variables and the solving time is 5.8 seconds.

Table 8.6 Generation Scheduling with Varying Wind Power

Hour	Units									
	1	2	3	4	5	6	7	8	9	10
1	180	150	69	86	25	0	0	0	0	0
2	223.87	150	20	31.13	25	0	0	0	0	0
3	285.23	150	20	39.77	25	0	0	0	0	0
4	356.71	150	20	38.29	25	0	0	0	0	0
5	412.83	153	20	39.17	25	0	0	0	0	0
6	449.67	208	20	27.333	25	0	0	0	0	0
7	331.68	263	40.32	50	25	0	0	0	0	0
8	449.8	208	20	37.2	25	0	0	0	0	0
9	455	263	71.333	90.667	25	20	25	0	0	0
10	455	355	130	130	25	20	25	10	0	0
11	455	263	100.67	121.33	25	20	25	10	10	0
12	455	305	130	130	25	20	25	10	10	10
13	455	258	89	108	25	20	25	10	10	10
14	455	243	81.333	100.67	25	20	25	10	0	0
15	455	150	107.33	122.67	25	20	0	0	0	0
16	455	190	130	130	25	0	0	0	0	0
17	455	250	130	130	25	0	0	0	0	0
18	455	320	130	130	25	0	0	0	0	0
19	455	410	130	130	25	0	0	0	0	0
20	455	455	130	130	155	20	25	10	0	0
21	455	455	130	130	70	20	25	10	0	0
22	455	285	20	20	25	20	25	0	0	0
23	322.44	180	0	0	25	22.56	0	0	0	0
24	384.97	155.03	0	0	0	20	0	0	0	0

3) Ramping Capabilities of Non-Wind Units and the Prediction Error of Wind Power

To show the impact of precision of wind power prediction, the standard deviation increase from 5% to 35% of the forecasted value with the ten-minutes ramping rate of non-wind units of 30MW/10-minute and the results are shown in Table 8.7. The security cost is defined as the difference between the operation cost with predicted wind power and that with variable wind power. The security cost in the fourth column reflects the cost of maintaining the security of the system when the wind power is uncertain. As shown in the table, the more accurate the prediction level is, the more the security costs needed to be paid.

The ramping requirements of non-wind units are strongly associated with the prediction errors of wind power. The results of increasing the ten-minutes ramping rate of non-wind units from 30 MW/10-minute to 50 MW/10-minute are shown in Table 8.8. The tolerance range of the volatility of wind power expands as the ramping capabilities increase, and vice versa. Owing to the faster ramping, the standard deviation of forecasted wind power is allowed to be 30%. Another benefit of faster ramping is that the cost to maintain the system in a secure and reliable state decreases.

Table 8.7 The Impact of Prediction Errors

Standard Deviation	Feasible/ Infeasible	Operation Cost ($)	Security Cost ($)
0	feasible	470586.0391	0
5%	feasible	470589.3508	3.3117
10%	feasible	470633.3167	47.2776
15%	feasible	471859.8933	1273.854
20%	feasible	482084.2494	11498.21
25%	feasible	486160.5988	15574.56
30%	Infeasible	/	/
35%	Infeasible	/	/

Table 8.8 The Impact of Ramping on Prediction Errors

Standard Deviation	Feasible/ Infeasible	Operation Cost ($)	Security Cost ($)
0	feasible	470586.0391	0
5%	feasible	470586.1657	0.1266
10%	feasible	470633.3167	47.2776
15%	feasible	470643.4630	57.4239
20%	feasible	474885.6065	4299.567
25%	feasible	475380.9308	4794.892
30%	Infeasible		
35%	Infeasible	/	/

4) Wind power as spinning reserve resource

Usually, wind power is not considered as a resource to supply spinning reserve, so spinning reserve of a power system is given by traditional power, etc. thermal plant, as shown in equation (25). With the development of wind power prediction technology and the increase of wind power installed capacity, it is necessary to consider wind power as offering a certain share of spinning reserve. Given this condition, wind power is looked upon as reliable power, which can give electricity assistance to satisfy the demand in order to keep the power system stable.

$$\sum_{i=1}^{NG} P_{i,\max}(t) + P_i^{W,f}(t) \geq D(t) + R(t) \tag{30}$$

Table 8.9 Total Operating Costs under Different Spinning Reserve Constraints

/	Non-Wind spinning reserve($)	Wind spinning reserve($)
The deterministic model	470586.0391	427893.6444
The stochastic model	470633.3167	431076.5314

The deterministic model and stochastic model can be reformed, if equation (25) is replaced by equation (30). Table 8.9 shows the total operation cost under different spinning reserve constraints. It is obvious that the total operation cost decreases when wind power is considered as a spinning reserve source. Similar to case 1, case 2 and case 3, security costs also need to be paid if the wind power is volatile.

5.2 A 100-unit System

The 100-unit system is generated by replicating the ten-unit system above ten times. A spinning reserve requirement of 10% of the load demand has to be met in each of the 24 hourly periods. The total installed wind power capacity is 10 times as big as that in the former system. In CPLEX, an optimality parameter can be specified to decide whether to find the optimal solution or to quickly obtain a suboptimal solution. In this case study, the execution of CPLEX was stopped when the value of the objective function was within 0.5% of the optimal solution (Carrión and Arroyo, 2006).

$$\text{The MIP Gap} = \left| \left(\frac{\text{Best Integer-Best LP}}{\text{Best LP}} \right| \times 100\ \%$$

The MIP Gap provides a good measure of optimality that can be considered as convergence criteria in (STREIFFERT et al, 2005). The deterministic model contains 98009 constraints, 50401 variables, 2400 binary variables. The MIP Gap in this model is 0.41% and the total cost is $4678421.242, which costs 125.8 seconds. The stochastic model contains 194249 constraints, 74401 variables, 2400 binary variables. The MIP Gap in this model is 0.45% and the total cost is $46810404.35, which costs 184.6 seconds.

6. Conclusions

A stochastic optimization approach is proposed for the unit commitment problem considering the uncertainty of wind power generation, based on the mixed-integer linear programming (MILP). The problem is formulated as minimizing the total cost of thermal units. To consider wind power generation, scenarios are generated using scenario generation techniques. The stochastic problem is hence transformed to a deterministic one.

Since LHS produces a stratified sample of the data, the variance of samples from LHS is smaller than that from simple Monte Carlo sampling. Time series model ARMA generates a fan with the white noise process which is implemented by LHS. In order to tackle the problem of a huge number of scenarios, scenario reduction technology is introduced. The MILP-UC algorithm developed is efficient, and scenarios reduction technology gives the possibility to explore a practical algorithm for considering varying wind power generation.

A 10-unit system and 100-unit system are employed for demonstrating the proposed model and method. It is shown by simulation results that the expected scheduling cost by using stochastic programming is generally more than that using the deterministic model. This is because the stochastic model took into account the situation that the thermal units cannot meet the prediction error in time caused by the variation of wind power. Hence, the ramping capabilities of units and prediction accuracy of wind power are crucial when wind power varies.

References

Department of Trade and Industry of UK. Energy white paper. (2003) Our energy future—creating a low carbon economy. http://www.dti.gov.uk/files/file10719.pdf

Congress of the United States of America. (2005) Energy policy act of 2005. http://frwebgate.access.gpo.gov/cgi-bin/getdoc.cgi?dbname=109_cong_bills&=f:h6enr.txt.pdf

Government of Canada. Moving forward on climate change: A plan for honouring our Kyoto commitment. http://www.climatechange.gc.ca/kyoto_commitments/report_e.pdf

BOUFFARD, F. & GALIANA F. D. (2008) Stochastic security for operations planning with significant wind power generation. IEEE Trans. Power System, 23, (2), 306-316.

HETZER, J., YU D.C. & BHATTARAI, K. (2008) An economic dispatch model incorporating wind power, IEEE Trans. Energy Conversion, 23, (2), 603-611.

CARPENTIER, P., COHEN, G., CULIOLI J.-C. & AUD, RENAUD A. (1996) Stochastic Optimization of Unit; Commitment: a New Decomposition Framework. IEEE Trans. on Power System, 11, (2), 1067-1073.

SAMER T., JOHN R.B., & ERIK L. (1996) A Stochastic Model for the Unit Commitment Problem. IEEE Trans. on Power Systems, 11, (3), 1497-1508.

UMMELS, B.C., GIBESCU, M. PELGRUM, E., KLING, W.L., & BRAND, A.J. (2007) Impacts of wind power on thermal generation unit commitment and dispatch. IEEE Trans. Energy Conversion, 22, (1), 44–51.

BARTH, R., BRAND, H., MEIBOM, P., & WEBER, C. (June 2006) A stochastic unit-commitment model for the evaluation of the impacts of integration of large amounts of intermittent wind power. Proc. Int. Conf. Probabilistic Methods Applied to Power Systems, 11–15.

WANG, J.H., SHAHIDEHPOUR, M., & LI Z.Y. (2008) Security-constrained unit commitment with volatile wind power generation. IEEE Trans. Power Systems, 23, (3), 1319-1327.

CARRIÓN, M., & ARROYO, J.M. (2006) A Computationally efficient mixed-integer linear formulation for the thermal unit commitment problem. IEEE Trans. Power Systems, 21, (3), 1371-1378.

PADHY, N.P. (2004) Unit commitment—A bibliographical survey. IEEE Trans. Power Syst., 19, (2), 1196-1205.

STREIFFERT, DAN., PHILBRICK, R., & OTT A. (June 2005) A Mixed Integer Programming Solution for Market Clearing and Reliability Analysis. Proc. Int. Conf. IEEE Power Engineering Society General Meeting, San Francisco, 2724-2731.

PAPPALA, V.S., ERLICH, I., ROHRIG, K. & DOBSCHINSKI J. (2009) A Stochastic Model for the Optimal Operation of a Wind-Thermal Power System. IEEE Trans. Power Syst., 24, (2), 940-950.

YAN, Y., YANG, S.H. WEN, F.S., & MACGILL I. (April 2009) Generation Scheduling with Volatile Wind Power Generation. Proceedings of SUPERGEN 2009.

GIEBEL, G. (2003) The state-of-the-art in short-term prediction of wind power A lit- erature overview. Position paper for the ANEMOS project. http://anemos.cma.fr.

FOCKEN, U., LANGE, M., & WALDL, H.P. (2001) Previento: a wind power prediction system with an innovation upscaling algorithm. Proc. Int. Conf. the 2001 European Wind Energy Association Conference, EWEC'01, 82-829.

MILLIGAN, M., SCHWARTZ, M. & WAN, Y. (2003) Statistical Wind Power Forecasting Models: Results for U.S. Wind Farms, Research Report.

BOX, G.E.P., & JENKINS, G.M. (1976) Time Series Analysis: Forecasting and Control. 2nd ed. Holden-Day Press.

MCKAY, M.D., BECKMAN, R.J. & CONOVER, W.J. (1979) A comparison of three methods for selecting values of input variables in the analysis of output from a computer code. Technometrics, 21, (1), 239–245.

JIRUTITIJAROEN, P. & SINGH, C. (2008) Reliability constrained multi-Area adequacy planning using stochastic programming with sample-average approximations. IEEE Trans. on Power Systems, 23, (2), 504–513.

http://www.vosesoftware.com/modelriskhelp/index.htm#monte_carlo_simulation/latin_hypercube_sampling.htm.

KAUT, M. & WALLACE, S.W. (2007) Evaluation of scenario generation methods for stochastic programming. Pac. J. Optimiz., 3, (2), 257–271.

DOMENICA, N.D., BIRBILIS, G., MITRA, G., & VALENTE, P. (2007) Stochastic programming and scenario generation within a simulation framework: an information systems perspective. Decision Support Systems, 42 , (4), 2197-2218.

KAUT, M. (2006) Scenario generation for stochastic programming a practical introduction. Tutorial on Scenario Reduction, http://work.michalkaut.net/papers_etc/scen-gen_intro.pdf.

SÖDER, L. (September 2004) Simulation of wind speed forecast errors for operation planning of multi-area power system. Proc. Int. Conf. PMAPS, Ames, 723-728.

ZHOU, Q., TESFATSION, L., & LIU, C.C. (March 2009) Scenario Generation for Price

Forecasting in Restructured Wholesale Power Markets. Proc. Int. Conf. IEEE Power Systems & Exposition Conference, 1-8.

HOYLAND, K. & WALLACE, S.W. (2001) Generating Scenario Trees for Multistage Decision Problems. Management Science, 47, (2), 295–307.

HOYLAND, K., KAUT, M. & WALLACE, S.W. (2003) A Heuristic for Moment-Matching Scenario Generation. Computational Applications and Optimization, 24, (2-3), 169-185.

GRÖWE-KUSKA, N., HEITSCH, H., & RÖMISCH, W. (June 2003) Scenario reduction and scenario tree construction for power management problems. Proc. Int. Conf. IEEE Bologna Power Tech, 1-7.

RÖMISCH, W., & HEITSCH, H. (2003) Scenario reduction algorithms in stochastic program. Computational Optimization and Applications, 24, (2-3), 187–206.

DUPAČOVÁ, J., GRÖWE-KUSKA, G., & RÖMISCH, W. (2003) Scenario reduction in stochastic programming. Mathematical Programming. 95, (3), 493–511.

HASCHE B. (2008) Scenario Tree Generation for an Electricity Market Model. Research Report.

CONCLUDING REMARKS

The research outcomes presented in this report cover the wind power forecasting, optimal siting and sizing of DGs, risk control in transmission system planning with wind generators, generation scheduling with wind generators, as well as the greenhouse gas abatement effect. The reported research is comprehensive and involves the planning and operation aspects associated with DGs.

The following research outcomes have been achieved:

1. An algorithm is developed for the calculation of the life cycle cost (LCC) and green house gas abatement. The algorithm determines the most economical and environmentally friendly hybrid DG unit combination that can be accommodated to an active distribution network. The algorithm offers the most beneficial distributed generation unit mix and their capacities respective to the geographical location of the system. The software program was developed and scripting the algorithm using IPLAN subroutines to work in conjunction with PSS®E software. The program facilitates to differentiate the LCC benefits, GHG emission levels, and combined effects. Such options are vital in trading off the business objectives of distributed energy business.
2. A RBF neural network based prediction model is developed based on the wind speed, temperature, and historical wind generator outputs. Prediction is conducted using the real 2009 annual data from a wind farm in Guangdong, China. The prediction achieved high accuracy with the prediction error below 10% most of the time. The simulation shows that the exceptional data must be eliminated in wind power forecasting in order to achieve higher precision of prediction. Although some progress achieved, wind power forecasting is still an issue not well solved.
3. For the optimal siting and sizing problem, much research work is presented in this report including a Modified Primal-Dual Interior Point Algorithm based and chance constrained programming based methods. In the chance constrained programming framework, a new mathematical model is developed to handle some uncertainties, with the objective of minimizing the equivalent annual cost as well as the security limits as chance constraints. Then, an approach for assessing the reliability of distribution systems containing DGs, capturing the inherent uncertainty, is presented. The work presented in this work is at its initial stage of our continuous development of new planning techniques for DGs, in which we believe the hybrid CCP approach is an appropriate technique and has more potential in dealing with various uncertainties appeared with introduction of DGs. Further development of the proposed method

is underway incorporating probabilistic indexes and additional realistic factor in DG planning, such as the transmission investment delay and emission reduction, into planning objective as well as more advanced reliability assessment.

4. Risk control in transmission system planning with wind generators is systematically investigated. A probability model is employed to simulate the uncertainties associated with the power output of wind generators integrated into a power system. The probability distribution of the branching power flow is obtained by the combined use of cumulants and Gram-Charlier series. This analytical approach has the advantages of low computation cost, efficiency and flexibility. Two case studies demonstrate that it is possible to achieve a good trade-off among the security, reliability and economics of transmission system programming (TSP) schemes by employing risk-controlling strategies. Consequently, the security risks of a system associated with the uncertainties due to wind generators can be controlled using the developed TSP model. Some further research is demanded to build the integrated/equivalent wind generator model for a wind farm with numerous small wind generators so as to reduce the computational burden of the transmission planning problem.
5. To address the generation scheduling problem with fluctuating wind power, a stochastic optimization approach is proposed for the unit commitment problem considering the uncertainty of wind power generation, based on the mixed-integer linear programming (MILP). The problem is formulated as minimizing the total cost of thermal units. A 10-unit system and 100-unit system are employed for demonstrating the proposed model and method. It is shown by simulation results that the expected scheduling cost by using stochastic programming is generally more than that using the deterministic model. This is because the stochastic model took into account the situation that the thermal units cannot meet the prediction error in time caused by the variation of wind power. Hence, the ramping capabilities of units and prediction accuracy of wind power are crucial when wind power varies. For the unit commitment problem in large scale power systems with numerous wind units, the computational efficiency of the solving algorithm is still an issue to be further investigated.

APPENDIX A

Table A1 Bus data of the 18-bus system

Bus no	Power of generator (MW)	power of load (MW)	Bus no	Power of generator (MW)	power of load (MW)
1	0	550	10	7500	940
2	3600	840	11	5400	7000
3	0	1540	12	0	1900
4	0	380	13	0	1100
5	7600	6390	14	5400	320
6	0	1990	15	0	2000
7	0	2130	16	4950	1320
8	0	880	17	0	4000
9	0	2590	18	1420	0

Table A2 Branch data of the 18-bus system

Branch no	Start bus no	End bus no	Reactance (p.u.)	Rating power (MW)	Original line number	Length (km)
1	1	2	0.0176	2300	1	70
2	1	11	0.0102	2300	0	40
3	2	3	0.0348	2300	1	138
4	3	4	0.0404	2300	1	155
5	3	7	0.0325	2300	1	129
6	4	7	0.0501	2300	0	200
7	4	16	0.0501	2300	0	200
8	5	6	0.0267	2300	1	106
9	5	11	0.0153	2300	0	60
10	5	12	0.0102	2300	0	40
11	6	7	0.0126	2300	1	50
12	6	13	0.0126	2300	0	50
13	6	14	0.0554	2300	0	220
14	7	8	0.0151	2300	1	60
15	7	9	0.0318	2300	0	126
16	7	13	0.0126	2300	0	50
17	7	15	0.0448	2300	0	178
18	8	9	0.0102	2300	1	40
19	9	10	0.0501	2300	1	200
20	9	16	0.0501	2300	0	200
21	10	18	0.0255	2300	0	100
22	11	12	0.0126	2300	0	50
23	11	13	0.0255	2300	0	100
24	12	13	0.0153	2300	0	60
25	14	15	0.0428	2300	0	170
26	16	17	0.0153	2300	0	60
27	17	18	0.014	2300	0	55

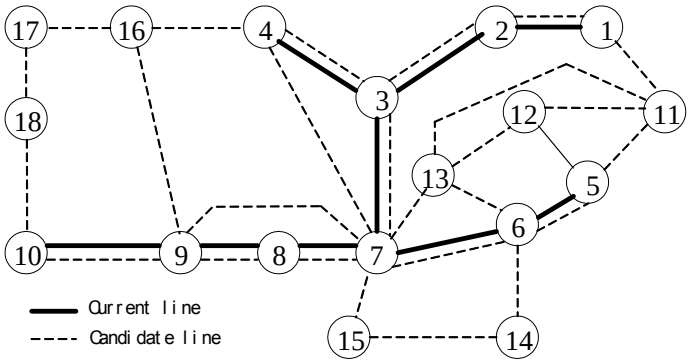

Fig A1 18-bus system

APPENDIX B

Table B1 Bus data of the 46-bus system

Bus no	Power of generator（MW）	power of load（MW）	Bus no	Power of generator（MW）	power of load（MW）
1	0	0	24	0	478.2
2	0	443.1	25	0	0
3	0	0	26	0	231.9
4	0	300.7	27	54	0
5	0	238	28	730	0
6	0	0	29	0	0
7	0	0	30	0	0
8	0	72.2	31	310	0
9	0	0	32	450	0
10	0	0	33	0	229.1
11	0	0	34	221	0
12	0	511.9	35	0	216
13	0	185.8	36	0	90.1
14	944	0	37	212	0
15	0	0	38	0	216
16	1366	0	39	221	0
17	1000	0	40	0	262.1
18	0	0	41	0	0
19	773	0	42	0	1607.9
20	0	1091.2	43	0	0
21	0	0	44	0	79.1
22	0	81.9	45	0	86.7
23	0	458.1	46	599	0

Table B2 Branch data of the 46-bus system

Branch no	Start bus no	End bus no	Reactance (p.u.)	Rating power (MW)	Original line number	Cost (10^3 dollar)
1	1	7	0.0616	270	1	4349
2	1	2	0.1065	270	2	7076
3	4	9	0.0924	270	1	6217
4	5	9	0.1173	270	1	7732
5	5	8	0.1132	270	1	7480
6	7	8	0.1023	270	1	6823
7	4	5	0.0566	270	2	4046
8	2	5	0.0324	270	2	2581
9	8	13	0.1348	240	1	8793
10	9	14	0.1756	220	2	11267
11	12	14	0.074	270	2	5106
12	14	18	0.1514	240	2	9803
13	13	18	0.1805	220	1	11570
14	13	20	0.1073	270	1	7126
15	18	20	0.1997	200	1	12732
16	19	21	0.0278	1500	1	32632
17	16	17	0.0078	2000	1	10505
18	17	19	0.0061	2000	1	8715
19	14	26	0.1614	220	1	10409
20	14	22	0.084	270	1	5712
21	22	26	0.079	270	1	5409
22	20	23	0.0932	270	2	6268
23	23	24	0.0774	270	2	5308
24	26	27	0.0832	270	2	5662
25	24	34	0.1647	220	1	10611
26	24	33	0.1448	240	1	9399
27	33	34	0.1265	270	1	8288
28	27	36	0.0915	270	1	6167
29	27	38	0.208	200	2	13237
30	36	37	0.1057	270	1	7025
31	34	35	0.0491	270	2	3591
32	35	38	0.198	200	1	12631
33	37	39	0.0283	270	1	2329
34	37	40	0.1281	270	1	8389
35	37	42	0.2105	200	1	13388
36	39	42	0.203	200	3	12934
37	40	42	0.0932	270	1	6268
38	38	42	0.0907	270	3	6116
39	32	43	0.0309	1400	1	35957
40	42	44	0.1206	270	1	7934
41	44	45	0.1864	200	1	11924
42	19	32	0.0195	1800	1	23423
43	46	19	0.0222	1800	1	26365
44	46	16	0.0203	1800	1	24319
45	18	19	0.0125	600	1	8178
46	20	21	0.0125	600	1	8178
47	42	43	0.0125	600	1	8178
48	2	4	0.0882	270	0	5965
49	14	15	0.0374	270	0	2884
50	46	10	0.0081	2000	0	10889
51	4	11	0.2246	240	0	14247

52	5	11	0.0915	270	0	6167
53	46	6	0.0128	2000	0	16005
54	46	3	0.0203	1800	0	24319
55	16	28	0.0222	1800	0	26365
56	16	32	0.0311	1400	0	36213
57	17	32	0.0232	1700	0	27516
58	19	25	0.0325	1400	0	37748
59	21	25	0.0174	2000	0	21121
60	25	32	0.0319	1400	0	37109
61	31	32	0.0046	2000	0	7052
62	28	31	0.0053	2000	0	7819
63	28	30	0.0058	2000	0	8331
64	27	29	0.0998	270	0	6672
65	26	29	0.0541	270	0	3894
66	28	41	0.0339	1300	0	39283
67	28	43	0.0406	1200	0	46701
68	31	41	0.0278	1500	0	32632
69	32	41	0.0309	1400	0	35957
70	41	43	0.0139	2000	0	17284
71	40	45	0.2205	180	0	13994
72	15	16	0.0125	600	0	8178
73	46	11	0.0125	600	0	8178
74	24	25	0.0125	600	0	8178
75	29	30	0.0125	600	0	8178
76	40	41	0.0125	600	0	8178
77	2	3	0.0125	600	0	8178
78	5	6	0.0125	600	0	8178
79	9	10	0.0125	600	0	8178

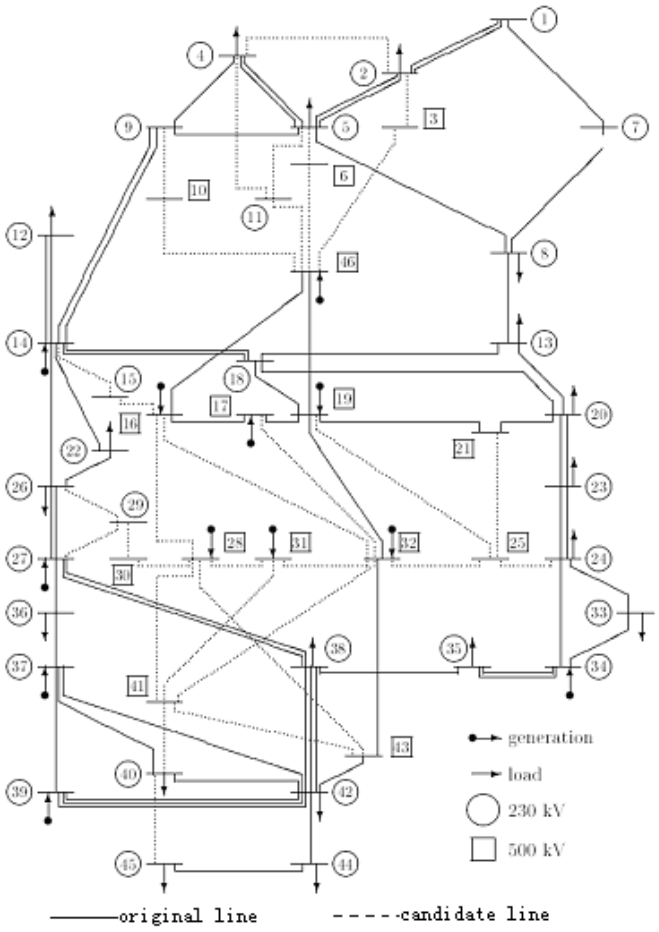

Fig B1 46-bus system